

# ALTERNATIVE FUELS AND CHEMICALS FROM SYNTHESIS GAS

## Quarterly Status Report No. 1

For the Period 1 October - 31 December 1994

Contractor

**AIR PRODUCTS AND CHEMICALS, INC.**  
7201 Hamilton Boulevard  
Allentown, PA 18195-1501

Prepared for the United States Department of Energy  
Under Contract No. DE-FC22-95PC93052  
Contract Period 29 December 1994 - 28 December 1997

19980313 124

07 JUL 19 8 AM 10:05  
DOE/PC/93052--T1

DISTRIBUTION OF THIS DOCUMENT IS UNLIMITED

**MASTER**

CLEARED BY  
PATENT COUNSEL

DTIC QUALITY INSPECTED 4

# **ALTERNATIVE FUELS AND CHEMICALS FROM SYNTHESIS GAS**

## **Quarterly Status Report No. 1**

For the Period 1 October - 31 December 1994

Contractor

**AIR PRODUCTS AND CHEMICALS, INC.**

7201 Hamilton Boulevard  
Allentown, PA 18195-1501

Prepared for the United States Department of Energy  
Under Contract No. DE-FC22-95PC93052  
Contract Period 29 December 1994 - 28 December 1997

## **DISCLAIMER**

This work was prepared as an account of work sponsored by the United States Government. Neither the United States nor the United States Department of Energy, nor any of their employees, makes any warranty, express or implied, or assumes any legal liability for the accuracy, completeness, or usefulness of any information, apparatus, product, or process disclosed, or represents that its use would not infringe privately owned rights. Reference herein to any specific commercial product, process, or service by trade name, mark, manufacturer, or otherwise, does not necessarily constitute or imply its endorsement, recommendation, or favoring by the United States Government or any agency thereof. The views and opinions of authors expressed herein do not necessarily state or reflect those of the United States Government or any agency thereof.

# Alternative Fuels and Chemicals from Synthesis Gas

## Quarterly Technical Progress Report

1 October - 31 December 1994

### Contract Objectives

The overall objectives of this program are to investigate potential technologies for the conversion of synthesis gas to oxygenated and hydrocarbon fuels and industrial chemicals, and to demonstrate the most promising technologies at DOE's LaPorte, Texas, Slurry Phase Alternative Fuels Development Unit (AFDU). The program will involve a continuation of the work performed under the Alternative Fuels from Coal-Derived Synthesis Gas Program and will draw upon information and technologies generated in parallel current and future DOE-funded contracts.

### Summary of Activity

- At the end of the quarter, DOE approved the Cooperative Agreement for the new Alternative Fuels and Chemicals program. The program was funded in full for FY95: \$8.8 million in total. Air Products and its industrial partners, Eastman Chemical and Bechtel, will contribute a 20% cost share ensuring us of all technology rights. We will now move to institute the subcontracts with Eastman and Bechtel, and the several universities who have been working with us. Next year promises to be a much more difficult time for fossil energy R&D funding.
- Work began on modifications for the hydrodynamic/methanol run scheduled for June 1995. Discussions were held with Piping Design for changes in the heater/cooler sequence in the utility oil system. Moving the heater downstream of the cooler is expected to improve the reactor temperature control. After a field inspection, it was decided to install additional piping instead of physically moving the equipment. Installing the piping would be cheaper than moving the equipment, and the oil pump has enough capacity to handle the additional pressure drop caused by the piping. Discussions have also begun for installation of a sump and a pad in the trailer area. This will improve our ability to handle spills. Air permit requirements for the hydrodynamic/methanol run were discussed between Process Engineering, Environmental Engineering, and Radian Corporation personnel. Radian will evaluate the proposed modifications and different operational options to determine whether we need a new air permit exemption.
- A confidentiality agreement was signed between Air Products and Syncrude Technology (STI). Technical discussions were held in a series of meetings between Air Products, STI, and DOE-PETC personnel for a proposed F-T run at La Porte. The objective of the run would be to evaluate performance of catalyst-reactor systems to confirm the design basis. A preliminary process flow diagram has been developed based on STI's desired operational envelope. The total cost of the run was initially expected to be \$2,028,000. A meeting was held in early November to further discuss the run plan and conduct a tour of the LaPorte

facility. Several potential investors of STI also joined for part of the meeting. Later discussions with STI indicated that the ~\$2 MM estimate for the run exceeded their current budget.

Another meeting was held with STI in December to discuss their goals and technical data base in detail. It appears that their catalyst requires a high level of inerts (~50% N<sub>2</sub>) in the feed for activity maintenance. To accommodate the inerts, the operating pressure and flow were doubled from the original design basis. They also want to maintain a high wax (dry) recycle to avoid catalyst agglomeration at the bottom of the reactor as well as maintain catalyst stability. STI would like to use Mott's sintered porous metal elements for catalyst-wax separation as they are unable to have their wire screen elements fabricated in a timely fashion. They have not done any commercial economic study since 1990 and would rely on an Engineering and Construction Contractor to update it. Air Products has decided not to kick off project work until economics from an ECC are updated and appear promising.

- A visit to Institut Francais du Petrole (IFP) revealed that they have stopped work on their (linear) higher alcohols process because of the unfavorable economics relative to MTBE production. They have switched their syngas work over to Fischer-Tropsch chemistry.
- A cesium doped copper/zinc oxide/chromia catalyst was tested at Lehigh University yielding isobutanol at a rate of 48 gm per hour per kilogram of catalyst. This yield almost meets the previous target for isobutanol set in the Alternative Fuels I program. Today's target is at least 400 gm/hour per kilogram of catalyst.
- The Ag/SrO catalyst for converting methanol to isobutanol has been modified with Cs. This modification has increased the lifetime of the catalyst and changed the mol % selectivity to oxygenates. The catalyst has been stable for 55 hours, and the combined isobutyraldehyde and isobutanol selectivity is 23-24 mol %. The catalyst Ag/Cs/SrO is very good at converting a C<sub>1</sub> to a C<sub>2</sub>.

To date the effect of Cs on extending the lifetime of the Ag on SrO catalyst for the conversion of methanol to isobutanol and isobutanol precursors appears to be a unique combination. Rapid deactivation occurs with other control catalyst systems: Cs on SrO; Ag, K on SrO; and Ir, Cs on SrO.

- The University of Aachen reports that their initial attempts to reproduce "Falter-type" catalysts have resulted in adequate activity with lower than expected selectivity to isobutanol.

TGA analysis of used Falter-type catalyst did not reveal any reasons for our lack of success in reproducing the previous Aachen results. The spent catalyst showed a higher degree of reduction and lost zinc at high temperatures, but neither of these phenomena were responsible for poor performance. Replacement of potassium with lithium in the Falter catalyst improved performance incrementally. This trend was the same as seen by Falter at Aachen. However, rate of reaction was still much lower than in the original Aachen work.

A visit to Aachen confirmed that the original Falter reactor was not isothermal. In addition, the reactor had both radial and axial gradients. It may be that the reactor characteristics had a great deal to do with the success of the original Falter catalyst. However, the deliberate imposition of steep axial temperature gradients in the packed bed reactor, like those observed in the previous work of Falter at Aachen did not improve the performance of the Li/Mn/Zn/Zr-based catalyst in syngas or syngas-plus-methanol conversion to isobutanol. The result, derived from experiments in a packed bed reactor designed like the one used in the original work, indicates that the most likely reason for our failure to reproduce the pre-performance results lies in the catalyst itself and not the testing method. Analytical measurement of the catalyst also indicates differences in catalyst.

- The University of Delaware has completed analysis of the factorial design based on the previous work of Styles. Some trends have been identified. Additional variables (e.g., alkalis and transition metals) will be screened.
- The cause of the rapid aging of the syngas to dimethyl ether catalyst system has finally been identified. Rapid aging of the mixed catalyst system is caused by an interaction between the methanol catalyst and the dehydration catalyst. Holding methanol catalyst and alumina under reducing conditions, with no reaction resulted in loss of activity, while the same conditions with no dehydration catalyst gave an active methanol catalyst. The exact nature of the interaction will be investigated further, since this understanding should hold the key to solving the problem.

In a parallel effort, we are testing new dehydration catalysts. None of the dehydration catalysts screened under LPDME conditions this month showed improved aging over the standard catalyst system. Tested were CuO-doped Catapal g-alumina, magnesium exchanged zeolite Y, and TiO<sub>2</sub>.

- A catalyst system consisting of BASF S3-86 methanol catalyst and silicon modified Catapal B g-alumina exhibited a 30% lower deactivation rate than that of the standard system (S3-86 plus virgin Catapal B alumina). While the initial activity is lower than the standard system, the new system demonstrated higher methanol equivalent productivity than the standard system after 50 hours on stream. Although the stability of the system is not completely satisfactory, the potential of improving the stability of LPDME catalyst systems by selecting proper dehydration catalysts has been demonstrated.

## **RESULTS AND DISCUSSION**

### **TASK 1: ENGINEERING AND MODIFICATIONS**

#### **1.1 Liquid Phase Hydrodynamic Run**

Air permit requirements for the hydrodynamic/methanol run were discussed among Process Engineering, Environmental Engineering and Radian Corporation personnel. Radian Corporation, contracted to evaluate air permit requirements, will review the proposed modifications and different operational options to determine whether we need a new air permit exemption.

Work began on modifications for the run scheduled for June 95. Discussions were held with Piping Design for changes in the heater/cooler sequence in the utility oil system. Moving the heater downstream of the cooler is expected to improve the reactor temperature control. After a field inspection, it was decided to install additional piping instead of physically moving the equipment. Installing the piping is cheaper than moving equipment, and the oil pump has enough capacity to handle the additional pressure drop caused by the piping. Discussions have also begun for installation of a sump and a pad in the trailer area to improve our ability to handle spills.

#### **1.2 Liquid Phase Fischer-Tropsch Demonstration**

A confidentiality agreement was signed between Air Products and Syncrude Technology (STI). Technical discussions were held at a meeting of Air Products, STI and DOE-PETC personnel for a proposed F-T run at LaPorte. The objective of the run is to evaluate performance of catalyst-reactor systems to confirm STI's design basis. A preliminary process flow diagram was developed based on STI's desired operational envelope. Four line specifications were generated for new equipment required at LaPorte. Equipment and materials costs for the modifications were estimated at \$425,000, and the total cost of the run was estimated at \$2,028,000.

A meeting was held in early November among Air Products, Syncrude Technology (STI) and DOE-PETC personnel to further discuss the run plan and conduct a tour of the LaPorte facility. Several potential investors in STI also joined for part of the meeting. The investors were impressed with our presentations and the facility. Later discussions with STI alone indicated that the ~ \$2 MM estimate for the run exceeds their current budget. However, they cannot reduce the scope of the run as they do need to recycle dry wax to sustain catalyst activity and breakup catalyst agglomeration at the reactor bottom. Air Products and DOE personnel believe that STI will not be ready for a demonstration run in September 95. Confirmation of the recycle idea is needed in their laboratory which will not be operational till at least May 95. Also, catalyst preparation at a large scale can involve significant development work. Therefore the run schedule has now been pushed back to early 96. This schedule works well with PS Engineering's manpower situation, as a current estimate for a project completion without a high priority is about 12 months.

A two-day working meeting was held with Syncrude Technology (STI) to discuss their technical data base in detail. It appears that their catalyst requires a high level of inerts (~50% N<sub>2</sub>) in the

feed for activity maintenance. To accommodate the inerts, the operating pressure and flow were doubled from the original design basis. STI would like to use Mott's sintered porous metal elements for catalyst-wax separation as they are unable to have their wire wound screen elements fabricated in a timely fashion. They have not done any commercial economic study since 1990 and would rely on an Engineering & Construction Contractor to update it. Air Products has decided not to kick off the project until economics from an ECC appear promising.

Bogdan Slomka from Iowa State University visited LaPorte in early November. He and his team have been working on sonic-assisted cross-flow filtration, and for removal of solids from coal liquefaction products, they have demonstrated a 2.7 fold increase in filtrate flux with sonic treatment. They plan to evaluate the F-T spent slurry from LaPorte (F-T I) next.

## **TASK 2: AFDU SHAKEDOWN AND OPERATIONS**

There is no progress to report this quarter.

## **TASK 3: RESEARCH AND DEVELOPMENT**

### **3.1 DME Catalyst Activity Maintenance**

In the last two quarterly reports from Contract No. DE-AC22-91PC90018 we have shown that DME and high water level are not directly responsible for the rapid aging of the catalyst system in the LPDME process. Since then, our focus has been on the effect of alumina on catalyst stability. Indeed, as shown below, an interaction between BASF S3-86 methanol catalyst and Catapal B g-alumina has been identified specifically as the cause of catalyst deactivation under LPDME conditions. The exact nature of this interaction is under investigation.

This finding shows that we need two catalysts that are compatible with each other. Considering the availability and the complex nature of methanol catalysts, alternative dehydration catalysts become an apparent solution. More efforts, therefore, have been directed at screening dehydration catalysts, an activity that had been started before the cause was found. Five dehydration catalysts have been tested in the past quarter. A catalyst system consisting of BASF S3-86 methanol catalyst and a silicon modified Catapal B g-alumina exhibited better stability and higher productivity (after 50 hours on stream) than that of the standard system (S3-86 plus virgin Catapal B alumina).

A literature review on the recent development (1990 to present) of the one step syngas-to-DME process has been conducted. The highlights include the following: 1) a novel catalyst has been developed by Eastman to convert syngas to methanol and DME, while all other catalyst systems are still some form of a mixture of a methanol synthesis and a dehydration component; 2) stable catalyst systems (up to 1000 hr) have been reported for syngas to DME under gas phase reaction conditions; 3) dehydration catalysts other than pure g-alumina appeared in the literature, providing leads for our catalyst screening; and 4) in terms of methanol equivalent productivity, there is no order-of-magnitude difference in the performance among the literature catalysts/processes and between them and the Air Products LPDME process.



### 3.1.1 Identifying the Cause of Catalyst Deactivation under LPDME Conditions

The effect of alumina on the stability of methanol catalysts was investigated using the following experimental scheme. Upon the standard catalyst reduction using 2% H<sub>2</sub> in N<sub>2</sub>, a catalyst mixture consisting of 80 wt.% of BASF S3-86 methanol catalyst and 20 wt.% of Catapal B g-alumina was left under flowing reduction gas (2% H<sub>2</sub> in N<sub>2</sub>, 50 sccm/min.) at 250°C for 117 hours. The activity of the catalyst system was then measured using Shell syngas to see if holding the two catalysts together at 250°C has any effect on their activity. This scheme avoids exposure of the catalyst system to syngas and reaction products during the holding period; therefore, any effect can be attributed to the mere presence of alumina.

Ideally, one would like to use an inert gas such as nitrogen or helium for the holding period. However, a previous experiment (13465-60) has shown that the methanol catalyst, when loaded by itself, deactivates under flowing nitrogen (APCI zero grade) at 250°C. In contrast, holding the methanol catalyst by itself at 250°C under 2% H<sub>2</sub> in N<sub>2</sub>, as shown below, exhibits little effect on its activity. Therefore, the reduction gas was used in the current alumina impact study to provide an inert medium.

The activity of this catalyst mixture (14045-26) is compared in Table 3.1.1 with that of similar catalyst mixtures from two previous LPDME life studies (11782-3 and 13467-11). Note that the initial activity of the current catalyst mixture, i.e., within 30 hours after the standard reduction, was not measured. This was done to avoid the complication that heavy products might be introduced from the initial activity check and remain in the slurry to deactivate the catalysts. We have confidence in catalyst reduction due to excellent reproducibility in the past. The hydrogen uptake during the current reduction was also found to be in the normal range. Therefore, it is assumed that the initial activity of the catalyst in the current run is similar to the other two DME life runs listed in the table, i.e., about 30 mol/kg-hr in productivity.

**Table 3.1.1 - Comparison of the Catalyst Activity of Different LPDME and LPMEOH Runs**  
**Reaction Conditions: 250°C, 750 psig, 6,000 sl/kg-hr, Shell gas**

Run	Catalyst S3-86:Al <sub>2</sub> O <sub>3</sub>	Time on Stream (hr)			MEOH Equiv. Prod. (mol/kg-hr)	Concentration (%)		Rate Constant	
		Rdctn gas	Syngas	Total		MEOH	DME	k <sub>m</sub> <sup>a</sup>	k <sub>d</sub> <sup>b</sup>
LPDME									
14045-26	80:20	117	26	143	13.7	0.27	2.66	0.84	6.4
11782-3	81.3:18.7	0	20	20	30.7	1.01	6.95	2.61	17.0
			139	139	22.9	0.85	4.71	1.65	10.5
13467-11	81.3:18.7	0	25	25	30.7	1.02	6.85	2.60	12.5
			140	140	21.6	0.78	4.37	1.66	8.7
14045-36	80:20	120	29	149	13.9	0.28	3.52	0.89	7.3
LPMEOH									
14045-28	100:0	17	7	24	15.7	6.80	0.006	1.51	
		128	14	142	14.8	6.28	0.006	1.29	
		128	39	167	15.0	6.34	0.004	1.32	

**Table 3.1.1 - (continued)**

Run	Catalyst S3-86:Al <sub>2</sub> O <sub>3</sub>	Time on Stream (hr)			MEOH Equiv. Prod. (mol/kg-hr)	Concentration (%)		Rate Constant	
		Rdctn gas	Syngas	Total		MEOH	DME	k <sub>m</sub> <sup>a</sup>	k <sub>d</sub> <sup>b</sup>
13467-90	100:0	0	24	24	14.4	5.9	0.08	1.81	
		0	140	140	15.0	6.2	0.03	1.74	

- a: Methanol synthesis rate constant calculated from  $R_m = k_m k_{CO_2} f_{H_2}^{2/3} f_{CO}^{1/3} (1 - appr.)$ , based on methanol catalyst weight.
- b: Methanol dehydration rate constant calculated from  $R_d = k_d f_{CO_2}^{-0.33} f_{MEOH}^{0.11} f_{CO}^{0.70} (1 - appr.)$ , based on alumina weight.

Table 3.1.1 shows that holding the methanol catalyst together with Catapal B alumina at 250°C for 117 hours results in a 55% drop in methanol equivalent productivity. Judging by the rate constants calculated from our current methanol synthesis kinetic model (with some confidence) and methanol dehydration kinetic model (with little confidence), their presence together causes both catalysts to deactivate. Since this observation of incompatibility of the two catalysts is important for the direction of our future work, the above experiment was repeated. As shown in Table 3.1.1, (Run 14045-36), the observation is reproducible.

In order to ensure that the presence of the reduction gas does not have any negative effect on catalyst stability, a similar holding-under-reduction-gas experiment was conducted with only the methanol catalyst loaded in the reactor. The results from this control experiment are also shown in Table 3.1.1 (14045-28), along with the results from a normal LPMEOH run under similar reaction conditions (13467-90). It can be seen that holding under the reduction gas for 128 hr has little effect on methanol catalyst activity. The small drop in activity between the first two measurements (15.7 mol/kg-hr at 7 hours under syngas to 14.8 at 14 hours) is expected when the catalyst burned out its initial hyperactivity under syngas. Upon exposure to the reduction gas for 128 hours, the catalyst has an activity similar to that under normal LPMEOH conditions. (The difference between two measurements in Run 13467-90 is within the noise level in that experiment.)

These results clearly indicate that there is a strong interaction between the methanol catalyst and the Catapal B g-alumina that deteriorates both catalysts. It is not clear what effect of syngas and reaction products would have on this interaction. However, the greater drop in activity under the reduction gas (55% in methanol equivalent productivity) than that under LPDME conditions for a similar length of time (33%) suggests that the interaction is more severe in the absence of syngas and LPDME products.

### 3.1.2 Understanding the Nature of the Interaction

#### Working Hypotheses

Understanding the exact nature of the detrimental interaction between the two catalysts is important for the development of stable catalyst systems for the LPDME process. The possible mechanisms are either chemical or physical. Chemically, there may exist spontaneous migration of active component(s) from the methanol catalyst to the alumina, since alumina is known as a good support material for metals, metal oxides and metal salts, i.e., a good chemical potential

sink. In many cases, a monolayer coverage of metal compounds on the alumina surface can be achieved spontaneously. Second, ion exchange can occur between metal ions in the methanol catalysts (e.g.,  $\text{Cu}^+$ ) and certain specific sites on alumina (e.g., Bronsted acid sites). Third, solid state reaction may take place between two catalysts, e.g., between ZnO (basic) and alumina (acidic), forming chemically bound agglomerates. Fourth, contaminants can be brought into the system by the alumina that poison the methanol catalyst. All of these mechanisms will result in the deactivation of both catalysts (except the fourth one) and can be categorized as *inter-catalyst mass transfer* or *inter-catalyst solid state reaction*.

Physically, agglomerates can be formed from the two catalysts, resulting in thermal sintering or a change in the sedimentation properties of the solids. The formation of fines as a result of the collision between the two catalyst powders in the slurry is another harmful factor. Would large surface area and the porous structure of alumina have any negative effects? What is the role of the mineral oil, serving as slurry fluid, in catalyst deactivation? Some of these physical processes may deactivate catalysts directly (e.g., thermal sintering and a change in sedimentation properties). Some may operate along with the chemical processes mentioned above. For example, formation of physical agglomerates will provide the long contact time necessary for inter-catalyst mass transfer or reaction. The mineral oil can provide a good mass transfer medium.

Even with this short list, a considerable number of parameters need to be examined to shed light on the development of stable catalyst systems. If alternative dehydration catalysts are chosen to be the solution, one needs to look at the following properties of dehydration catalysts:

- Acid types and strength
- Dispersing ability as a support material
- Hardness
- Pore structure and surface area
- Hydrophilic vs. hydrophobic

Thus there are many areas in catalyst screening that need to be explored. Understanding the nature of the interaction will decrease the number of catalyst candidates to be screened. Several possible mechanisms have been investigated in the last quarter.

### **Gas Phase DME Life Study**

A gas phase DME life study has been carried out to shed light on the mechanism of possible mass transfer between the two catalysts. Some of the ways in which migration of material from one catalyst component to the other catalyst component could occur are:

- (1) transport of a soluble species through the slurry liquid
- (2) transport of a volatile species through the gas phase
- (3) surface diffusion when the catalyst particles are in direct contact

Any of these transport mechanisms could occur in a slurry reactor. However, for a packed bed reactor the situation is different; only routes (2) and (3) are possible. Route (2) could certainly be operative in any situation where the two catalysts are in the same packed bed reactor, but route (3) could only be operative if the two components were in close contact.

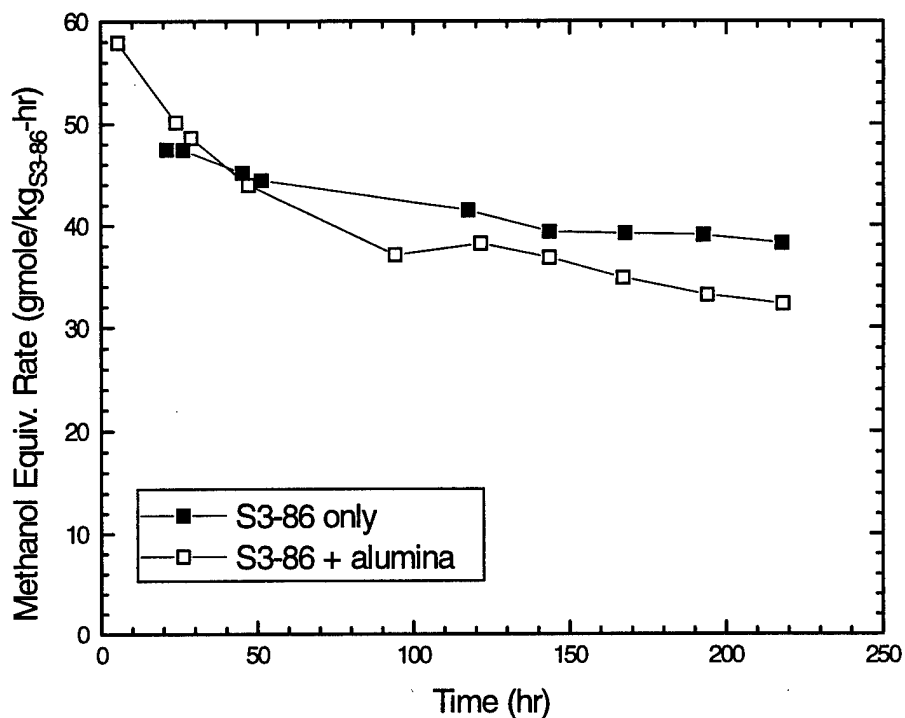
Thus, to test the hypothesis of inter-catalyst mass transfer and to narrow the field of possibilities on mechanisms of transport, deactivation studies were done using a packed bed reactor. Two packed bed life test runs were conducted: one with S3-86 alone to establish a deactivation baseline and the other with an intimate physical mixture of S3-86 and alumina powders. Both tests were run at differential reaction conditions, i.e., very low CO conversion. In this case, the DME productivity is very low for the S3-86/alumina mixture. Thus, the effect of alumina on the S3-86 component is observed, in the absence of appreciable concentrations of products from the alumina and also in the absence of a liquid phase. Specifically, the goal of this experiment was to test whether alumina provides a sink for Cu and/or Zn transported from the S3-86 by one or more of the above mechanisms.

For each run, powder was pressed into pellets approximately 0.5 mm in diameter. The same quantity of S3-86, 0.11 g, was used in each case. To minimize the exotherm (and the concentration of DME) in the packed bed, the conversion was kept very low (<2% CO) by operating at high GHSV (130,000 sl/kg-hr in each case). The calculated adiabatic temperature rise is 32°C at 2% CO conversion. Because of constraints imposed by the reactor configuration and the extremely small bed size, it was not possible to measure the actual temperature of the catalyst particles. Instead the temperature a short distance upstream from the catalyst particles was maintained at 250°C. Due to the very high GHSV the DME productivity for the S3-86/alumina mixture was approximately 5% of the methanol productivity. In fact, the reactor exit DME concentration was comparable to that observed in methanol synthesis over S3-86 alone at typical integral conversions of CO. (For S3-86 alone under differential conversion, the DME productivity and exit concentration was zero.)

The methanol production rates (methanol equivalent rate for the S3-86 plus alumina mixture) as a function of time on stream for both cases are shown in Figure 3.1.1. Initial rates are comparable for both cases. The deactivation rate for the S3-86 alone is higher than typically observed in a LPMEOH run at integral conversion at 250°C. This is likely due to the fact that the catalyst particles in the packed bed experiment are probably at a temperature higher than 250°C because of the reaction exotherm. The deactivation rate for S3-86 is known to increase with increasing temperature. The deactivation rate for the S3-86/alumina mixture appears to be slightly greater than that for S3-86 alone, but the magnitude of the apparent difference is small. In fact, it is not possible to conclude with any confidence that there is a significant difference between the two rates of deactivation. The current experiment does not demonstrate that alumina provides a sink for Cu and/or Zn from the S3-86 component transported by the mechanisms appropriate for a packed bed reactor.

An experiment utilizing Robinson-Mahoney basket internals in a 300 CC autoclave is now being conducted. The liquid phase reaction can run isothermally, thus avoiding the complications involved with reaction exotherms in the packed bed. This experiment uses pellets of S3-86 and alumina, thus making possible several studies which cannot currently be done in the slurry reactor. For example, analysis of the individual catalyst components that have been used in reaction will be possible. Also, spatial separation of the two catalyst components is possible to provide information as to whether inter-catalyst transport of Cu, Zn, or Al is operative.

**Figure 3.1.1 - Methanol Synthesis Life Tests using a Differential, Packed Bed Reactor**



### Effects of Large Surface Area Materials

To find out if the large surface area ( $265 \text{ m}^2/\text{g}$ ) and porous structure (average pore diameter 100 Å) of the Catapal alumina are responsible for the deactivation of the catalyst mixture, a holding-under-reduction-gas experiment was conducted using a silica gel (Davison grade 55,  $\text{SA}=300 \text{ m}^2/\text{g}$ , average pore diameter = 150 Å) mixed with S3-86 methanol catalyst. The initial activity of the mixture was measured using syngas upon reduction. As shown in Figure 3.1.2, the initial methanol synthesis activity of the mixture is similar to that of a pure methanol catalyst. Judging by the product distribution, the activity is solely due to the methanol catalyst, and the silica gel is completely inert under the reaction conditions. The activity of the methanol catalyst was checked again after the system was maintained under 2%  $\text{H}_2$  in  $\text{N}_2$  for 117 hr ( $250^\circ\text{C}$ , 750 psig, 50 sccm). In contrast to the S3-86/Catapal B g-alumina system, no significant drop in the activity was observed. This indicates that a high surface area material is not solely the problem.

The above catalyst system was left under syngas for an additional 173 hr, and a continuous decrease in the activity was observed (Fig. 3.1.2). Figure 3.1.3 shows the normalized methanol synthesis rate constant, calculated from the process engineer's model, as a function of time on syngas stream for this run, along with the constant when pure S3-86 or a S3-86/Catapal B mixture was used. It can be seen that the silica gel causes deactivation of the methanol catalyst under LPMEOH conditions, but at a much slower rate than Catapal B alumina under LPDME conditions. The results shown in Figures 3.1.2 and 3.1.3 indicate that silica may be more compatible to the methanol catalyst than alumina. Therefore, more silica-based dehydration catalysts will be examined.

**Figure 3.1.2 - Compatibility Study of S3-86 and Silica Gel System**

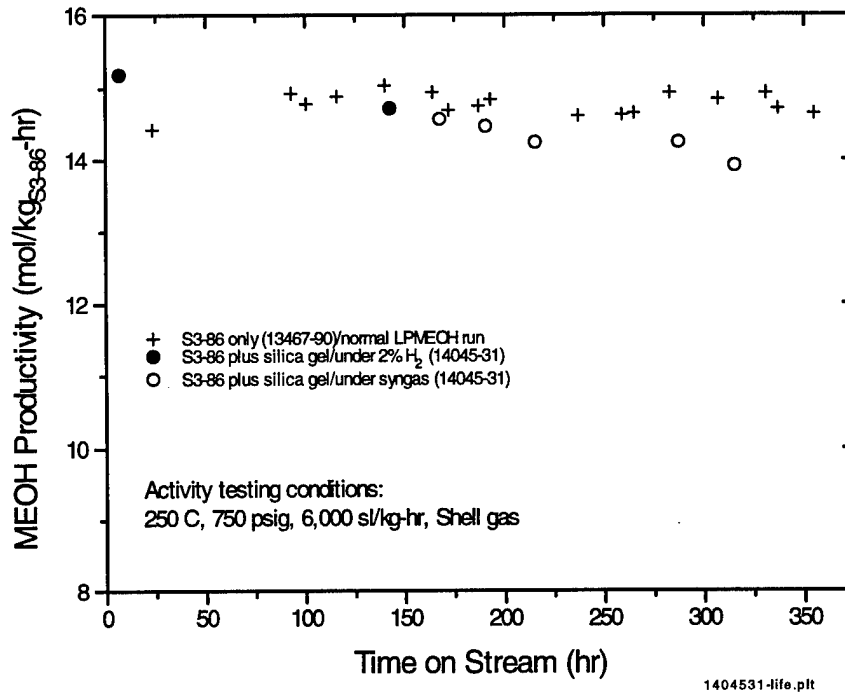
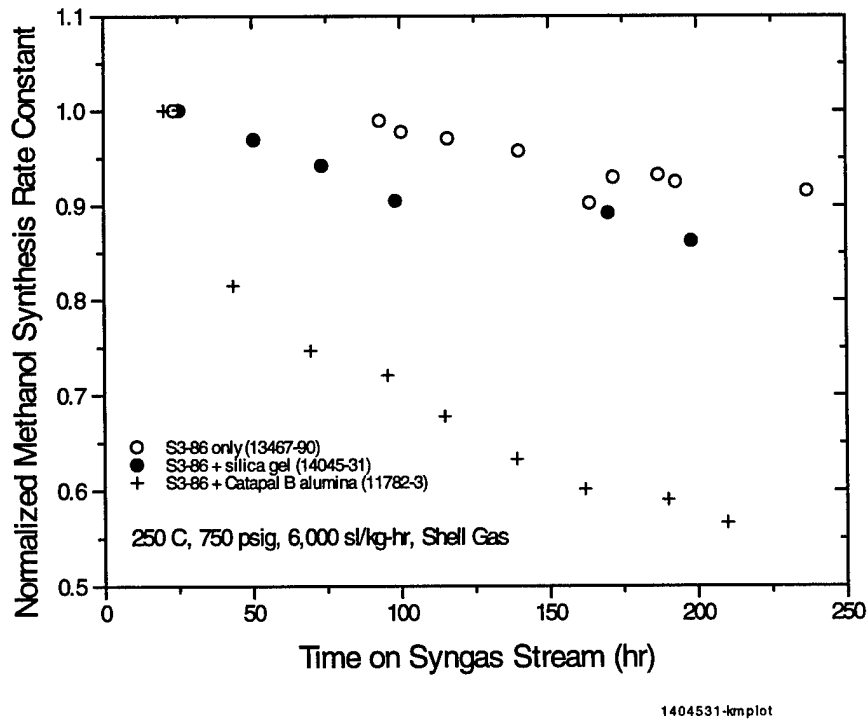


**Figure 3.1.3 - Methanol Catalyst Stability with Different Dehydration Catalysts**



### Possibility of Sediment Formation

The possibility of sediment formation was also examined. Scanning electron micrographs have shown that many fine methanol catalyst and alumina particles are formed under LPDME conditions, apparently due to the collision between catalyst particles. It is possible that the formation of these fines changes the sedimentation properties of the slurry system. For example, large agglomerates with poor dispersing properties could be formed, or the fines themselves may stick to the walls of the reactor, therefore, reducing the activity of the system. Should sedimentation be the cause of catalyst deactivation, increasing stirring rate would bring some of the sediments back into the slurry, resulting in higher activity. Based on this thinking, the activity of a deactivated catalyst system consisting of BASF S3-86 methanol catalyst and a Si-modified Catapal B g-alumina (see Run 14191-36 in the next section) was measured after the stir rate was changed from the normal rate at 1,600 rpm to 2,500 rpm. However, little effect on the activity was observed. This simple experiment rules out the sedimentation hypothesis.

### Contamination from Alumina?

Another possible effect of the Catapal B alumina on the methanol catalyst is that the impurities in the alumina, including known methanol catalyst poisons such as Fe, Ni, S and Cl, may migrate onto the methanol catalyst, leading to its deactivation. To check this possibility, bulk elemental analysis of the Catapal B alumina was conducted, and the results are shown in Table 3.1.2 below. Also included in the table is the bulk composition of the methanol catalyst. It can be seen that the level of poisonous elements in the alumina sample is very low, actually lower or comparable to that in the methanol catalyst. Therefore it is unlikely the alumina is a source of contamination to the methanol catalyst. The high purity of Catapal alumina is due to its production method (ethoxide route).

**Table 3.1.2 - Elemental Analysis of Catapal B g-Alumina and S3-86 Methanol Catalyst**  
(in ppmw)

Sample	Fe	Ni	Cu	Zn	Ti	Ca	Mg	S	Cl
Catapal B alumina (LaPorte 91 run)	<7.3	<10	<1	<5	840	<8.3	<1.4	<100	<100
S3-86 (91/14638)	100	11							33

The surface composition of a deactivated sample of S3-86 and Catapal alumina mixture (S3-86:alumina = 81:19, 500 hr on stream, #13467-11) was analyzed using XPS, and the result is compared in Table 3.1.3 with the surface composition of a pure methanol catalyst of normal activity (#13467-90). No conclusion can be drawn from this analysis because the concentrations of Cl, Fe and Ni in both samples are below the detecting limit of the instrument.

**Table 3.1.3 - XPS Analysis of the Surface Composition of Methanol Catalyst Samples\***

Sample ID	Cu	Zn	C	O	Al	Cl	Ni	Fe
13467-11	4.2	5.3	33.1	34.2	23.2	ND	ND	ND
13467-90	3.9	5.2	36.0	33.0	21.9	ND	ND	ND

\* Composition in atomic percentage; ND: not detected; detection limit: 0.1 atomic%.

### Plan for the Coming Quarter

In addition to the study utilizing Robinson-Mahoney internals, efforts are being made 1) to characterize the surface composition of Catapal alumina before and after deactivation under LPDME conditions, and 2) to understand the effect of the acid properties of a dehydration catalyst (type and strength) on the aging of a catalyst system. The first investigation, primarily using scanning electron microscopy (SEM), will reveal if there is mass transfer between the two catalysts; and if true, what species is transferred. The second study, assisted by IR characterization, will hopefully demonstrate if catalyst deactivation is specifically related to certain acid sites on a dehydration catalyst.

#### 3.1.3 Catalyst Screening

Even before the detrimental interaction between the two catalysts was identified, efforts had been started to search for stable catalyst systems based on the hypothesis of mass transfer or reaction between two catalysts. The approaches included stabilizing the methanol catalyst and examining alternative dehydration catalysts. It was soon realized that the temperature ceiling (ca. 300°C) for a stable methanol catalyst leaves little room for modification of a commercial methanol catalyst, and the methanol catalyst is too delicate a system to manipulate. Therefore, primary efforts have been on screening alternative dehydration catalysts. In the past quarter, a modified methanol catalyst and five alternative dehydration materials have been tested.

#### Cr<sub>2</sub>O<sub>3</sub> -Modified S3-86

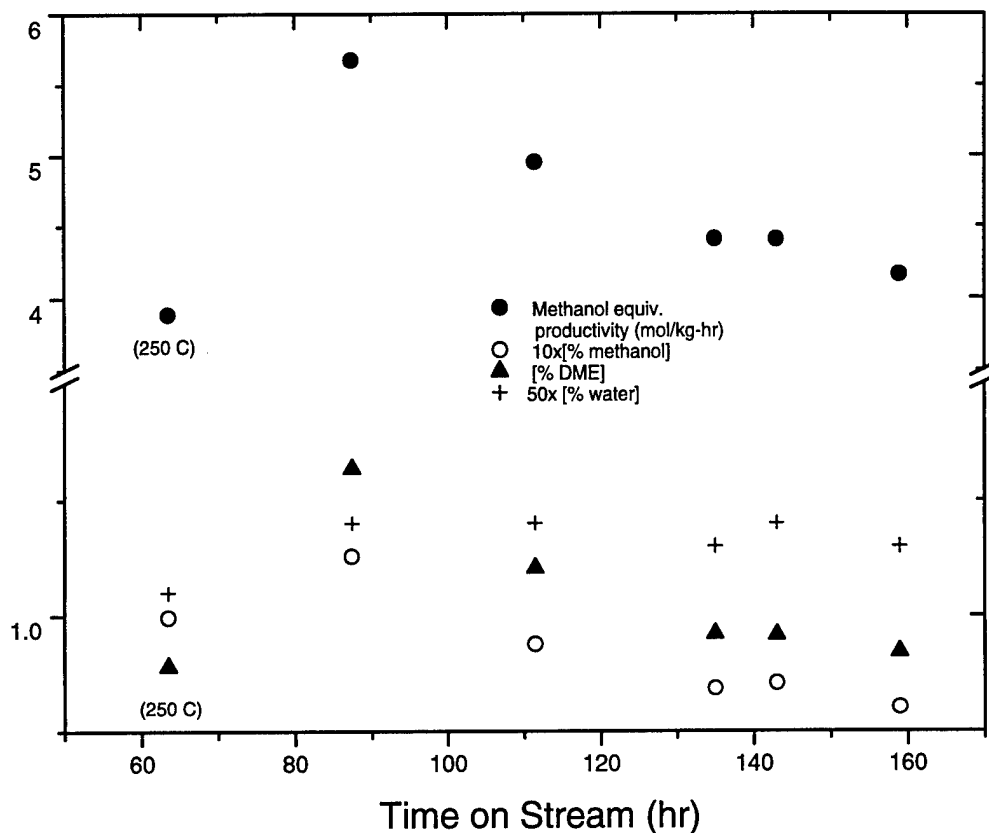
The BASF S3-86 methanol catalyst was modified by Cr<sub>2</sub>O<sub>3</sub> according to a literature method [P. G. Bondar et al., US Patent 4,107,089, 15 August 1978]. This modification reportedly should result in high thermal stability. The modified catalyst, combined with Catapal B g-alumina, was tested using Shell gas. As shown in Figure 3.1.4, the activity of the methanol catalyst is very low at 250°C, an initial methanol equivalent productivity of 4 mol/kg-hr. A previous run using virgin BASF S3-86 under similar conditions (13467-11) shows an initial methanol equivalent productivity of 30.7 mol/kg-hr. The activity of the modified S3-86 catalyst is also an order of magnitude lower than that of the Cr<sub>2</sub>O<sub>3</sub> -modified catalyst reported in the original patent, indicative of the difficulty in reproducing the literature preparation. Nevertheless, we proceeded to test the stability of the catalyst system. In order to start at a reasonable activity, the test was conducted at 270°C. Aside from the low activity, the figure shows that this Cr<sub>2</sub>O<sub>3</sub>-modified catalyst does not have good stability.

#### Si-Modified Catapal B g-Alumina

A 1979 patent by Snamprogetti [G. Manara, et al., US Patent 4,177,167 (1979)] shows that the stability of a mixture of methanol catalyst and g-alumina for a *gas phase* one step syngas-to-DME process can be greatly improved if the alumina is treated with a silicon compound. We prepared a silicon-modified Catapal B alumina sample (Si-Catapal B) according to the patent. A LPDME life test using the Si-Catapal B sample and S3-86 methanol catalyst was conducted at 250°C and 750 psig using Shell gas, and the results (14191-25) are shown in Figure 3.1.5 along with the results from a previous LPDME run using S3-86 and virgin Catapal B alumina (11782-3).



**Figure 3.1.4 - Catalyst Screening Run Using Cr<sub>2</sub>O<sub>3</sub>-Modified S3-86 (14191-2)**  
**Conditions: 270 C, 750 psig, 5,000 sl/kg-hr, Shell Gas**  
**Catalysts: Cr<sub>2</sub>O<sub>3</sub>-Modified BASF S3-86 (13467-77) plus Catapal Alumina (4:1)**



The methanol equivalent productivity of the Si-Catapal B system is fairly low initially. However, it increases with time on stream, reaches a maximum at ca. 50 hours, and then continuously decreases. The induction behavior in the first 50 hours can be attributed to the conditioning of the dehydration catalyst under the reaction conditions. As shown in Figure 3.1.6, the methanol concentration drops rapidly in this period, accompanied by an increase in DME concentration, indicating that the dehydration catalyst is activated in this period. This is understandable because the highest temperature seen by the Si-Catapal B sample during preparation is 200°C, 50°C lower than the reaction temperature. In order to reduce this induction behavior and to see if better stability can be obtained, another Si-Catapal B sample was calcined at 500°C for 5 hours and tested in a separate run (14191-36). As shown in Figure 3.1.5, this calcined Si-Catapal B sample still exhibits an induction period (ca. 115 hr), during which the activity increases slightly. The catalyst system containing the calcined Si-Catapal B sample does not show a better stability than the one without calcination. The activities of the two systems actually become similar to each other upon 200 hr on stream.

The system consisting of S3-86 and Si-Catapal B appears to be more stable than that of S3-86 and virgin Catapal B alumina. As shown in Figure 3.1.5, the methanol equivalent productivity of

the Si-Catapal B system becomes higher than that of the virgin Catapal B system after 50 hr on stream, partly due to rapid deactivation of the latter system.

**Figure 3.1.5 - LPDME Life Study Using S3-86 and Si-Modified Catapal B Alumina**

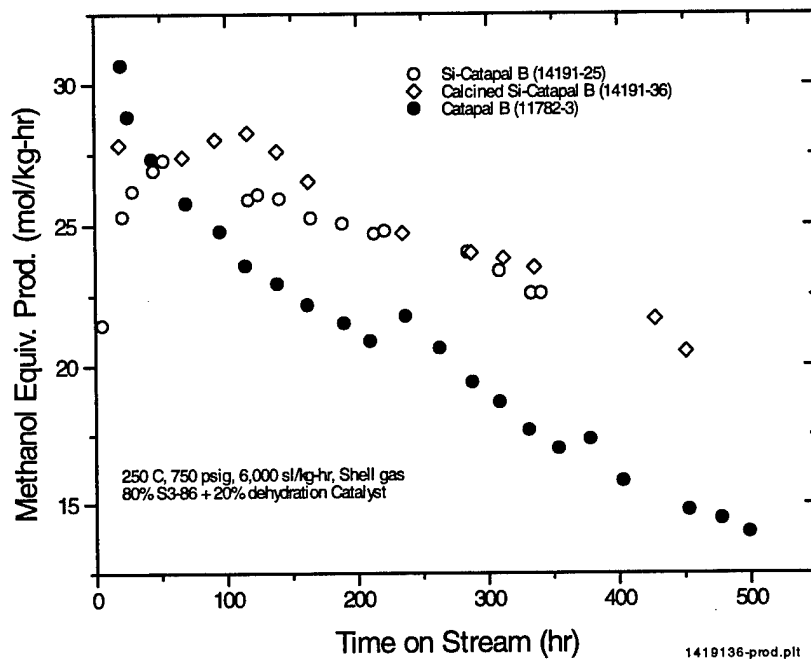
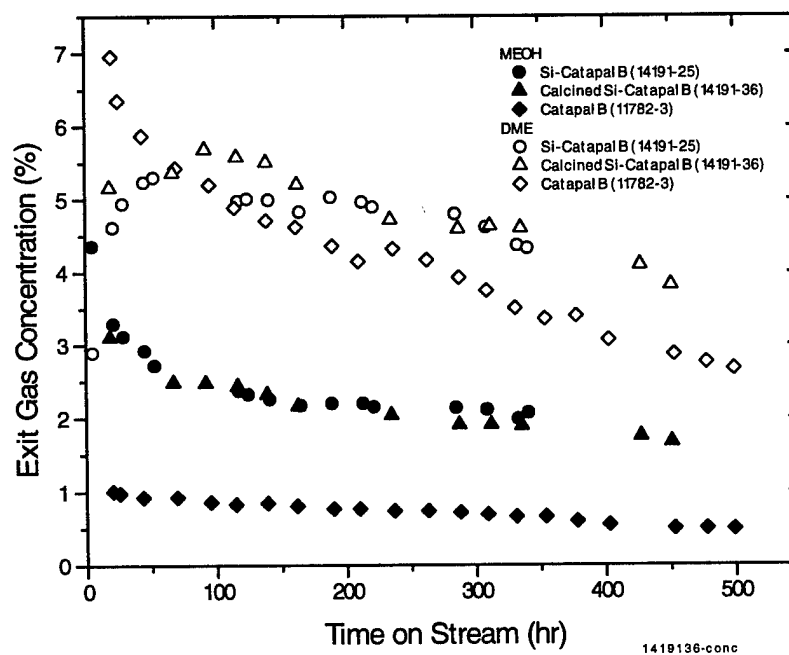


**Figure 3.1.6 - Methanol and DME Concentration in the Effluent as a Function of Time on Stream**

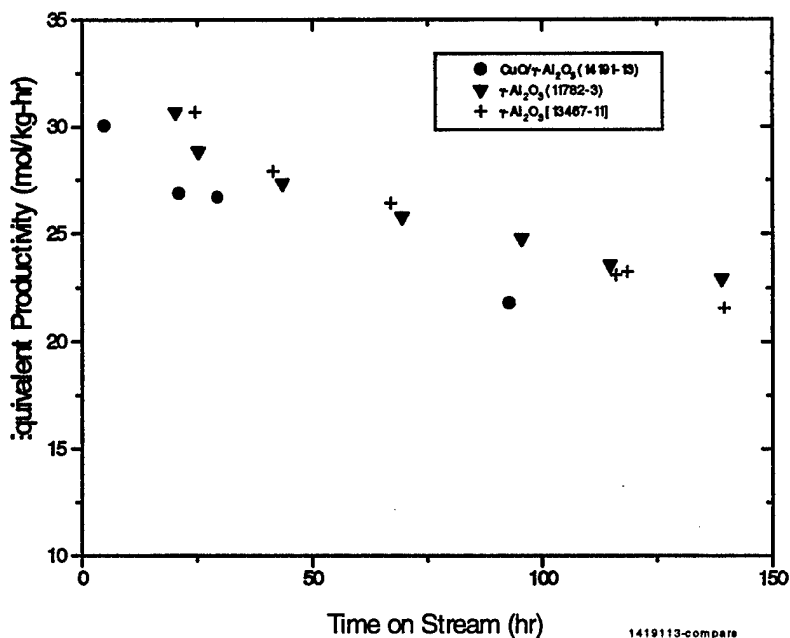


The difference between the two systems becomes larger with increasing time on stream because the deactivation rate of the Si-Catapal B system is smaller by a factor of 0.7. This result is encouraging because it shows the potential of improving the stability of LPDME catalyst systems by selecting proper dehydration catalysts.

### CuO-Doped Catapal B g-Alumina

CuO doped g-alumina was tested as a dehydration catalyst for the following two reasons. First, it is reported [K. Fujimoto et al., EP patent 591,538 (1994)] that CuO doped g-alumina is more active than pure g-alumina for one-step syngas-to-DME process. Second, if the migration of the active components from the methanol catalyst to alumina (especially, a Cu-containing species) would be the cause of the catalyst deactivation under LPDME conditions, doping with CuO might make the alumina a lesser acceptor, therefore reducing the migration/deactivation process. A CuO doped g-alumina was prepared in this lab from the Catapal B alumina. The catalyst contains 6.2 wt.% of CuO and exhibits no CuO XRD powder pattern, indicative of perfect dispersion. This loading corresponds to a 20% monolayer CuO coverage on the alumina surface. This catalyst and S3-86 methanol catalyst were loaded into a 300 cc autoclave, and the test result (14191-13) is shown in Figure 3.1.7, along with two previous LPDME life runs under similar conditions (11782-3 and 13467-11) using virgin Catapal B alumina. It can be seen that the deactivation pattern of the catalyst mixture containing CuO-doped alumina is similar to that of virgin alumina. Contrary to the literature report, the methanol equivalent productivity of the system containing CuO-doped g-alumina is slightly lower than that of virgin alumina.

**Figure 3.1.7 LPDME Runs Using Different Dehydration Catalysts**  
250°C, 750°C, 6,000 sl/kg-hr, Shell gas, S3-86:alumina=80:20



### Chabazite

A chabazite dehydration catalyst developed at Air Products for a commercial methyl amine process was tested along with S3-86. The chabazite catalyst was chosen because it is a weaker acid than many other zeolites such as H-ZSM5 and Y-zeolite. (Strong acidity reportedly results

in the formation of low alkanes, therefore poor DME selectivity, and potentially, coke formation). The test was started at 250°C, the normal reaction temperature for LPDME. Figure 3.1.8 shows that at this temperature the chabazite is not an active dehydration catalyst, yielding, initially, 1% DME in the effluent compared to 6.8% when the Catapal B alumina is used (run 13467-11). Furthermore, this dehydration activity dropped by a factor of 5 in the next 15 hours, accompanied by an increase in the methanol effluent concentration. However, after 20 hours on stream, both the methanol synthesis and dehydration activity of the system became rather stable. The DME concentration in the effluent was about 0.17%, an order of magnitude higher than when the dehydration catalyst was not present. More oxygenates and low alkanes were detected, amounting to 0.3% in the effluent compared to 0.02% when alumina was used.

Next, we increased the reaction temperature to 270°C, the level at which the chabazite is normally used as a methyl amine synthesis catalyst. The DME production was doubled at 270°C, accompanied by a decrease in methanol concentration. The methanol equivalent productivity was lower than that at 250°C. Apparently, the increase in the dehydration activity was not enough to compensate for the increase in the equilibrium approach of the methanol synthesis reaction (from 38% at 250°C to 61% at 270°C), which slows down the reaction. Again, the noteworthy observation from this run was the stability of the catalyst system even at 270°C.

**Figure 3.1.8 - Catalyst Screening Run 14191-6**  
**BASF S3-86 plus APCI Chabazite**  
**Dehydration Catalyst (83.3:16.7)**  
**750 psig, 5,000 sl/kg-hr, Shell gGas**

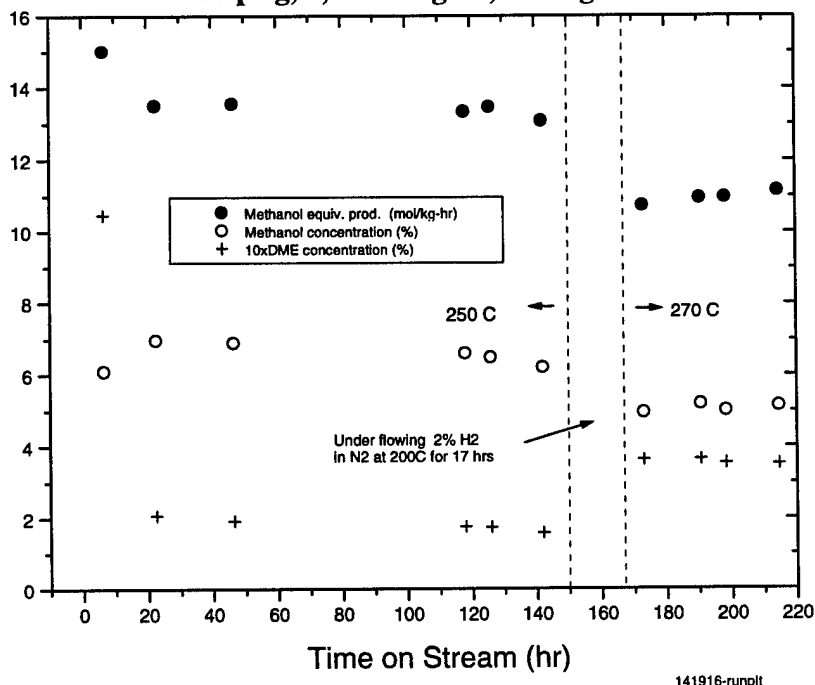


**Figure 3.1.9 - The Stability of Different Catalyst Systems**  
 250°C, 750 psig, 5,000-6,000 sl/kg-hr, Shell gas

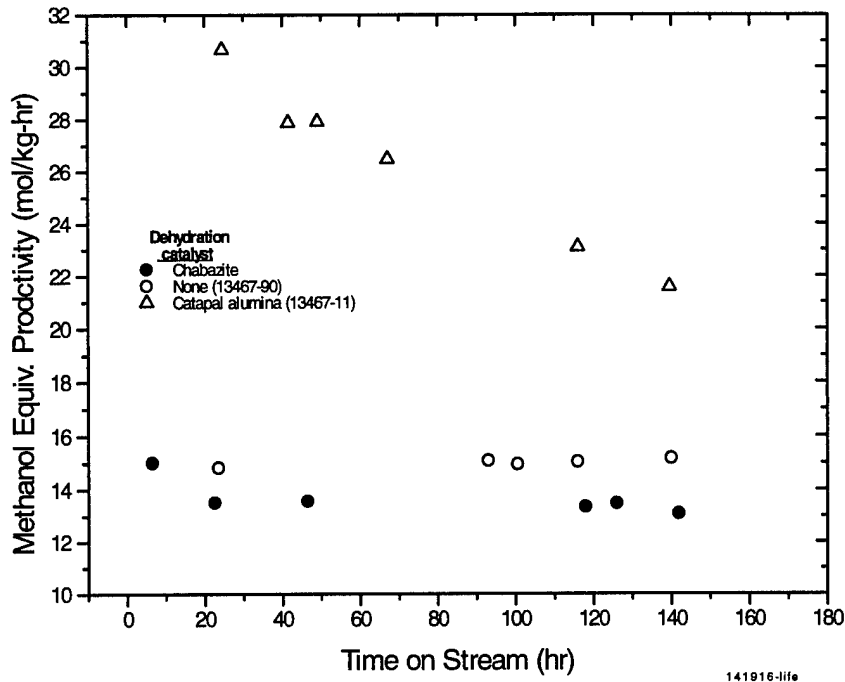


Figure 3.1.9 compares the stability of different catalyst systems at 250°C in terms of methanol equivalent productivity. It can be seen that the stability of the chabazite system is comparable to that of pure S3-86, and much better than that of the Catapal B alumina system.

### Mg-Y

The second zeolitic material we tested, along with S3-86, is a magnesium ion-exchanged zeolite Y (14191-17). The reaction was conducted at 250°C, 750 psig, 6,000 sl/kg-hr in space velocity, using Shell gas. The dehydration activity of the catalyst upon 22 hour under syngas was very low, resulting in a methanol equivalent productivity of 15.3 mol/kg-hr compared to 30 when Catapal B alumina was used under similar conditions. No life test was conducted for this catalyst.

A noteworthy observation from the two runs using zeolitic materials was the very fast deactivation of dehydration catalysts at the beginning of the runs. From 6 to 22 hr under a syngas stream, the DME concentration decreased by a factor of 5 for chabazite, and 2.3 for Mg-Y. The activity in these two runs within 6 hr on stream was not monitored with GC. However, the exit gas flowrate measurement (the higher the activity, the smaller the exit gas flow) in the run using Mg-Y suggests that, within an hour under syngas, the catalyst had a dehydration activity comparable to the Catapal B alumina. In other words, Mg-Y lost 90% of its dehydration activity in the first 6 hr under syngas. It appears that both zeolite samples were much more vulnerable under LPDME conditions than the Catapal B alumina. However, in both cases, the methanol catalyst did not seem to deteriorate along with the zeolite catalysts. The stability of the

S3-86/chabazite system shown in Figures 3.1.8 and 3.1.9 corresponds to a chabazite that has lost most of its dehydration activity.

## TiO<sub>2</sub>

A commercial TiO<sub>2</sub> powder (anatase) from Aldrich was tested. Although it is reported in the literature that TiO<sub>2</sub> is a dehydration catalyst, little dehydration activity was detected in our LPDME run (14191-21) using the TiO<sub>2</sub> sample. A later BET measurement shows that this sample has a surface area of only 9 m<sup>2</sup>/g.

### 3.1.4 Literature Review on One Step Syngas-to-DME Synthesis

A literature search on DME synthesis covering the work from 1967 to 1990 was conducted when the LPDME project was begun in the early 90's. A more recent search of Chemical Abstracts and Derwent from 1990 to the present was conducted on one step DME synthesis from syngas. Except for a novel catalyst by Eastman Kodak, the development of both catalyst and process in recent years still follows the same path, i.e., the catalyst system is some form of mixture of methanol and dehydration catalysts, and the process utilizes either a packed bed or a slurry phase reactor. However, a richer data base is now available from the new publications, providing a broader range of catalysts we can examine, many other methods we can apply to alter DME catalysts, and more information on issues of interest such as catalyst stability.

#### Catalysts

A 1993 patent by Eastman Kodak [G. Irick, Jr., P. N. Mercer and K. E. Simmons, US Patent 5,254,596, 19 October, 1993] discloses a novel catalyst for one step DME synthesis from syngas. The catalyst consists of "chemically mixed" titanium-zinc oxide, Zn<sub>x</sub>Ti<sub>y</sub>O<sub>z</sub>, with x ranging from 0.025 to 0.58 and z from 2.03 to 2.58 at y equal to 1. Note that this catalyst contains neither common components in traditional methanol synthesis catalysts such as Cu, Cr, Al and Pd, nor a typical acidic solid for dehydration. The test reaction was run in a packed bed reactor. Methanol was the primary product when the temperature was below 300°C, but DME selectivity increased to 60% at 325°C. The methanol equivalent productivity of the catalyst was comparable to the Air Products LPDME process when the reaction temperature was above 300°C.

Two patents by Mitsubishi Heavy Ind. Co., LTD, Japan, demonstrate how the activity and stability of a catalyst depend on the details of catalyst preparation. In a 1991 patent [Japanese patent 3,008,446, 19 January 1991], two methanol catalysts were prepared by co-precipitation of Cu, Zn, Cr, and Al nitrates. The resulting methanol catalysts of 150-250 mm were then mixed with g-alumina of the same size, and pressed into 600-1000 mm pellets. The activity and stability of the two catalysts were tested in a 2 cc fixed bed reactor, and the results are shown below. Among the differences between catalysts A and B, although both had the same elemental composition, was the order in which one nitrate was added into another during methanol catalyst preparation. No DME selectivity data were reported in the patent.

<u>Catalyst</u>	<u>Initial CO %conversion</u>	<u>CO %conversion after 100 hr</u>
A	61	54
B	39	21

Reaction conditions: 250°C, 50 ATM, GHSV = 8,000 hr<sup>-1</sup>, H<sub>2</sub>:CO = 2:1..

The second Mitsubishi patent [Japanese Patent 2,280,836, 16 November 1990] shows that DME catalysts of supported form have better activity and stability than a physical mixture of methanol and dehydration catalysts. Catalysts of supported form were prepared by depositing Cu, Zn, and Al on the surface of various metal oxides. The metal oxides served as both catalyst support and dehydration catalyst. The following example illustrates the difference between a catalyst in the supported form and a catalyst mixture:

<u>Catalyst</u>	Initial CO <u>%conversion</u>	CO % conv. <u>after 1,000 hr</u>
CuO-ZnO-Al <sub>2</sub> O <sub>3</sub> /Al <sub>2</sub> O <sub>3</sub> (100:75:25/65), supported	65	61
CuO-ZnO-Al <sub>2</sub> O <sub>3</sub> + Al <sub>2</sub> O <sub>3</sub> (100:75:25/65), mixture	53	18

Reaction conditions: 250°C, 50 atm, 4,000 l/hr, H<sub>2</sub>:CO = 2.

A noteworthy point in the patent is the wide range of metal oxides that were employed as the support and dehydration component for the supported form catalysts. These included Al<sub>2</sub>O<sub>3</sub>, TiO<sub>2</sub>, Fe<sub>2</sub>O<sub>3</sub>, SnO<sub>3</sub>, and ZrO<sub>2</sub>, and all exhibited similar activity.

Stable catalyst systems were observed in these two Mitsubishi patents. In a better Air Products LPDME run using Texaco gas, CO conversion dropped by 45% upon 500 hr on stream. In contrast, catalyst A in the first patent exhibited only an 11% decrease in CO conversion upon 1,000 hr on stream, while the catalyst of supported form in the second patent dropped only 6% upon 1,000 hr on stream. Stable bifunctional catalyst systems under gas phase reaction conditions were also reported by Topsoe [J. B. Hansen, and F. Joensen, in "Natural Gas Conversion Symposium Proceedings" (Ed. A. Holman) 1991, p 457]. An aging test showed only a modest activity loss during a 1,800 hr test period. No detail catalyst information and test data of aging test were presented.

A patent by Snamprogetti [G. Manara, B. Notari and V. Fattore, US Patent 4,177,167, 4 December 1979] shows how the stability of a catalyst system depends on the dehydration catalyst. When a methanol catalyst is used with a g-alumina, the system shows fast deactivation (61% decrease in CO conversion after 310 hrs at 300°C). When the methanol catalyst is mixed with a g-alumina that has been modified by silicon compounds, the system exhibits good DME productivity and exceptionally good stability at 280 - 330°C (virtually no decrease in CO conversion after 500 hours on stream in certain cases).

When a catalyst mixture is used, the intimate contact between the methanol synthesis component and dehydration component appears to play a role in the catalyst activity. NKK Corporation, Japan, issued a patent in 1994 [K. Fujimoto, T. Shikada, Y. Yamaoka, and T. Sumigama, European Patent 591,538, 13 April 1994] on the LPDME process and catalyst. Two types of catalysts were disclosed. The first type involved a procedure for the preparation of a powder mixture of methanol and dehydration catalysts. First, a commercial methanol catalyst (BASF S3-85 or ICI 51-2) and g-alumina were co-pulverized into 20 mm in a ball mill, and then the powder was compressed at 300 kg/cm<sup>2</sup> for about 24 hr to adhere. The pressed pellets were pulverized again to < 120 mm. The final powder was used as a DME catalyst in a slurry phase autoclave reactor. The procedure of co-pulverization-compression-re-pulverization is aimed at bringing two catalysts together, therefore shortening the mass transfer distance in the sequential

reactions of methanol synthesis and methanol dehydration. Comparative examples are given below:

<u>Catalyst</u>	<u>CO % conversion</u>	<u>DME % yield</u>
Co-pulverized, compressed, re-pulverized	41.5	30.3
Co-pulverized without compression	33.3	23.1

Reaction conditions: 280°C, 30 atm, H<sub>2</sub>:CO = 1:1, 6,000 sl/kg-hr, 100 cc autoclave with 30 g of n-hexadecane, methanol catalyst:alumina = 2:1 by weight.

The second type of catalyst was made by co-pulverizing (no compression) a commercial methanol catalyst and CuO doped g-alumina. A very interesting observation is that methanol catalyst plus CuO-doped alumina has higher activity than methanol catalyst plus pure alumina.

<u>Catalyst</u>	<u>CO % conversion</u>	<u>DME % yield</u>
Methanol catalyst + CuO/g-alumina	51.0	34.4
Methanol catalyst + g-alumina	37.8	30.7

The same reaction conditions as shown above.

A study at the Institute of Coal Chemistry (ICC), China, also examined the role of intimate contact between methanol synthesis and dehydration catalysts in DME production [J. L. Tao, Y. Q. Liu and Z. H. Chen, Tianranqi Huagong 16 (1991) 17]. One catalyst tested in a 1 cc packed bed reactor was a mixture of methanol catalyst and g-alumina powders of 400-800 mm (*mixture*). The other catalyst was prepared by mixing methanol catalyst and g-alumina powders of <150 mm, followed by pressing and sieving them into 400-800 mm pellets (*pellet*). The results demonstrated that the pellet exhibited a slightly lower CO conversion, but much higher DME selectivity than the mixture, indicative of the benefit of good interaction between two catalysts.

Different dehydration catalysts were examined in a study by Sofianos and Scurrall [A. C. Sofianos and M. S. Scurrall, Ind. Eng. Chem. Res. 30 (1991) 2372], including g-alumina, silica alumina, Y zeolite, mordenite, and ZSM-5. DME catalysts were prepared by intimate mixing of finely milled methanol catalyst and dehydration catalyst, followed by molding the powder mixture under pressure into 300-500 mm. Catalyst performance was tested in a packed bed reactor using a H<sub>2</sub>/CO (2:1) gas mixture. As shown in the table below, of all the dehydration catalysts, g-alumina was found to be the best. Silica-alumina, with its known strong acidity, did not show significant higher activity than g-alumina when the temperature was above 250°C, yet produced twice as much CO<sub>2</sub> as g-alumina. Zeolitic materials exhibited CO conversion comparable to g-alumina at 275°C, but poorer DME selectivity due to higher conversion to CO<sub>2</sub> and low alkanes (C<sub>1</sub>-C<sub>4</sub>). Mordenite reportedly exhibited very poor stability.



<u>Dehydration component</u>	<u>CO %conversion</u>		
	<u>Total</u>	<u>To DME</u>	<u>To CO<sub>2</sub></u>
g-alumina	41.0	25.8	13.2
silica-alumina	47.3	17.9	27.8
H-ZSM5	28.3	17.1	9.6
H-Y zeolite	37.5	16.4	17.6
ZM 760 mordenite	32.3	11.9	16.9

Reaction conditions: 275°C, 40 atm, H<sub>2</sub>:CO = 2:1, GHSV = 16,000 1/hr.

The same study also demonstrates that the catalyst system consisting of methanol catalyst and g-alumina deactivates rapidly. At 275°C, CO conversion drops by 38% after 120 hr on stream. Catalyst activity, however, can be restored momentarily by treating the deactivated catalyst at the same temperature with air for 2 hr.

A 1991 German patent [K. Decker, H. J. Bisinger, L. Ebner, H. Mere, G. Ohlmann, A. Seidel, K. D. Vollgraf, H. Zarmer (Akad Wissenschaften DDR), German Patent 291,937, 18 July 1991] also examined ZSM-5 as a dehydration component in pelletized DME catalyst made of methanol and dehydration catalyst powders (a binder was used). However, in a different temperature range, a different result was obtained. As shown in the table below, ZSM-5 yielded higher DME productivity than g-alumina at 210 and 230°C.

<u>Dehydration component</u>	<u>CO conversion (%)</u>		<u>DME productivity (g/lit-hr)</u>	
	<u>210°C</u>	<u>230°C</u>	<u>210°C</u>	<u>230°C</u>
ZSM-5	28.4	56.6	70.2	116.9
g-alumina	37.8	56.7	57.3	97.9

Reaction conditions: 50 atm, 1,930 lit/lit-hr, H<sub>2</sub>:CO = 85:15.

ZSM-5 with Si/Al ratio ranging from 12 to 98 were tested, showing no significant difference. No data above 230°C were reported.

### Performance

Table 3.1.4 summarizes the typical performance of DME synthesis reported in the above literature, in terms of CO conversion and/or methanol equivalent productivity. Also included are typical Air Products LPDME results using different types of syngas. Deactivation factor is ignored in the table, and initial activity is used whenever possible. That is, the data in the table represent the best performance of each catalyst/process. It is impossible to make a legitimate or true comparison of these catalysts/processes versus Air Products' process, since different reaction conditions (e.g., T, P, SV, catalyst ratio, feed gas composition) are used. However, in spite of the wide range of reaction conditions, the methanol equivalent productivity from most of the runs falls between 20 and 40 mole/kg-hr. The productivity in the German case is much lower than the others. However, the reaction temperature and space velocity are also very low in that study. In brief, it appears that none of the catalysts/processes is outperforming the others by an overwhelming advantage.

**Table 3.1.4 - Comparison of Different Catalysts and Processes for One Step Syngas-to-DME Synthesis**

Developer	Catalyst	Process	Gas H <sub>2</sub> :CO:CO <sub>2</sub>	Temp (C)	Press. (atm)	SV (sl/kg-h)	CO conv. (%)	MEOH prod. (mol/kg-h)	DME prod. (mol/kg-h)	Methanol equiv. prod. (mol/kg-hr)
Eastman	Zn <sub>x</sub> Ti <sub>y</sub> O <sub>z</sub>	pkd bed	67:33:0	250	70	12,000	1	1.6	0.04	1.7
Eastman	Zn <sub>x</sub> Ti <sub>y</sub> O <sub>z</sub>	pkd bed	75:25:0	300	83	12,000	13	13.4	2.2	17.8
Eastman	Zn <sub>x</sub> Ti <sub>y</sub> O <sub>z</sub>	pkd bed	67:33:0	325	70	12,000	73	25	25.9	50.9
Mitsubishi	CuO-ZnO-Al <sub>2</sub> O <sub>3</sub> /g-Al <sub>2</sub> O <sub>3</sub> pressed mixture	pkd bed	67:33:0	250	50	8,000	61	n.a.	n.a.	n.a.
Mitsubishi	CuO-ZnO-Al <sub>2</sub> O <sub>3</sub> /g-Al <sub>2</sub> O <sub>3</sub> supported	pkd bed	67:33:0	250	50	8,000	65	n.a.	n.a.	n.a.
NKK Co.	methanol catalyst/g-Al <sub>2</sub> O <sub>3</sub> co-pulverized, compressed re-pulverized	slurry	50:50:0	280	30	6,000	41.5	1.2	8.4	18.0
NKK Co.	methanol catalyst/CuO/ g-Al <sub>2</sub> O <sub>3</sub> , co-pulverized	slurry	50:50:0	280	30	6,000	51.9	1.7	12.0	25.7
ICC	methanol catalyst/g-Al <sub>2</sub> O <sub>3</sub>	pkd bed	67:33:0	250	20	6,150	28.3	0	10.0	20.0
ICC	methanol catalyst/g-Al <sub>2</sub> O <sub>3</sub>	pkd bed	67:33:0	260	20	6,150	38.6	1.1	13.0	27.1
ICC	methanol catalyst/g-Al <sub>2</sub> O <sub>3</sub>	pkd bed	67:33:0	275	20	6,150	45.8	0.4	16.0	32.4
Sofianos	methanol catalyst/g-Al <sub>2</sub> O <sub>3</sub>	pkd bed	67:33:0	275	40	16,000	41.0	4.8	30.4	65.2
Sofianos	methanol catalyst/H-ZSM5	pkd bed	67:33:0	275	40	16,000	28.3	0	21.0	21.0
Sofianos	methanol catalyst/g-Al <sub>2</sub> O <sub>3</sub>	pkd bed	1:1:0	250	40	6,670	34			35
German	methanol catalyst/ZSM-5	pkd bed	85:15:0	210	50	2,000	28.4	0.5	1.5	3.5
German	methanol catalyst/ZSM-5	pkd bed	85:15:0	230	50	2,000	56.6	0.7	2.5	5.7
APCI	BASF S3-86/Catapal alumina	slurry	35:51:13 (Texaco)	250	52	6,000	34.3	7.6	11.5	30.6
APCI	BASF S3-86/Catapal alumina	slurry	30:66:3 (Shell)	250	52	6,000	23.4	2.1	13.4	28.5
APCI	BASF S3-86/Catapal alumina	slurry	70:24:6 (H <sub>2</sub> -rich)	250	52	3,600	70	10	6	22

## 3.2 New Fuels from Dimethyl Ether (DME)

### 3.2.1 Overall 1QFY95 Objectives

The following set of objectives appeared in Section III of Quarterly Technical Progress Report No. 16 written under Contract No. DE-AC22-91PC90018.

- Continue to develop the concept of methanol to isobutanol over compositions of Ag on SrO with the goal of increasing oxygenate selectivity and extending catalyst lifetime.
- Initiate catalyst development work on the cracking of ethylidene diacetate to vinyl acetate and acetic acid.
- Initiate the design and construction of small-scale continuous reactor to study DME to ethylidene diacetate conversion.

### 3.2.2 Chemistry and Catalyst Development

#### Methanol to Isobutanol

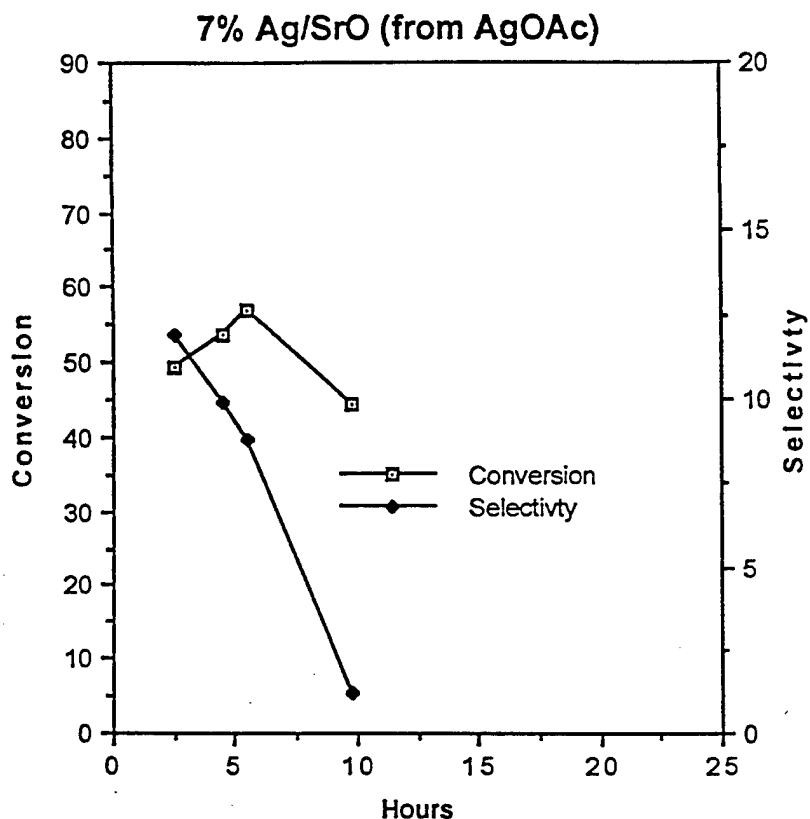
In the previous quarterly, it was mentioned that several Ag/SrO compositions were waiting to be verified by wet analysis. In one example, the expected wt % was 28-30 by method of preparation. Silver analysis put the exact value at 27.52%. Therefore calcination in an inert crucible, like Au, prevents the loss of Ag. Calcination in a quartz tube put the Ag loss at approximately 40%.

All Ag/SrO compositions prepared to date show catalytic activity for the conversion of methanol to isobutanol. Lifetime and selectivity to isobutanol and isobutylaldehyde has been a continuing problem with only slight improvements through the research effort.

A 7% Ag/SrO catalyst prepared from Ag acetate was loaded on top of a Cu screen in a Cu reactor with a Au covered thermocouple. An attempt was made to remove all sources of stainless steel from the reactor zone. With a 24.8 mol % of MeOH in N<sub>2</sub> feed stream, the resulting MeOH conversion and isobutanol selectivity is shown in Figure 3.2.1. The carbon balance was between 74-81 mol %, which was lower than normal, suggesting that the new capillary column must be re-calibrated with respect to molar response factors. Total isobutylaldehyde and isobutanol selectivity fell from an initial value of ~14 mol % to ~2 mol % in 10 hours.

With a fresh catalyst sample from the same batch but now with a 49.6 mol% MeOH in N<sub>2</sub> feed stream, the resulting MeOH conversion and isobutanol selectivity is shown in Figure 3.2.2. The carbon balance was between 62-71 mol %. The direction of the carbon balance suggests that a non-linear response exists for the methanol. In both of these examples, the methanol conversion is nearly identical but the latter has more methanol in the feed. The total isobutylaldehyde and isobutanol selectivity fell from an initial value of ~10 mol % to 0.5 mol % in 20 hours.

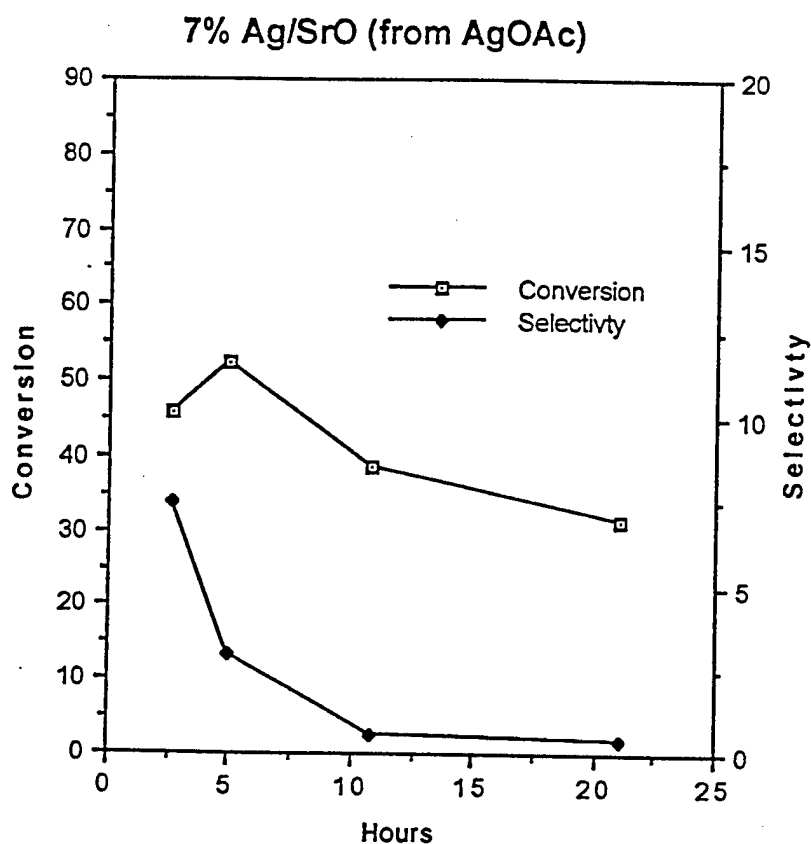
Figure 3.2.1 - 7% Ag/SrO Performance for Isobutanol at 380°C, 1 atm and 13.3 Total sccm



The capillary column was re-calibrated at several different concentrations of methanol in  $N_2$ . The results indicate that the molar response factors at all concentrations are the same. This suggests that the missing carbon is being deposited on the catalyst.

A 17 wt % Ag/SrO prepared from  $AgNO_3$  was tested as before with a 24.8 mol % of MeOH in  $N_2$  feed stream. MeOH conversion and isobutanol selectivity are shown in Figure 3.2.3. The carbon balance ranged from 75-88 mol %. The selectivity to isobutanol was about 6 mol % for the first 6 hours.

Figure 3.2.2 - 7% Ag/SrO Performance for Isobutanol at 380°C, 1 atm and 13.3 Total sccm



The same catalyst that gave the results in Figure 3.2.1 was tested again. The methanol conversion and isobutanol selectivity is shown in Figure 3.2.4. Carbon balance was between 75 - 81 mol %. Total isobutylaldehyde and isobutanol selectivity fell from an initial value of ~16 mol % to ~4 mol % in 6 hours. The conversion/selectivity profiles were similar except for a shift in reaction time. The reactor system was producing near reproducible results.

Figure 3.2.3 - 17 % Ag/SrO Performance for Isobutanol at 380°C, 1 atm and 13.3 Total sccm

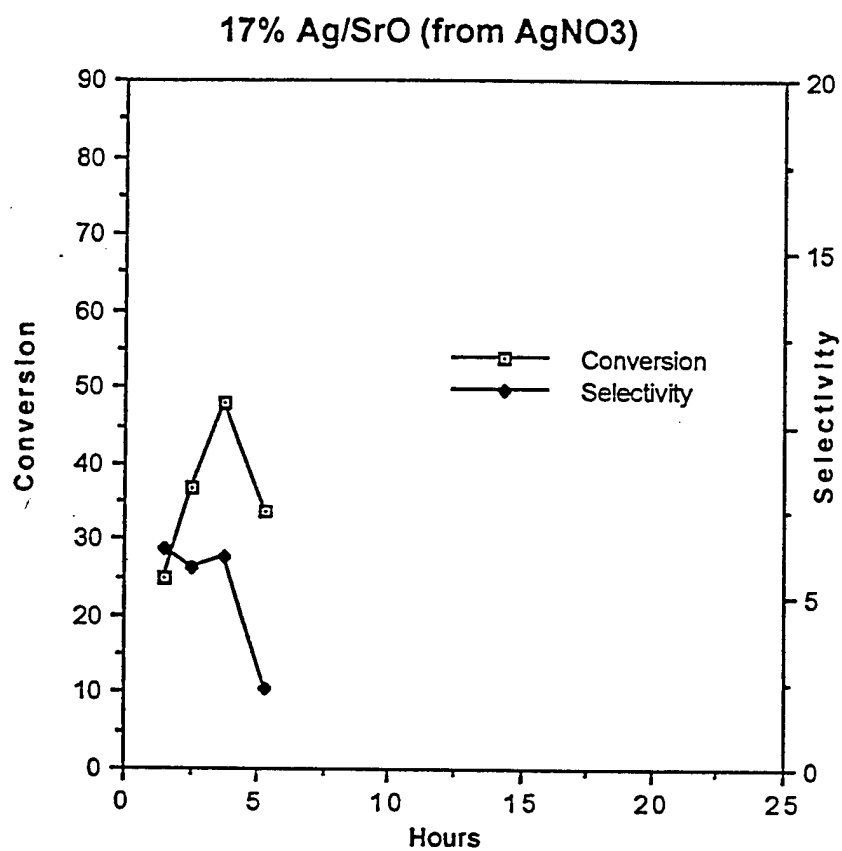
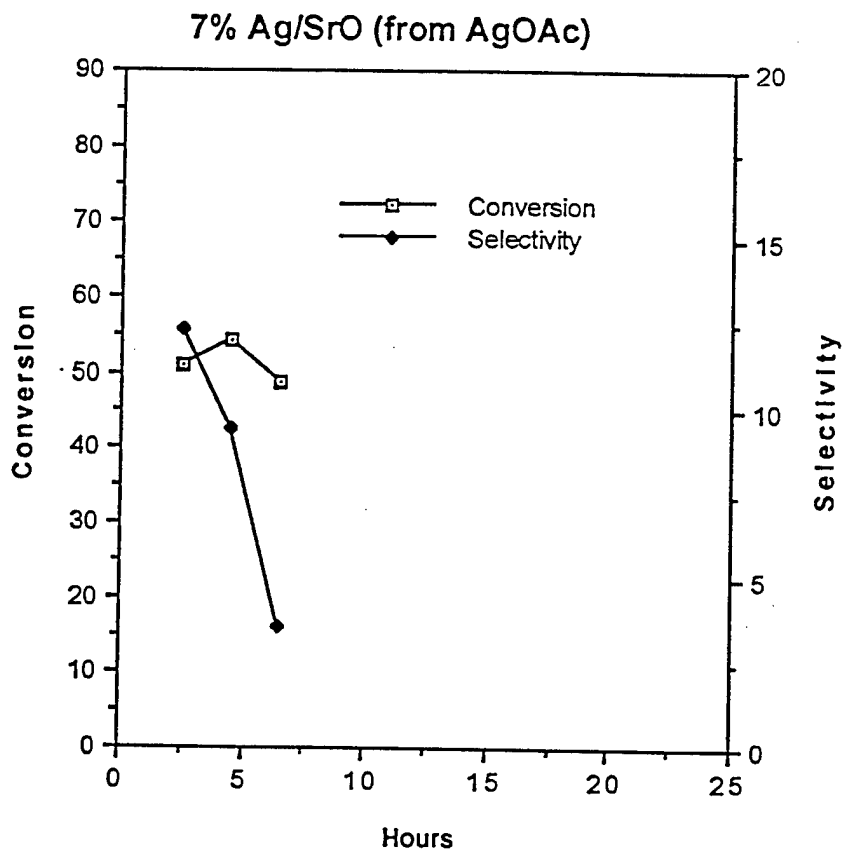


Figure 3.2.4 - 7% Ag/SrO Performance for Isobutanol at 380°C, 1 atm and 13.3 Total sccm



It was also noted that carbon balances improved as the catalyst deactivated suggesting that carbon may have been deposited on the catalyst surface.

A set of four Ag/SrO catalysts was prepared according to Table 3.2.1, and each catalyst was evaluated with a 24.8 mol % in N<sub>2</sub> feed. In each case, there was a decay in activity regardless of the method of calcination. The catalysts lost the ~10 mol % selectivity for isobutanol after 5-6 hrs. on stream.

---

**Table 3.2.1 - Ag/SrO Compositions**

<u>Ag Precursor</u>	<u>Wt % Ag by Prep.</u>	<u>Calcination</u>	<u>Avg. C. Bal.</u>
AgOAc	7	quartz tube	74%
AgOAc	7	Au crucible	76%
AgNO <sub>3</sub>	7	quartz tube	81%
AgNO <sub>3</sub>	7	Au crucible	76%

---

These catalysts should be compared with a Ag/Cs on SrO catalyst that is being evaluated for methanol conversion. In Figure 3.2.5, the plot clearly shows that the performance did not change after 60 hours of operation. The loading of Ag and Cs was 5.8 and 7.3 wt %, respectively. The plotted selectivity refers to combined isobutyraldehyde and isobutanol. At 48 hours the product composition is shown in Table 3.2.2. The carbon balance was 86%, and C<sub>2</sub> and C<sub>3</sub> hydrocarbons were also detected along with propionaldehyde. These components should increase the carbon balance to 100% and probably slightly change the useful C<sub>3</sub> and C<sub>4</sub> selectivity. The appropriate response factors are being determined. The most important finding is that the addition of Cs produces a more stable catalyst and decreases the amount of CO produced. The CO<sub>2</sub> that before appeared to react with the SrO to form a carbonate now is detected in the gas phase.

---

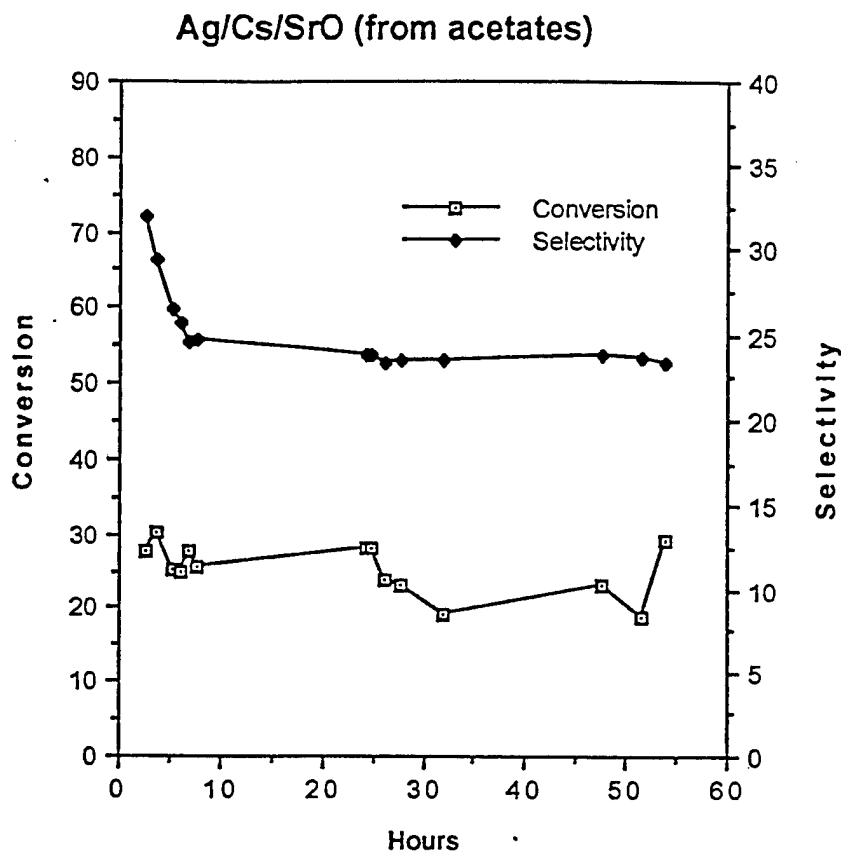
**Table 3.2.2 - Mol % Product Selectivity at 48 Hours**

<u>Product</u>	<u>Mol %</u>
CH <sub>4</sub>	6.1
DME	1.1
isobutyraldehyde	17.5
isobutanol	6.1
C <sub>6</sub> <sup>+</sup>	4.0
CO	39.3
CO <sub>2</sub>	25.9

---



**Figure 3.2.5 - Methanol Conversion and C<sub>3</sub> - C<sub>4</sub> Oxygenate Selectivity vs. Time on Stream at 380°C, 1 atm, and 13.3 Total sccm**



Since the initial report of ~60 hrs. on-stream the same catalyst has now been extended to ~200 hrs. During this time interval, the temperature was increased from 380 to 410°C at 170 hrs. Two plots are provided: Figure 3.2.6, which is a time extension of Figure 3.2.5, reflects selectivity to isobutyraldehyde and isobutanol and Figure 3.2.7 reflects selectivity to isobutyraldehyde, isobutanol, ethanol, propionaldehyde and 1-butanol. Typical product slates at 380°C and 410°C are shown in Table 3.2.3. In general, the carbon mass balance is between 77-90 mol %, the catalyst is operating at 1 atm of pressure, the mol % of methanol in the feed is 24.8 (balance N<sub>2</sub>), the contact time is ~2 seconds, and the wt. % Ag and Cs is 5.8 and 7.3, respectively.

---

**Table 3.2.3 - Product Compositions From Methanol over Ag, Cs on SrO**

<u>Compound</u>	<u>Mol % Selectivity</u>	
	<u>380°C</u>	<u>410°C</u>
Methane	7.3	10.0
Ethylene	0.5	0.5
Ethane	2.8	2.8
Propylene	0.5	0.6
Propane	1.6	1.1
DME	1.2	0.9
Methyl formate	-----	0.3
Ethanol	-----	0.4
Propionaldehyde	4.2	3.2
Isobutyraldehyde	9.7	7.3
n-butanol	2.5	2.3
isobutanol	4.8	3.8
C <sub>6</sub>	1.7	1.3
CO	42.4	49.2
CO <sub>2</sub>	20.8	16.2
MeOH Conv (%)	34.8	44.2

---

The effect of Cs is dramatic with respect to lifetime. Other controls are in progress: Cs only on SrO; Ag, K on SrO; variation of Ag/Cs on SrO and other Group VIII on SrO to determine if lifetime can be enhanced with Cs.

The first control, Cs on SrO, when tested under standard conditions of one atmosphere, 380°C, mol % methanol of 24.8, and contact time of ~2 seconds, quickly deactivates. Figure 3.2.8 illustrates the decay profile. Carbon balance is between 64-81%. Therefore the composition for an active catalyst is Ag, Cs on SrO.

The Cs was replaced with K in the Ag, Cs on SrO composition and tested under the above conditions. Figure 3.2.9 shows the typical deactivation profile. The carbon balance is between 65-84%. Of the Group 1 metals, Cs is superior to K.

**Figure 3.2.6 - Methanol Conversion and Isobutyraldehyde and Isobutanol Selectivity vs. Time On Stream**

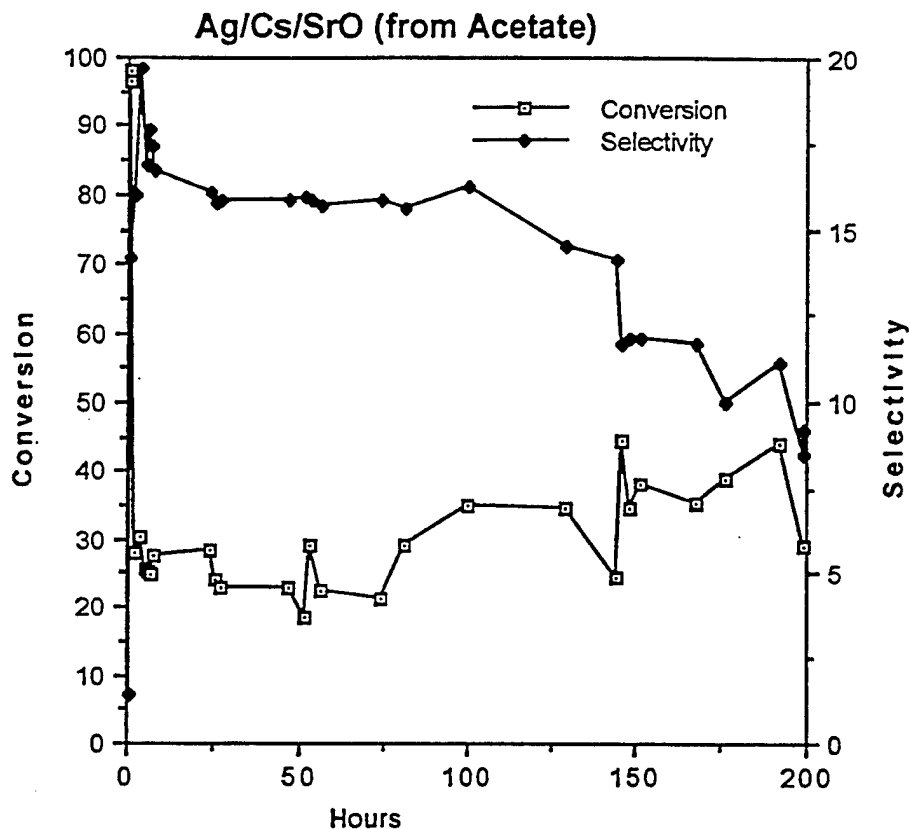


**Figure 3.2.7 - Methanol Conversion and Ethanol + Propionaldehyde + Isobutyraldehyde + n-Butanol + Isobutanol Selectivity vs. Time On Stream**

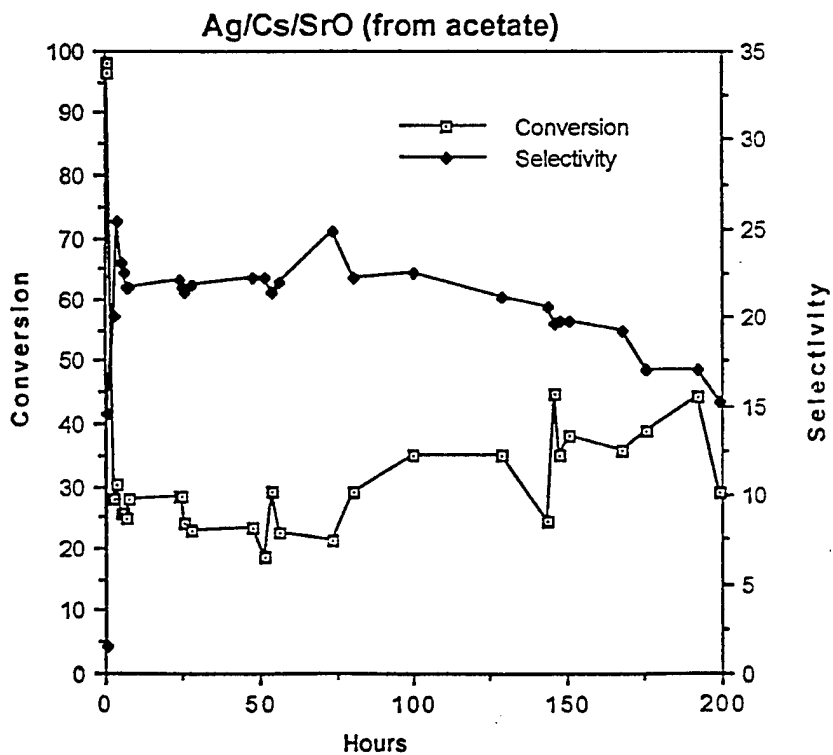


**Figure 3.2.8 - Methanol Conversion and Ethanol + Propionaldehyde + Isobutyraldehyde + n-Butanol + Isobutanol Selectivity vs. Time On Stream**

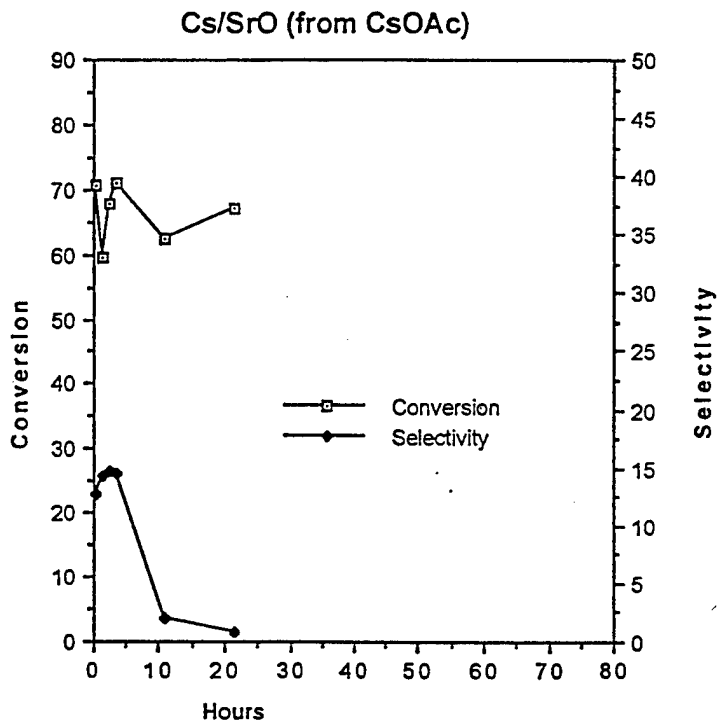
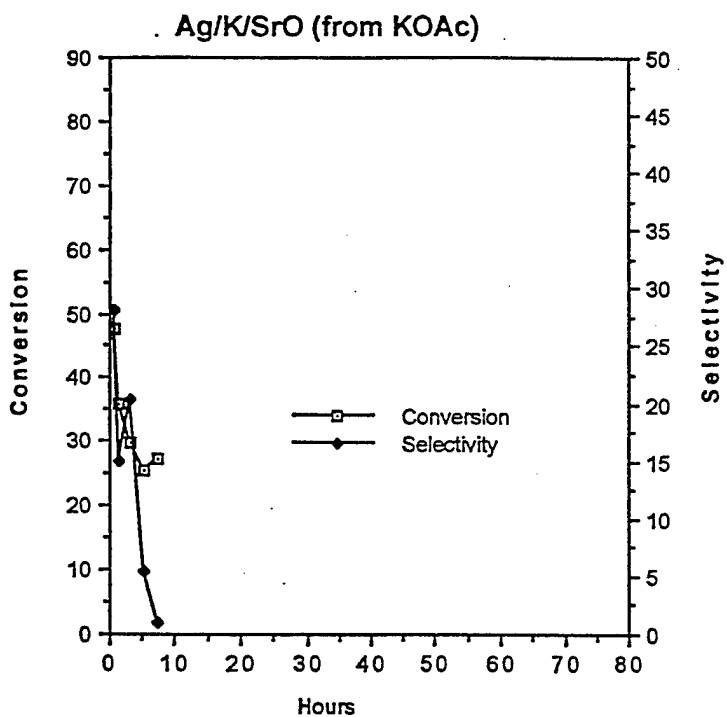


**Figure 3.2.9 - Methanol Conversion and Ethanol + Propionaldehyde + Isobutyraldehyde + n-Butanol + Isobutanol Selectivity vs. Time On Stream**



Previous catalyst compositions of Ir on SrO were active for the conversion of methanol to isobutanol; however, the catalysts deactivated quickly. Cesium was added to this composition, but a gain in lifetime was not observed. Carbon balance was between 57-80%.

The composition of Ag, Cs on SrO has the best lifetime of the catalysts tested to date. In addition it appears that this three component system is unique.

### **Dimethyl Ether to Ethylidene Diacetate**

An attempt was made to run three identical batch autoclave runs on the hydrocarbonylation of dimethyl ether to ethylidene diacetate and to represent these runs as product selectivity vs time. The existing autoclave did not have sampling capabilities. Table 3.2.4 summarizes the three individual experiments.

The product selectivity vs. reaction time, Figure 3.2.10, appears to be consistent with the sequential reactions of DME to methyl acetate to acetic anhydride and then to ethylidene diacetate. The ethyl iodide probably comes from the sequence of methyl iodide to ethyl iodine and begins to appear at the longer reaction time. However, the ethyl acetate at 30 minutes is probably from the reaction between methyl acetate, lithium iodide and ethyl iodide. This suggests that ethyl iodide is made and reacted at 30 and 45 minutes.

During the depressurization of the autoclave after the run is cooled to room temperature, it is most likely some unreacted DME and some of the most volatile products, like acetaldehyde, is lost. The % recovered MeI is consistent with a venting loss of volatile organics. If the yield based on DME charged is normalized to an initial charge of 0.1978 mol DME, then the yields become 79.9, 81.3 and 72.4, respectively.

One research area has been identified that would simplify the homogeneous hydrocarbonylation of dimethyl ether to ethylidene diacetate, especially with respect to catalyst separation from the organic products. This involves heterogenizing the homogeneous hydrocarbonylation catalyst.

**Table 3.2.4 - Identical Batch Autoclave Runs to Represent Reaction Product Profile vs Time**

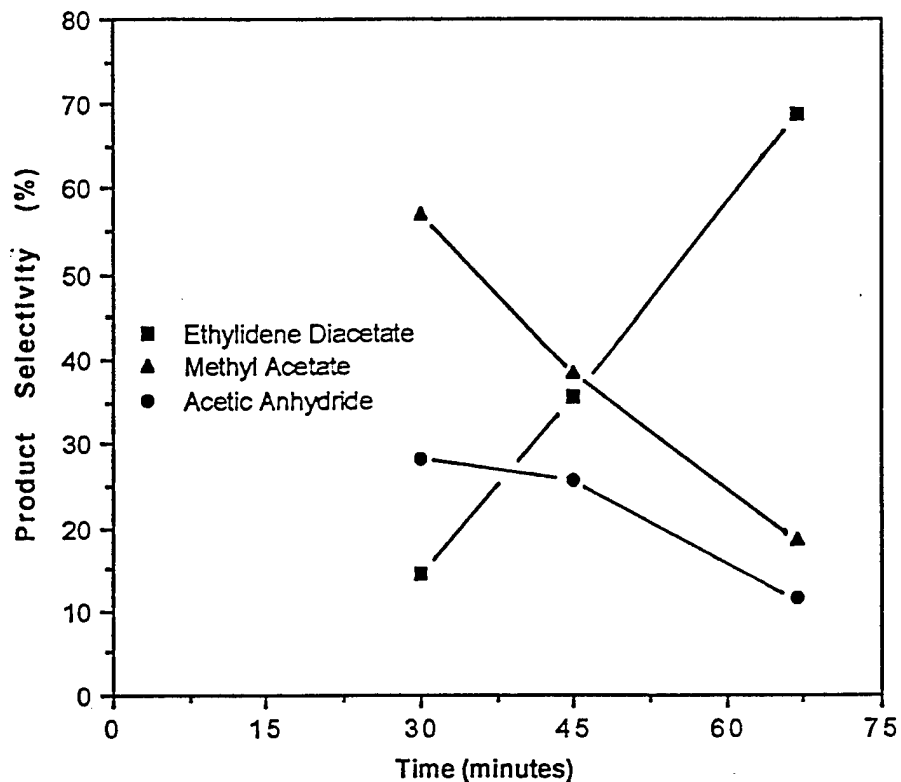
	MMOL	MMOL DME EQUIV.	Sel	MMOL	MMOL DME EQUIV.	SEL	MMOL	MMOL DME EQUIV.	SEL
DME init.	213	---	---	197.8	----	---	208.7	----	---
AcH*	---	---	---	0.1	0.1	0.1	0.1	0.1	0.1
MeOAc	90.3	90.3	57.1	61.7	61.7	38.4	26.7	26.7	18.6
EtI*	---	---	---	---	---	---	0.2	---	---
EtOAc*	0.05	0.05	0.03	0.4	0.4	0.2	1.2	1.2	0.8
HOAc*	2236.2	---	---	2254	---	---	2252.8	---	---
Ac2O*	44.8	44.8	28.3	41.4	41.4	25.7	16.6	16.6	11.6
EDA*	11.5	<u>23.0</u> 158.2	14.5	28.6	<u>57.2</u> 160.8	35.6	49.3	<u>98.6</u> 143.2	68.9
Rxn Time (min) **			30			45			67
Yield based on DME									
Charged:		74.3			81.3			68.6	
Recovered									
MeI:		62.2			62.2			60.0	

\*From GC analysis

\*\* Mol DME equiv. per mol Rh per min: 7.0, 4.7 and 2.8, respectively

\*\*\* RhCl<sub>3</sub>.3H<sub>2</sub>O, 0.75 mmol; MeI, 63.4 mmol; LiI, 11.2 mmol; LiOAc, 12.1 mmol

**Figure 3.2.10 - Product Selectivity vs Time Profile for the Hydrocarbonylation of Dimethyl Ether to Ethylidene Diacetate**



A literature search was initiated to find references on heterogenizing a carbonylation catalyst.

### 3.2.3 2QFY95 Objectives

Future plans for Task 3.2 will focus on the following areas:

- Continue to develop the concept of methanol to isobutanol over compositions of Ag, Cs/SrO with the goal of increasing oxygenate selectivity.
- Initiate catalyst development work on the cracking of ethylidene diacetate to vinyl acetate and acetic acid.
- Prepare carbonylation catalyst candidates for immobilization on supports.

### 3.3 New Processes for Alcohols and Oxygenated Fuel Additives

#### 3.3.1 Oxygenate via Synthesis Gas

##### 3.3.1.1 Overall 1QFY95 Objectives

(i) Complete the kinetic analysis of the methanol/isobutanol and ethanol/isobutanol coupling reactions to form ethers and dehydration reactions to form olefins and dimethylether over Amberlyst-35.

(ii) Conclude the experimental research and computational modelling of selective dimethylether synthesis from methanol/isobutanol mixtures over H-mordenite.

(iii) Complete all experiments using isotopically labelled ethanol and chiral alcohols over Nafion-H and Amberlyst-35 catalysts and write a detailed report that clarifies the mechanistic pathways that control product composition in the synthesis of ethers from alcohols.

(iv) Make substantial progress in establishing the accessibility, number, type (Lewis or Bronsted) and strength of the active surface acid sites by volumetric and HR-XPS analyses after pyridine adsorption on the sulfated zirconia catalyst that is highly active for the selective dehydration of isobutanol to isobutene from methanol/isobutanol reactant mixtures.

(v) Continue studies of increasing the surface area and catalytic activity of Cs/Cu/ZnO/Cr<sub>2</sub>O<sub>3</sub> catalysts for higher alcohol synthesis from H<sub>2</sub>/CO synthesis gas and review methods to attain high surface area Cu/ZrO<sub>2</sub> catalysts that are candidates for the synthesis of C<sub>1</sub>-C<sub>5</sub> alcohols, in particular, branched products such as isobutanol.

##### 3.3.1.2 Results and Discussion

###### A. Kinetic Analysis of Methanol/Isobutanol and Ethanol/Isobutanol Coupling Reactions

A systematic study of the dehydration and coupling of alcohols, i.e., methanol/isobutanol and ethanol/isobutanol binary mixtures, was previously carried out over the Amberlyst-35 resin catalyst, and kinetic analysis of the large amount of acquired experimental data was continued. A 2-page abstract entitled "Kinetic Evaluation of the Direct Synthesis of Ethers From Alcohols Over Sulfonated Resin Catalysts" was submitted for a presentation [1] at the First World Conference on Environmental Catalysis that will be held in Pisa, Italy during May 1-5, 1995. A draft of the 4-page manuscript that will be included in the proceedings volume has been written and is being revised. An expanded 8-page manuscript is being prepared for publication in a special issue of Catalysis Today.

###### B. Selective DME Synthesis Over H-Mordenite

Final experiments were carried out and reported during the previous quarter. A comprehensive report on this research will be written.

###### C. Mechanistic Pathways for Ether Synthesis

No additional experiments were carried out, but computations centered on the S<sub>N</sub>2 reaction of ethanol with chiral S-2-pentanol were completed. The goal was to determine if the transition state complex formed by the coupling reaction would be accommodated in the H-ZSM-5 zeolite.



The geometry of the transition state was optimized by using the Spartan *ab initio* program (RHF/STO-3G model). It was found that the transition state could be accommodated at the intersection of the channel structure of the zeolite. The results indicate that the acid sites at the intersection of the two types of channels are responsible for catalyzing the dehydrative coupling of ethanol and 2-pentanol to the chiral 2-ethoxypentane product with very high selectivity to the inversion product. A communication has been written for publication, and it is near a final version that incorporates a graphic representation of the transition state complex.

In addition, previously obtained experimental data, reported in part in quarterly technical progress reports for January-March 1994 [2] and April-June 1994 [3] (Alternative Fuels I program), have been analyzed in greater detail and included in a communication [4] to be presented at a symposium sponsored by the Division of Fuel Chemistry at the national meeting of the American Chemical Society in Anaheim, CA in May 1995. The manuscript is entitled "Mechanistic Studies of the Pathways Leading to Ethers *via* Coupling of Alcohols," co-authored by Q. Sun, L. Lietti, R. G. Herman, and K. Klier. In particular, the reaction mechanisms for the solid acid-catalyzed dehydrative coupling of methanol and ethanol with isobutanol and 2-pentanol to form ethers were examined by using the data from the previous isotopic labelling, i.e., 180-ethanol, and chiral inversion experiments. It was shown that the solid acid-catalyzed direct coupling of alcohols to form ethers over Nafion-H, Amberlyst-35, and H-ZSM-5 zeolite proceeds primarily through a surface-mediated  $S_N2$  reaction pathway that is far more efficient than either a carbenium or olefin pathway. However, the methyl tertiarybutyl ether (MTBE) and ethyl tertiarybutyl ether (ETBE) products were formed *via* a carbenium intermediate. The efficient surface  $S_N2$  reaction gave rise to high selectivity to configurationally inverted chiral ethers when chiral alcohols were used. This was especially observed in the case of the H-ZSM-5 zeolite catalyst with ethanol/2-pentanol reactants, in which the minor carbenium ion or olefinic intermediate paths were further suppressed by "bottling" of the 3-ethoxypentane product by the narrow zeolite channels and 97% inversion of the chiral center was observed.

#### **D. Investigation of Surface Acidity by X-Ray Photoelectron Spectroscopy**

The surface acidity of solid superacids can be determined by measuring core level binding energy shifts obtained by X-ray photoelectron spectroscopy (XPS). The binding energy measured is related to the charge on the atom being investigated, i.e., an increase in the positive charge on an atom yields an increase in the measured binding energy. For solid acids, it is expedient to adsorb nitrogen-containing bases such as pyridine or ammonia because the nitrogen 1s core level is very sensitive to changes in the environment, e.g., charge on the atom. The N 1s binding energy for pyridine increased by 2-3 eV upon protonation to form the pyridinium ion. This occurred when pyridine was adsorbed on and interacted with Brønsted-type solid acids. The resultant N 1s binding energy shift was readily measured by XPS. Our research using this technique has shown that the sulfated zirconia catalyst has accessible both Lewis and Brønsted acid sites, with the Lewis acid sites having lower N 1s binding energy of adsorbed pyridine than the Brønsted sites. A few additional XPS analyses have been carried out during this quarter, and they will be described in a full report that is currently being written.

A number of computational methods have been employed to calculate the charge on the nitrogen atom in pyridine and pyridinium ion to aid in the quantitative measurement of acidity. The charges have been calculated using electronegativities and partial ionic character [5] and by

partial equalization of orbital electronegativity [6]. The computational results are being compared with experimental XPS results, and further refinements are being incorporated into the calculations being carried out.

### E. Alcohol Synthesis Catalysts

During the previous quarter, a Cu/ZnO/Cr<sub>2</sub>O<sub>3</sub> catalyst was prepared *via* coprecipitation of a hydrotalcite-like precursor using a standard procedure [7], and it was subsequently doped with 3 mol% cesium formate under nitrogen atmosphere, reduced with a 2 vol% H<sub>2</sub>/N<sub>2</sub> mixture, and then tested for higher alcohol synthesis under various reaction conditions. Additional testing was carried out, and a manuscript was submitted for presentation at a symposium sponsored by the Division of Fuel Chemistry at the national meeting of the American Chemical Society in Anaheim, CA in May 1995. The manuscript [8] is entitled "Higher Alcohol Synthesis Over a Cs-Cu/ZnO/Cr<sub>2</sub>O<sub>3</sub> Catalyst: Effect of the Reaction Temperature on Product Distribution and Catalyst Stability."

As described in the manuscript and in the text below, the influence of reaction temperature on methanol and higher alcohol synthesis has been investigated in the range of 310-340°C. Optimal conditions for selective production of 2-methyl primary alcohols included a reaction temperature of 340°C and synthesis gas H<sub>2</sub>/CO = 0.75. Deactivation features were observed after 300 hr on stream, but no significant growth of Cu<sup>o</sup> crystals or reduction in surface area was observed for the catalyst after testing.

*Introductory Remarks.* The Cu/ZnO/M<sub>2</sub>O<sub>3</sub> systems (M = trivalent metal) are well-known catalysts for methanol and higher alcohol synthesis (HAS) [9-12]; their performances are reported in the literature with particular attention being paid to the optimization of both the catalyst composition (amount of alkaline dopant, metal ion ratios) and the operating conditions [10-13]. The application of these catalysts is commonly limited to reaction temperatures not exceeding 310-325°C in order to avoid sintering phenomena that are recognized as the major constraint and drawback of all the copper-containing catalysts. At these temperatures, methanol formation is highly favored, and only by carrying out the reaction at low H<sub>2</sub>/CO ratios can significant quantities of C<sub>2+</sub> oxygenates be obtained. No specific studies have so far addressed the thermal stability of Cu/ZnO-based systems at high temperatures. However, the strong demand for selective production of branched higher oxygenates supports more extensive exploration of the range of allowable reaction temperatures that can be utilized with copper-based catalysts. Indeed, an increment in the temperature is expected to result in the desired promotion of higher alcohol production and a concurrent decrease in methanol formation. In the following, a study of the effect of reaction temperature on HAS over a Cs-doped Cu/ZnO/Cr<sub>2</sub>O<sub>3</sub> catalyst is presented, and the principal interests are the changes in the product distribution and the catalyst thermal stability.

*Catalyst Preparation.* The methodology has been described by Nunan et al. [11,14], and consists of the precipitation of a hydrotalcite-like precursor Cu<sub>2.4</sub>Zn<sub>3.6</sub>Cr<sub>2</sub>(OH)<sub>16</sub>CO<sub>3</sub>·4H<sub>2</sub>O [15], followed by stepwise calcination to 350°C to give the mixture of oxides, CuO/ZnO/Cr<sub>2</sub>O<sub>3</sub>. Cesium doping was achieved by adding the catalyst to a N<sub>2</sub>-purged aqueous solution of CsOOCH, which was then slowly evaporated to dryness under flowing N<sub>2</sub>. The amount of

dopant (3 mol%) was chosen on the basis of previous studies of the optimal catalyst composition with respect to higher alcohol synthesis [11]. The catalyst was finally reduced with a 2 mol%  $H_2/N_2$  mixture at 250°C.

Activity Tests. The apparatus has been extensively described elsewhere [16]. It is noted that charcoal and molecular sieve traps, an internally copper-lined stainless-steel reactor, as well as a copper thermocouple-well were used during the catalytic testing to prevent the formation and deposition of iron-carbonyls, which are well-known deactivating agents [17,18]. The catalysts were tested under steady-state conditions at 7.6 MPa with synthesis gas of various  $H_2/CO$  compositions flowing with a gas hourly space velocity of 5300 l/kg cat/hr. The reaction temperature was varied between 310 and 340°C.

The exit product mixture was sampled every 30-60 min using an in-line, automated, heated sampling valve and analyzed in a Hewlett-Packard 5390 gas chromatograph. The products were analyzed *via* a Poraplot-Q capillary column alternatively connected to a flame ionization detector and to a thermal-conductivity detector (TCD) and a Molsieve capillary column connected to TCD. The sensitivity factors of the instrument were determined on the basis of calibrated mixtures. The gas-phase on-line analyses were coupled with the analysis of liquid samples collected downstream from the reactor (atmospheric pressure) by liquid nitrogen cooled traps. The identification of the products (more than 50 components) was obtained by comparison of their retention times with those of known standards and from analysis of the liquid samples by a HP GC/MS instrument. All of the experimental data were obtained in a steady-state regime that was reached about 6-8 hr after setting the operating conditions.

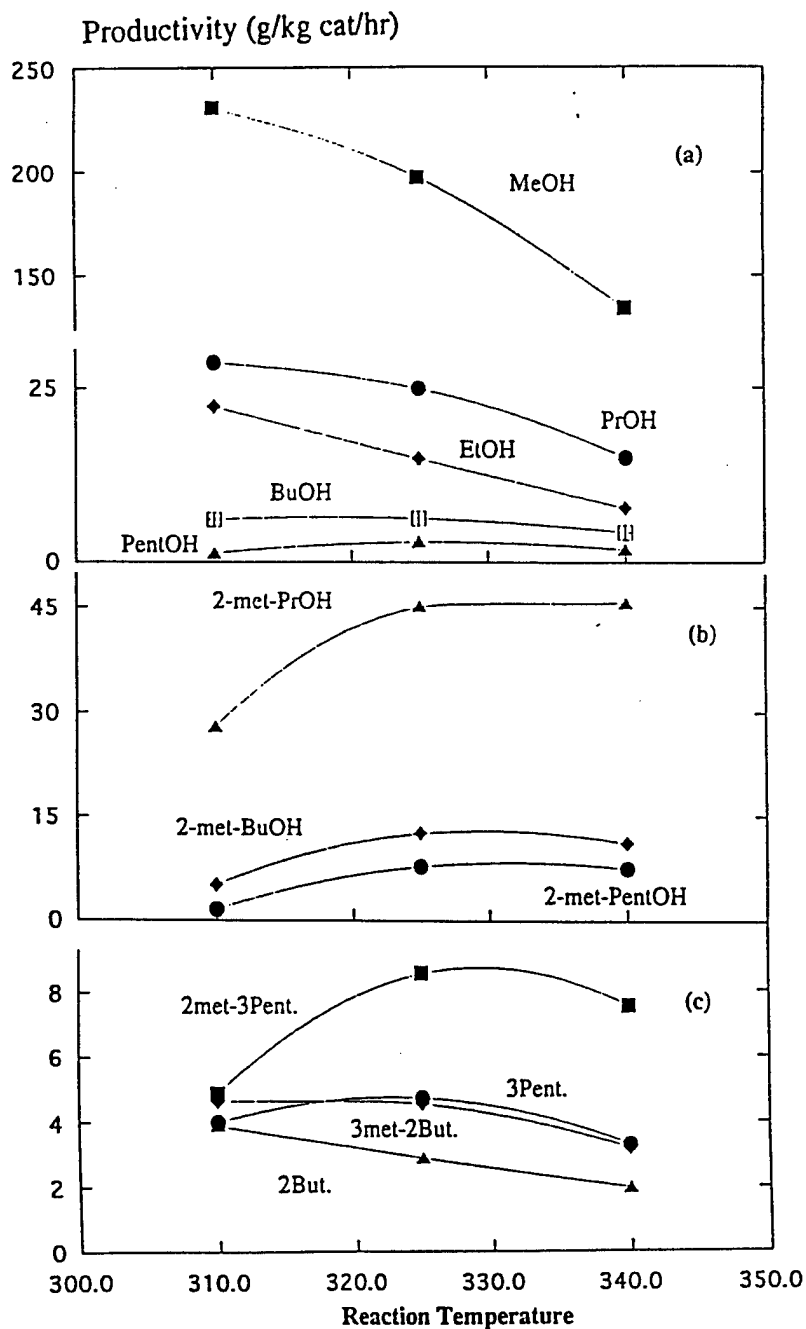
Catalyst Characterization. BET measurements and XRD analyses were performed at each stage of the catalyst preparation and after testing to determine the catalyst surface area and crystalline phases, respectively.

Effect of the Reaction Temperature on the Product Distribution. In Figure 3.3.1, the productivities of the most abundant oxygenated products are reported as a function of the reaction temperature, which was increased from 310°C up to 340°C over a period of about 160 hr. As the temperature was increased, a decrease of methanol productivity was observed, in line with the thermodynamic constraints that govern methanol synthesis. As shown in Figure 3.3.1a, the productivities of all the linear higher alcohols exhibited decreasing trends with increasing reaction temperature. In fact, the product mixture tends to become depleted in intermediate species (ethanol, propanol) and more enriched in the branched oxygenates that play a terminal role in the chain-growth process. At 325°C, a promotion of all the 2-methyl alcohols was observed (Figure 3.3.1b). It is noted that the molar ratio between methanol and the totality of  $\alpha$ -branched alcohols passed from a value of about 16 at 310°C to the value of about 5 at 340°C. In the case of secondary alcohols (whose productivities are summed in Figure 3.3.1c with those of the corresponding ketones), it is observed that high temperatures favor the formation of high molecular weight species (e.g., 2-methyl-3-pentanol) at the expense of the intermediate species (e.g., 2-butanol).

**Figure 3.3.1 - Experimental Effect of Reaction Temperature on Methanol and Higher Oxygenates Productivities**

In 1-c: 2met-3Pent = 2methyl-3-pentanol + 2 methyl-3-pentanone, 3-Pent. = 3-pentanol + 3-pentanone, 3met-2But. = 3-methyl-2-butanol + 3-methyl-2-butanone, 2-But. = 2 butanol + 2-butanone.

Operating Conditions:  $H_2/CO = 0.45$ ,  $P = 7.6$  MPa,  $GHSV = 5300$  l/kg cat/hr.



The formation of methane and  $C_2^+$  hydrocarbons was also observed to increase with increasing reaction temperature (Figure 3.3.2). The overall production of hydrocarbons, equal to 15.7 g/kg cat/hr at 310°C, grew to the value of 39.4 g/kg cat/hr at 340°C. It is worth noting that, contrary to the case of oxygenates, hydrocarbons appear to keep an almost constant relative product distribution, which could support the hypothesis of a formation pattern independent from the higher alcohol chain-growth process.

Finally, it is noted that the productivities of all the methyl-esters detected in the product mixture decreased monotonically with increasing reaction temperature. This trend was especially evident in the case of methyl-formate and methyl-acetate, while it was less pronounced for the higher homologs (methyl-propionate, methyl-isobutyrate, methyl-butyrate).

*High Reaction Temperature: Effect of  $H_2/CO$  Ratio.* At the reaction temperature of 340°C, kinetic runs were performed to investigate the combined effects of high temperature and  $H_2/CO$  feed ratio on HAS product distribution. The results are reported in Figure 3.3.3, and the data show that an excess of  $H_2$  exclusively promoted methanol formation. The production of higher oxygenates appears to be significantly inhibited at high  $H_2/CO$  ratios. Specifically, all of the primary alcohols tended to show a maximum in productivity, with the highest value being associated with the  $H_2/CO$  value of 0.75 (Figure 3.3.3a,b).

With respect to the formation of hydrocarbons, the data reported in Figure 3.3.4 indicate that while the synthesis of  $C_2^+$  hydrocarbons was strongly slowed by decreasing CO partial pressure, methane productivity was approximately constant as a function of the  $H_2/CO$  ratio.

*High Reaction Temperature: Catalyst Stability.* The operating conditions of  $T = 340^\circ\text{C}$ ,  $H_2/CO = 0.45$ , 7.6 MPa, and GHSV = 5300 l/kg cat/hr were periodically reproduced in order to check the stability of the catalyst. The results of the experiments are reported in Figure 3.3.5, where the averaged FID signals, in arbitrary units, for the most abundant products have been plotted vs the time of testing. As previously noted, a period of about 160 hr occurred before the final temperature of 340°C was reached, and at this high temperature a stable catalytic activity was observed during 125 hr. Subsequently, a slow loss of selectivity of the higher oxygenates in favor of an increment in methanol productivity was detected. Similar results were obtained in the past when deactivation caused by the deposition of iron carbonyls onto Cu/ZnO catalysts was studied [17]. Even though the cause of the behavior shown in Figure 3.3.5 cannot be assessed,  $Cu^\circ$  sintering can be excluded as playing a major role, where the XRD pattern of the tested catalyst (300 hr on stream at 340°C) revealed the presence of metallic copper with crystallite size in the range of 100Å, which is comparable with the dimension of  $Cu^\circ$  crystallites observed in the binary Cu/ZnO systems after the reduction stage and before testing [17]. Moreover, BET measures showed that no reduction in the catalyst surface area occurred during the kinetic runs, being 85 m<sup>2</sup>/g and 89 m<sup>2</sup>/g before and after testing, respectively.

Figure 3.3.2 - Effect of Temperature on C<sub>1</sub>-C<sub>6</sub> Hydrocarbon Production and Distribution

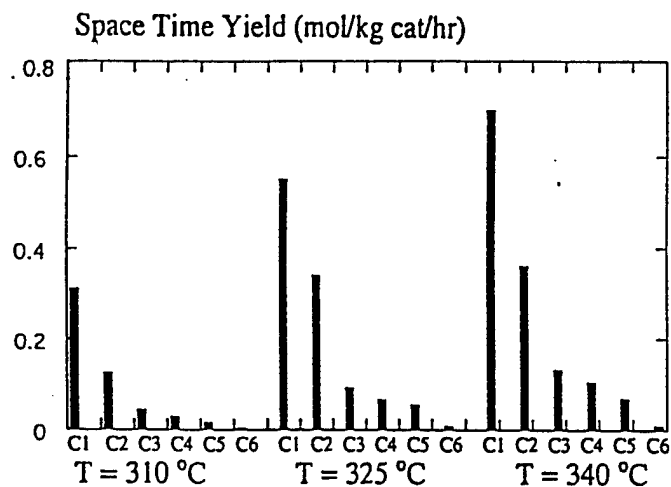


Figure 3.3.3 - Effect of H<sub>2</sub>/CO Ratio; T = 340°C, P = 7.6 MPa, GHSV = 5300 l/kg cat/hr

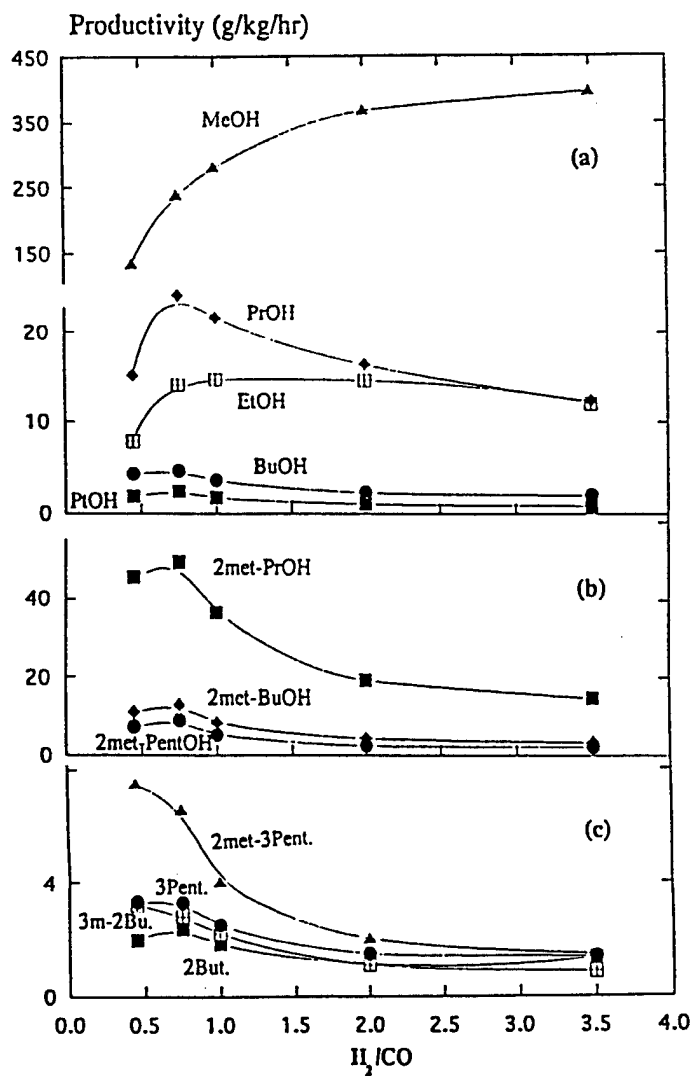


Figure 3.3.4 - Effect of H<sub>2</sub>/CO Ratio Hydrocarbon Formation. Conditions as in Figure 3.3.3

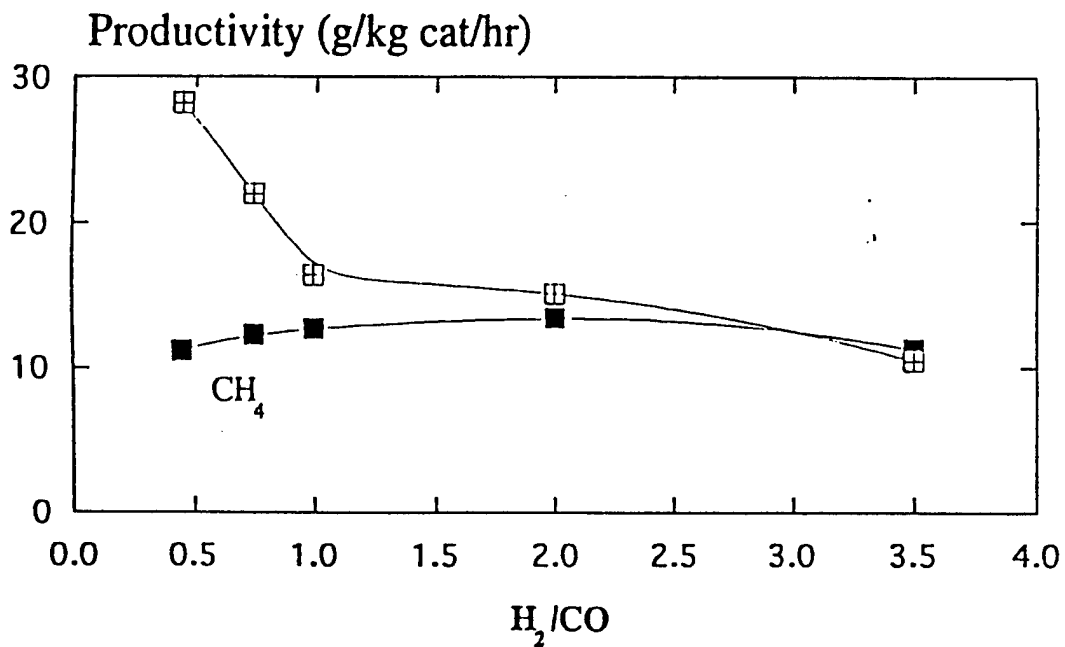
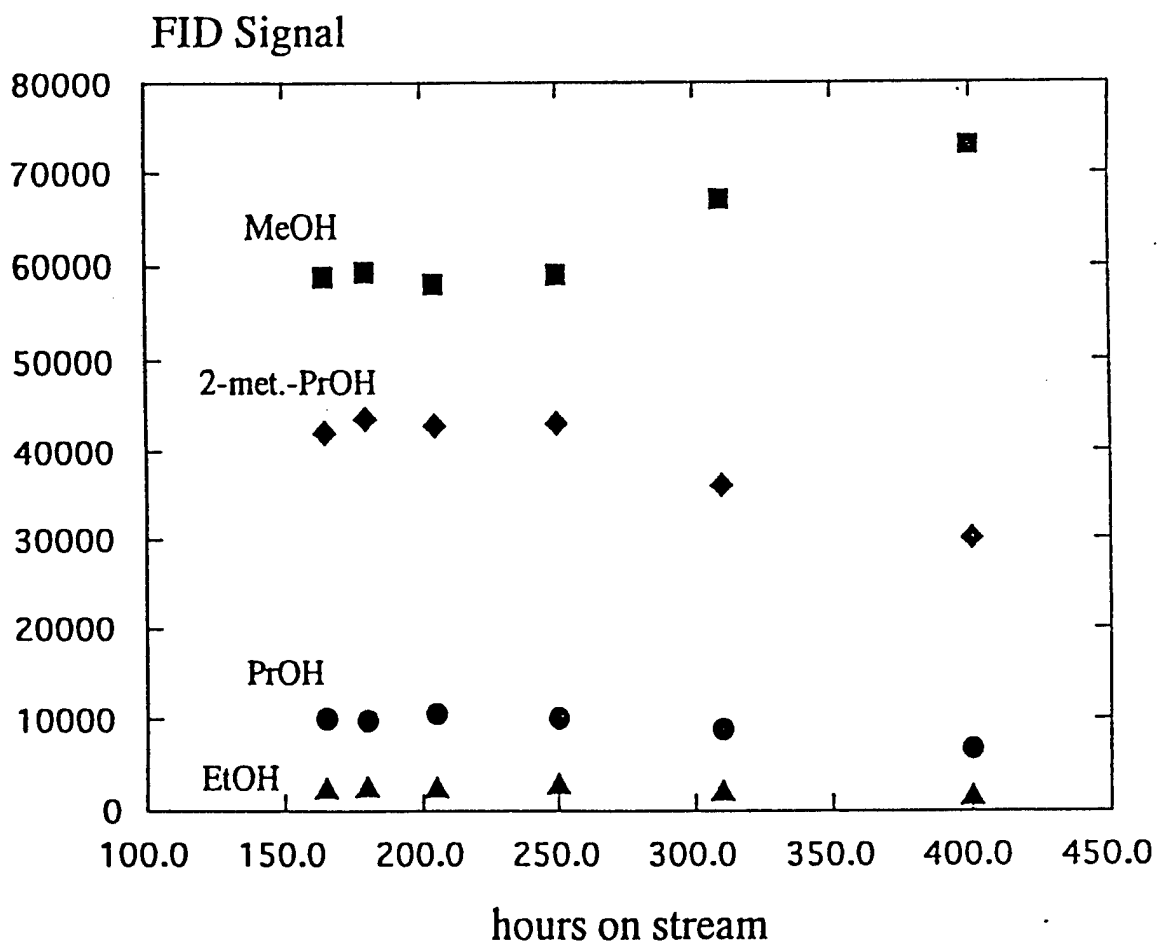


Figure 3.3.5 - Change of Product Distribution with Time as Detected by FID



Conclusions. The experimental results for the synthesis of higher alcohols over the Cs/Cu/ZnO/Cr<sub>2</sub>O<sub>3</sub> catalyst suggest that:

- (1) The productivity of  $\alpha$ -branched species benefits significantly from an increment of the reaction temperature to 325°C. For further increments of temperature, the productivities of higher alcohols are almost constant, but the methanol/higher alcohols molar ratio increases progressively.
- (2) At high temperature, the H<sub>2</sub>/CO feed ratio of 0.75 is optimal with respect to higher oxygenate formation. Under such conditions, an equal amount of methanol but *twice* the amount of branched higher alcohols can be obtained, compared to the optimal low temperature conditions (T = 310°C, H<sub>2</sub>/CO = 0.45).
- (3) No significant Cu sintering or surface area reduction occurred upon testing at the reaction temperature of 340°C; however, iron-carbonyl formation and deactivation of the catalysts under high temperature conditions need to be studied further.

## REFERENCES

1. Lietti, L., Sun, Q., Herman, R. G., and Klier, K., "Kinetic Evaluation of the Direct Synthesis of Ethers From Alcohols Over Sulfonated Resin Catalysts," to be presented at the *First World Conference on Environmental Catalysis* (Pisa, Italy) and to be published in *Catal. Today*, 8 pp (1995); accepted based on a 2-page abstract.
2. Klier, K., Herman, R. G., Lietti, L., Sun, Q., Johansson, M. A., and Feeley, O. C., Quarterly Technical Progress Report on "Oxygenates *via* Synthesis Gas" for January-March 1994.
3. Klier, K., Herman, R. G., Sun, Q., Johansson, M. A., Lietti, L., and Feeley, O. C., Quarterly Technical Progress Report on "Oxygenates *via* Synthesis Gas" for April-June 1994.
4. Sun, Q., Lietti, L., Herman, R. G., and Klier, K. "Mechanistic Studies of the Pathways Leading to Ethers *via* Coupling of Alcohols," *Preprint, Div. Fuel Chem., ACS*, 40 (1995); in press.
5. Nordberg, R., Albridge, R. G., Bergmark, T., Ericsson, U., Hedman, J., Nordling, C., Siegbahn, K., and Lindberg, B. J., *Arkiv för Kemi*, 28, 257 (1968).
6. Marsili, M. and Gasteiger, J., *Croat. Chem. Acta*, 53, 601 (1980).
7. Nunan, J. G., Himelfarb, P. B., Herman, R. G., Klier, K., Bogdan, C. E., and Simmons, G. W., *Inorg. Chem.*, 28, 3868 (1989).



8. Beretta, A., Sun, Q., Herman, R. G., and Klier, K., "Higher Alcohol Synthesis Over Cs-Doped Cu/Zn/Cr Oxide Catalysts: Effect of Reaction Temperature on the Product Distribution and Catalyst Stability," Preprint, Div. Fuel Chem., ACS, 40 (1995); in press.
9. Natta, G., Colombo, U., and Pasquon, in "*Catalysis*," Vol. 5, Chap. 3, ed. by P. H. Emmett, Reinhold (1957).
10. Smith, K. J. and Anderson, R. B., J. Catal., 85, 428 (1984).
11. Nunan, J. G., Herman, R. G., and Klier, K., J. Catal., 116, 222 (1989).
12. Herman, R. G., in "*New Trends in CO Activation*," ed. by L. Guzzi, Elsevier, Amsterdam, 265 (1991).
13. Boz, I., Sahibzada, M., and Metcalfe, I., Ind. Eng. Chem. Res., 33, 2021 (1994).
14. Nunan, J. G., Himelfarb, P. B., Herman, R. G., Klier, K., Bogdan, C. E., and Simmons, G. W., Inorg. Chem., 28, 3868 (1989).
15. Busetto, C., Del Piero, G., Manara, G., Trifiro, F., and Vaccari, A., J. Catal., 85, 260 (1984).
16. Nunan, J. G., Bogdan, C. E., Klier, K., Smith, K. J., Young, C.-W., and Herman, R. G., J. Catal., 116, 195 (1989).
17. Bogdan, C. E., Nunan, J. G., Santiesteban, J. G., Herman, R. G., and Klier, K., in "*Catalysis-1987*," ed. by J. W. Ward, Elsevier, Amsterdam, 745 (1988).
18. Hindermann, J. P., Hutchings, G. J., and Kiennemann, A., Catal. Rev.-Sci. Eng., 35, 1 (1993).

## II. 2QFY95 Objectives

Future plans for Task 3.3 will focus on the following area:

- 3.3 New and improved catalysts and processes for the synthesis of mixed higher alcohol and other oxygenates.

### 3.3.2 The Effect on Performance of Axial Temperature Gradients in the Packed Bed

#### 3.3.2.1 Motivation for Investigation

Thus far, all modifications to the preparation procedure for Falter's Li/Mn/Zn/Zr catalyst have resulted in approximately the same performance in syngas or syngas-plus-methanol conversion. Therefore, the possibility exists that catalyst preparation may not be the key issue in trying to reproduce Falter's results. Thus, differences in testing methods between Air Products and Falter's

original work have been considered to account for the discrepancy between the performance results obtained in this work and his.

One difference noted was that the design of Falter's packed bed reactor was quite different from the design of either packed bed Reactor #1 or Reactor #2. Falter's reactor, which was very long and narrow, resulted in a very large axial temperature gradient (temperature increased steeply with axial distance down the bed). By contrast, the design of Reactors #1 and #2 attempted to minimize axial gradients (i.e., approximate isothermality) by using a relatively short reactor bed located deep within a heated zone surrounded by an aluminum block to provide good thermal conductivity. The steep temperature gradient observed in Falter's work, caused by the exothermicity of the syngas reaction coupled with reactor geometry, may have impacted the measured performance of the Li/Mn/Zn/Zr-based catalyst in Falter's work.

One hypothesis is that the steep gradient could have provided a unique, but favorable, set of conditions for the production of isobutanol. In fact, the existence of a cool upstream reaction zone followed by a hotter downstream reaction zone is the concept that the current work is attempting to demonstrate in the two-stage isobutanol synthesis process (low temperature methanol synthesis followed by methanol conversion to isobutanol). To investigate the influence of axial temperature gradients in more detail, Reactor 3 was constructed to approximate Falter's original reactor design, in an attempt to create the same steep axial temperature gradient during reaction. It was deliberately designed long and narrow without an aluminum heating block to allow for axial temperature gradients.

### **3.3.2.2 Results Obtained Using Reactor #3**

Since the catalyst bed was much longer in this reactor than in Reactors #1 and #2, more catalyst was required to fill it (20 g vs. 5 g previously used); thus it was necessary to precipitate more Li/Mn/Zn/Zr catalyst. Since Pd impregnation was previously shown to have no impact on performance, the Li/Mn/Zn/Zr material, without impregnated Pd, was tested in this new reactor. This new sample of catalyst was prepared in the 3 liter precipitator without N<sub>2</sub> purge at pH=10, and was tested at the previously used conditions of 1500 psig and a GHSV of 10,000 std.lit./kg-hr of 50% H<sub>2</sub>/50% CO feed gas.

The measured axial temperature gradient during this run is compared with Falter's gradient in Figure 3.3.6. Clearly, the new reactor design was successful in establishing a steep temperature gradient comparable to Falter's, though Falter's is slightly steeper in the first half of the bed.

**Figure 3.3.6 - Packed-Bed Axial Temperature Gradients during Syngas Conversion**

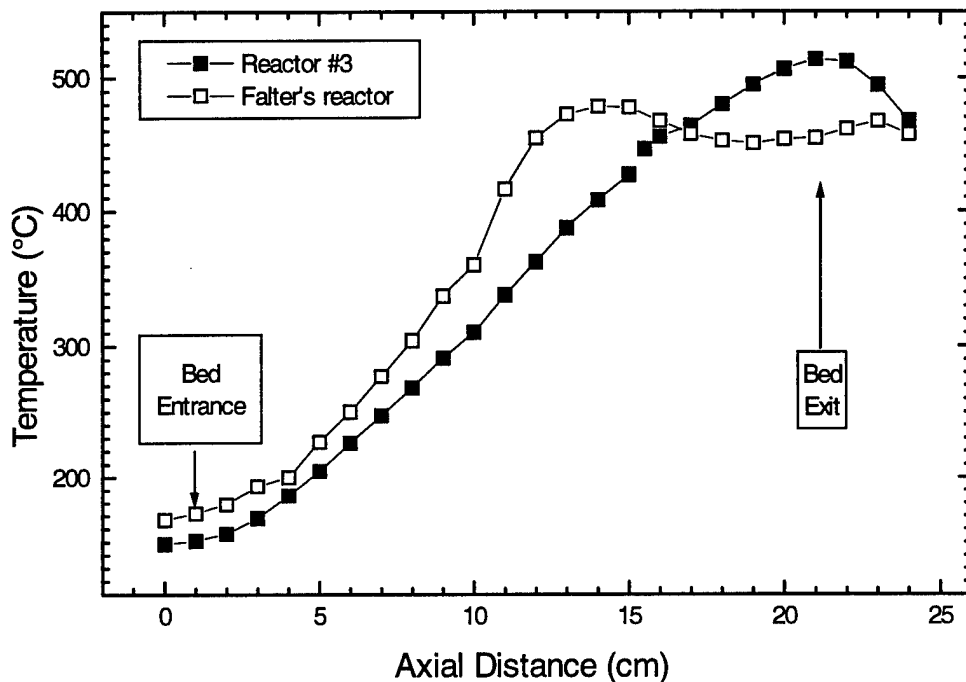
Catalyst: Li/Mn/Zn/Zr (#14183-18-1)

No Catalyst in Microclave

Run: 14047-25

1500 psig, 425°C, GHSV=10000 std.lit./kg-hr Syngas Comp.: 50%H<sub>2</sub>/50%CO

Packed Bed Reactor #3



Even though a steep axial temperature gradient was established in these tests, this resulted in a lower measured catalyst performance than that observed using the old reactor. Table 3.3.1 shows the performance results for syngas conversion and methanol-plus-syngas conversion for the Li/Mn/Zn/Zr catalyst, and syngas conversion for the Pd-impregnated version of this catalyst. Compared with the previously discussed results obtained using Reactors #1 and #2, the isobutanol production rate is much lower in Reactor #3, and lower than expected based on Falter's data.

Evidently, the existence of a steep axial temperature gradient in the reactor does not explain the high performance measured in Falter's original work. The reason that Falter's original performance cannot be reproduced is still not known. However, the current results indicate that it is the catalyst itself rather than the method of testing. Further investigation may reveal the reason.

**Table 3.3.1 - Effect of Imposed Axial Temperature Gradient on Performance**

Catalysts: Li/Mn/Zn/Zr (#14183-18-1) and Pd/Li/Mn/Zn/Zr (#14183-18-2)

No Catalyst in Microclave

Runs: 14047-25, -34 1500 psig, 425°C, GHSV=10000 std.lit./kg-hr,

Syngas Comp.: 50% $H_2$ /50%CO

Packed Bed Reactor #3

catalyst	reactor feed	Reactor Exit Rate (g/kg-hr)				
		methanol	ethanol	1-propanol	isobutanol	DME
Li/Mn/Zn/Zr	syngas	30.8	0.3	9.3	20.4	22.7
Li/Mn/Zn/Zr	syngas + 10 mole% methanol	36.5	0.3	8.8	22.0	132
Pd/Li/Mn/Zn/Zr	syngas	39.9	0.3	10.0	31.5	34.5

**3.3.2.3 Catalyst Analysis****Elemental Analysis and BET Surface Area of Catalysts used in Reactor #3**

Table 3.3.2 shows the results of elemental analysis and BET surface area determinations for unused samples of the catalysts used in packed bed Reactor #3. Also shown are results reported in Falter's thesis for his version of the catalyst. The catalysts used in the current work are significantly lower in Li content than Falter's version. However, results reported previously indicate that Li content had no impact on performance. For unknown reasons, the Zn content of these catalysts was much higher than that reported by Falter. The proportions of the starting materials for the catalysts were the same as Falter used in his preparation. Measured BET surface area for the Pd-impregnated version was comparable to that for Falter's catalyst.

**Table 3.3.2. Elemental Analysis and BET Surface Area of Li/Mn/Zr/Zn and Pd/Li/Mn/Zr/Zn Catalyst Used in Reactor #3**

Element	Analysis (wt%)		
	Li/Mn/Zn/Zr (#14183-18-1)	Pd/Li/Mn/Zn/Zr (#14183-18-2)	Falter's Pd/Li/Mn/Zn/Zr Catalyst
manganese (Mn)	13.8	14.3	15.4
zirconium (Zr)	35.3	36.0	30.5
zinc (Zn)	16.0	16.9	8.6
lithium (Li)	0.24	0.23	1.5
palladium (Pd)	---	0.22	Not reported
BET Surface Area (m <sup>2</sup> /g)	246	193	209

The elemental analysis and surface area measurements provide no significant clues as to why Falter's performance cannot be reproduced.

### Thermogravimetric Analysis (TGA) of Fresh and Used Catalysts

The effect of temperature on the structure and composition of the Li/Mn/Zn/Zr-based catalyst was investigated in light of the steep temperature gradients observed in Falter's work. To investigate possible thermally induced changes in the catalyst in more detail, fresh and used samples of a Li/Mn/Zn/Zr material (#14183-11-1) were examined by TGA. This catalyst was used in run 14047-4 (performance results were previously presented in Table 3.3.1). Nitrogen, air, and H<sub>2</sub> were used for both the fresh and used materials to compare the effect of inert, oxidizing, and reducing atmospheres, respectively. For these investigations, a new sample was loaded in the TGA for each run, i.e., the individual TGA samples were not reused.

Figures 3.3.7 and 3.3.8 show TGA results for the three gases for the fresh and spent Li/Mn/Zn/Zr samples, respectively. For the fresh catalyst, the weight loss curves for air and N<sub>2</sub> are very similar. There is an initial large weight loss before 100°C that is most likely due to H<sub>2</sub>O adsorbed from the atmosphere during handling. However, for H<sub>2</sub> on the fresh catalyst there are two distinct weight losses at higher temperatures: between approximately 300°C and 400°C and between 500°C and 800°C. The weight loss from 500°C to 800°C also occurs for H<sub>2</sub> TGA in the used sample (Figure 3.3.8), but the lower temperature loss (300°C to 400°C) is absent. Also evident in the TGA results for the used sample is a considerable weight gain in air between 300°C and 800°C.

The TGA results are interpreted as follows, considering that the fresh catalyst most likely consists of the metal oxides, Li<sub>2</sub>O, MnO, ZnO, and ZrO<sub>2</sub>. The 20% weight loss between 500°C and 800°C for H<sub>2</sub> TGA, which occurs for both fresh and spent samples, is likely due to the vaporization of metallic, elemental zinc, which had been previously produced by reduction of ZnO (ZnO is the most easily reduced oxide present). The magnitude of the weight loss is consistent with the total quantity of zinc in the catalyst (approximately 24 wt%). Moreover, the temperature range at which the weight loss occurs is consistent with the volatility of elemental zinc (Zn melts at 520°C, boils at 911°C, and has a significantly large vapor pressure between 500°C and 800°C). The vaporization of Zn has been confirmed by elemental analysis of the spent sample after the H<sub>2</sub> TGA, which showed no Zn present.

The cause of the lower temperature (300° to 400°C) weight loss for the fresh sample during H<sub>2</sub> TGA is not known, but probably represents reduction of some part of the catalyst. Since this weight loss does not occur in the used sample, the unknown reduction has probably already occurred during exposure of this sample to syngas at the 425°C reaction temperature. The weight gain during the air run on the used sample probably indicates a reoxidation of this reduced material. This weight loss probably does not correspond to reduction of ZnO to Zn, since Zn vaporization would be expected but does not occur in N<sub>2</sub> for the used sample. Further analysis is necessary to identify the cause of the 300-400°C weight loss in H<sub>2</sub> for the fresh sample.

The TGA results provide no clues as to why we have not been able to reproduce Falter's catalyst performance. The most dramatic, thermally-induced change in the catalyst is the apparent loss of Zn at temperatures greater than 500°C. Our reaction temperature (425°C in run 14047-4) and Falter's peak reactor temperature (approximately 475°C) are less than the temperature range at which reduction of ZnO and vaporization of Zn take place. Apparently, no major thermally-induced changes in the catalyst occur at temperatures near the reaction temperature range of interest (425°C-475°C); at least none that can be identified by TGA.

### 3.3.7 - TGA of Fresh Li/Mn/Zn/Zr Catalyst

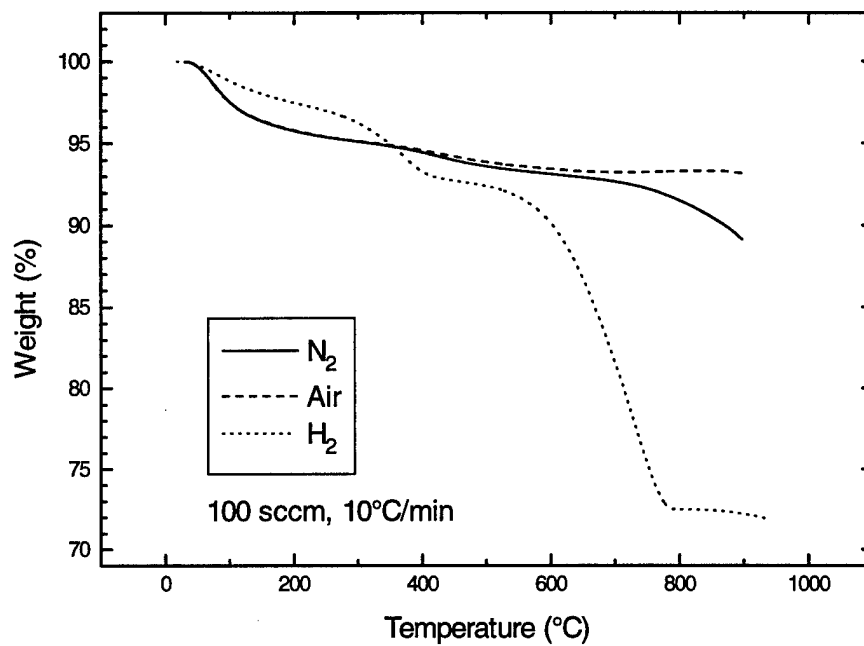
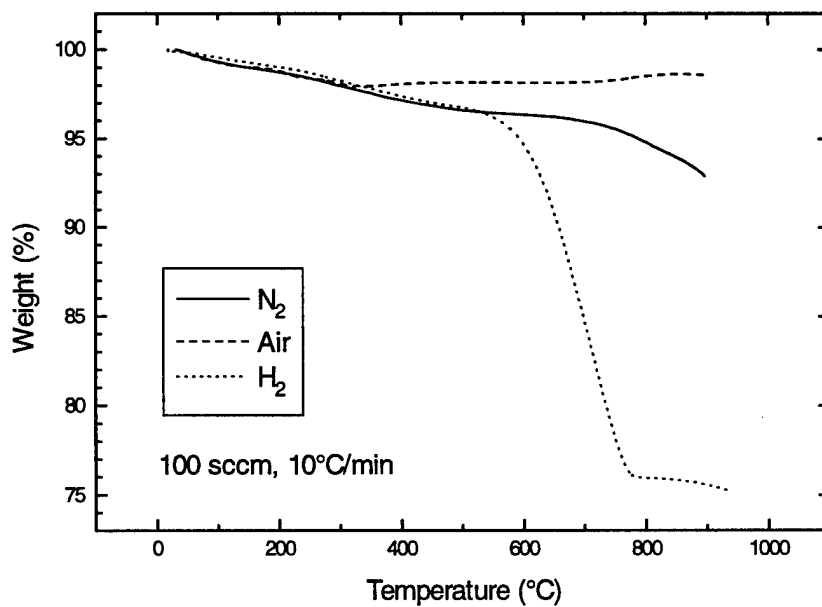


Figure 3.3.8 TGA of Li/Mn/Zn/Zr Used in Syngas Reaction



### 3.3.2.3 Effect of Precipitating with Potassium Hydroxide instead of Lithium Hydroxide

Thus far, the investigations indicate that the performance of the Li/Mn/Zn/Zr-based catalyst is fairly insensitive to preparation procedure, metal precursors, and whether or not Pd is present. To provide more information on the influence of preparation procedure, the effect of the alkali metal used in the preparation was investigated. To this end, the precipitation was done with KOH instead of the previously used LiOH. Falter had also prepared catalysts with both Li and K, and found Li to be the most effective at promoting isobutanol synthesis. This catalyst was prepared at pH=10 without N<sub>2</sub> purge.

Results for the performance of Pd/K/Mn/Zn/Zr for syngas conversion and syngas-plus-methanol conversion are shown in Table 3.3.3. Comparison with the previously reported results for the lithium-precipitated catalysts indicate that the Li-containing catalyst is slightly more effective at producing isobutanol than the K-containing catalyst for both types of feed. This trend is in agreement with the previous results of Falter. The K-containing catalyst is not effective at methanol-plus-syngas conversion to isobutanol either. In addition, the K-containing catalyst exhibited a higher rate and selectivity to hydrocarbons.

**Table 3.3.3 - Performance Results for Pd/K/Mn/Zn/Zr**

Catalyst: Pd/K/Mn/Zn/Zr (#14183-14-2)

No Catalyst in Microclave

Run: 14047-10

1500 psig, 425°C, Syngas Comp.: 50%H<sub>2</sub>/50%CO

Packed Bed Reactor #2 (Copper-Lined)

Feed Gas	Syngas GHSV (std.lit./ kg-hr)	Production Rate at Packed Bed Exit (g/kg-hr)*					
		Methanol	Ethanol	1-propanol	Isobutanol	C <sub>1</sub> -C <sub>6</sub> Hydro- carbons	DME
syngas	10000	113	0.3	8.3	45.0	47.2	4.9
syngas	15000	162	0.5	11.0	59.7	53.6	6.2
syngas + methanol*	15000	233	0.5	10.1	59.8	44.0	100

\*methanol feed concentration=14 mol% (addition rate=3400 g/kg-hr).

### 3.3.2.4 Summary of Status on Two Bed Work

The development of a two-stage process for the production of isobutanol remains a challenge. Though Falter's original work indicates that a Pd/Li/Mn/Zn/Zr catalyst would be very effective as the second-stage catalyst in this process, that effectiveness could not be reproduced in the present work.

Table 3.3.4 shows the extent to which the results are disparate. Falter's reaction conditions were not reproduced exactly in the present work, but the conditions are comparable. Shown in Table 3.3.4 are results from Falter's thesis compared with results obtained in the present work, for syngas conversion and syngas-plus-methanol conversion. For syngas conversion, isobutanol productivity observed in this work is about 50% of that seen by Falter. However, the larger

difference is in syngas-plus-methanol conversion, where Falter's isobutanol rate is 4.5 times that measured in this work under comparable reaction conditions.

The performance of the Li/Mn/Zn/Zr-based catalysts prepared in the present work, particularly with respect to syngas-plus-methanol conversion to isobutanol, is relatively insensitive to catalyst preparation variables such as the:

- (1) presence or absence of supported Pd
- (2) Li content
- (3) extent of mixing during precipitation
- (4) drying and pelletizing procedure
- (5) inclusion or exclusion of N<sub>2</sub> purging during precipitation.

In addition, the performance of the Li/Mn/Zn/Zr-based catalysts prepared in this work have been shown to be fairly insensitive to certain variable involved in testing the catalysts, such as the:

- (1) reactor material of construction
- (2) presence or absence of steep axial temperature gradients.

The reason why Falter's original work can not be reproduced is, at this time, a mystery. The problem is, most likely, the inability to reproduce the exact catalyst. Work at Aachen has reproduction of this catalyst as a primary goal. No further work will be done on the two bed process until the original preparation has been reproduced at Aachen. Solving this mystery will be especially difficult given the absence of a sample of Falter's original material and the scarcity of characterization work done on the sample. However, the remarkable ability of that material to catalyze syngas-plus-methanol conversion cannot be ignored if economical isobutanol production is to continue to be a development target.

**Table 3.3.4 - Comparison of Performance Results from This Work with Results Published by Falter**

Catalyst	Temp. (°C)	Press. (psig)	Feed Gas	Syngas GHSV (hr <sup>-1</sup> )	Production Rate (g/liter-hr)	
					methanol	isobutanol
Falter - Pd/Li/Mn/Zn/Zr*	427	1435	50% H <sub>2</sub> /50% CO	20,000	45	165
This work - Pd/Li/Mn/Zn/Zr**	425	1500	50% H <sub>2</sub> /50% CO	19,500	188	84
Falter - Pd/Li/Mn/Zn/Zr*	427	1435	43% H <sub>2</sub> /43% CO/14% methanol	15,000	85	450
This work - Pd/Li/Mn/Zn/Zr**	425	1500	43% H <sub>2</sub> /43% CO/14% methanol	19,500	323	101

\* W. Falter, PhD thesis, RWTH-Aachen, 1988, pp. 161.

\*\* This work, run 14047-7.



### **3.3.2.5 Isobutanol Synthesis in a Three Phase System**

#### **Engineering Aspects**

The activities within the last quarter of the year were testing catalysts and improving our analytical procedures. The unit is now equipped with two high-grade analysis systems. The best results found in catalytic runs showed a selectivity to isobutanol in the liquid product of more than 25% with a space-time yield over 300 g/(l\*h).

#### **1. Slurry Reactor**

The slurry reactor has nearly been finished. A reamer needed for machining the inner surface of the reactor was four weeks late. First tests with this continuous slurry reactor will be in February 1995.

#### **2. Fixed Bed Reactor**

To study the impact of temperature in more detail, the temperature indicating and controlling system at the fixed bed reactor was optimized. Initially the process variables to control the jacket heatings were obtained directly at the jacket heatings themselves according to Falter. The temperature profile was determined by a combination of external heating, the strongly exothermic reaction and the loss of heat. Under reaction conditions, the three thermocouples inside the fixed bed always indicated a higher temperature than the temperature at the jacket heatings.

These three thermocouples show that process temperature controls jacket heating. Thus, the temperature inside the fixed bed can be controlled exactly; temperature gradients must be produced artificially.

#### **3. On-Line Screening**

The unit has been equipped with a capillary system for the calibration gas. With this calibration gas a random failure was found. The on-line screening system consisting of bypass, sample injector, gas chromatograph and integrator was checked and optimized. Some experimental difficulties due to instrumental failure were found and fixed. Residual high boiling products remaining in the bypass capillary were found to vary the pressure drop along the bypass. To avoid the influence of this effect on the reliability of the analysis, the possibility of injecting the sample without pressure will be investigated in January.

#### **4. Product Sampler**

The product sampler as described in a previous progress report has been finished and is operating well. It was tested in several runs using a downstream trap cooled by dry ice or liquid nitrogen. The product sampler operates with a mass loss of 30% (depending slightly on the gas mass stream). The composition of probes collected in the product sampler and in the topped trap were identical, i.e., the product composition was not effected.

#### **5. Experiments**

Irrespective of the results shown at the beginning, the influence of variations in reaction conditions on isobutanol synthesis are discussed in below in terms of:

- The effect of a temperature gradient at the entrance zone of the fixed bed inside the reactor and
- Changes in reduction conditions and the use of glass particles for the fixed bed within this quarter.

As a result of changing temperature measurement, the axial temperature gradient must be produced artificially. Switching off heating jacket 2W1 decreases the temperature TIC 205 by about 90°C. The resulting temperature gradient is 1.5°C/mm. The effect of this gradient compared with a gradient-free run is non-uniform and depends on pressure, gas mass flow and to a lesser extent on the catalyst. The effect on the space-time yield of methane and methanol was found to depend on the residence time given by pressure and gas mass flow. A long residence time at the heated entrance zone filled only with glass particles led to an increased methane production. It was observed that the amount of formed methane in these cases was up to 2.5 times higher than in the case where the first heating jacket was switched off. In contrast methanol production showed the opposite behavior, having maximum productivities when the first heating jacket was switched off. However, the space-time yield i-BuOH remained nearly constant.

After reduction conditions were changed and glass particles were used for the fixed bed, catalyst BJ 17 was tested a second time and showed a different behavior. The selectivity to isobutanol decreased, and its space-time yield increased. The results of the older run CH 14 and the actual run CH 28 are listed in Table 3.3.5.

**Table 3.3.5 - Results from Catalyst Tests in a Fixed Bed Reactor**

<b>org. information</b>				
test No.:	CH 14:02	CH 14:03	CH 28:02	CH 28:03
cat. No.:	BJ 17			
<b>set point</b>				
GHSV [1/h]	20000			
pressure [bar]	236	236	250	250
temperature [°C]	375	400	445	415
volume flow [NI/h]	100	100	80	80
<b>results</b>				
% Methanol	18.52	9.72	31.95	62.18
% 2,4-Dimethylpentanon-3	0.98	1.05	1.37	0.66
% n-Propanol	1.22	0.96	0.80	0.60
% i-Butanol	49.16	46.60	27.36	16.28
% 2,4-Dimethylpentanol-3	2.11	1.41	0.69	0.35
% 2-Methylbutanol-1	6.01	5.19	3.33	1.53
% 2-Methylpentanol-1	2.62	3.60	2.60	1.01
space-time yield i-BuOH [g/(l*h)]	45	62	311	142

The catalyst is from the same batch. The differences in the reaction conditions are minor. Higher set temperatures in run CH 28 are the result of changing the indicating temperature and controlling system. In run CH 14 the set temperature was measured at the jacket heatings. The fixed bed temperature was about 20°C higher. In run CH 28 the set temperature was measured at the fixed bed.

In contrast to the explanation in his thesis, Falter reduced the catalysts both inside and outside the reactor in a special apparatus. The differences in both reduction methods are substantial. We have tested both methods. The reaction conditions of each run are listed below:

#### **Scheme 1: Reduction Conditions for Run CH 14**

gas:	hydrogen
mass flow:	60 NI/h
pressure:	ambient pressure
heating rate:	< 4 °C/min
temperature:	200°C
reduction time:	2h

---

#### **Scheme 2: Reduction Conditions for Run CH 28**

gas:	hydrogen
mass flow:	30 NI/h
pressure:	3 MPa
heating rate:	4 °C/min
temperature:	225°C
reduction time:	2h

---

The second significant modification is the use of glass particles in the fixed bed since the inner tube was changed. Glass particles were also used by Falter.

As a result of these experiments, another batch of catalyst BJ 17 will be prepared according to the formerly used procedure and tested in further runs. Both reduction methods will be used to obtain more information. The influence of the kind of glass and/or the structure of the fixed bed will be examined, and the set of twelve catalysts will be further tested.

### **Chemical Aspects**

This section will discuss the catalyst design strategy used to optimize the isobutanol catalyst.

#### ***1. Coprecipitated Zr/Zn/Mn-Catalysts***

The set of Falter catalysts described previously has been completed. A typical procedure for the synthesis of these catalysts is described below:

A solution of  $ZrO(NO_3)_2$ ,  $Zn(NO_3)_2$ ,  $Mn(NO_3)_2$  (0.17 mole each) in 1 liter of deionized water was simultaneously added with a 2 M aqueous solution of LiOH (or KOH) into a vessel

containing 1 liter of water. This procedure is done under vigorous stirring, at a temperature of 353 K and a constant pH (resp. 9, 10 or 1 liter). After the addition, which normally takes 90 min, the suspension is stirred for 12-14 h, filtered, suspended again in 1 liter of deionized water and stirred for 1 h. After this washing procedure the solid is filtered again and pelletized in teflon matrices (3 x 3 mm). Subsequently the pellets are dried at 400 K for 12 h. The pellets were calcined in a quartz tube using flowing air (heating rate 5°/min; 3 h constant at 600 K).

Impregnation with 0.25 wt% Pd(acac)<sub>2</sub> is performed in acetonitrile solution (30 ml) without stirring. After disappearance of the yellow color, the solution is decanted. After drying under flowing air at ambient temperature the pellets are calcined as described above.

This set of twelve catalysts includes Falter's best catalysts compared to other less active and less selective ones described in his thesis. Their behavior will enable us to compare the present isobutanol unit with the former one.

Analysis of these samples, using AAS, BET and XRD is in progress and will be presented when all data are available. As mentioned before, a laboratory spray dryer has been installed, and, in addition to pelletizing, some of the above described catalysts were spray dried for later use under slurry conditions.

## ***2. Semibatch (Discontinuous) Slurry Reactions***

In order to gain information about the catalysts in a shorter time, semibatch reactions are carried out. For this purpose more laboratory autoclaves are needed. Within the next week the institute workshop will finish new autoclaves that can withstand a pressure of 300 bars and temperatures up to 700 K. With this setup, catalysts can be screened for their selectivity towards oxygenated products, especially isobutanol and methanol.

## ***3. Objectives of Catalyst Design***

To optimize the catalysts it is important to obtain information regarding composition, surface, porous structure and crystalline or amorphous phases.

The good properties of the alkaline-promoted Zr/Zn/Mn-system have been shown. Falter found that the pH of the precipitation has a major impact on catalyst behavior. However, it was not clear in what way pH change influenced the catalyst. For that reason current research aims at investigating one specific variable, keeping the others constant.

The final alkaline content in the Falter catalyst after precipitation is determined by the washing procedure. The influence of this factor has been investigated by preparing a set of catalysts at constant pH, only varying the amount of washing water. Another approach to introduce an exact amount of alkaline metal would be the impregnation of an alkaline free catalyst. To meet with this objective we plan to synthesize alkaline-free Zr/Zn/Mn catalysts.

Precipitations are performed using complexing agents, e.g., mono- and bidentate ligands, containing oxygen or nitrogen. In fact, ammonia and hydroxyl can be regarded as the smallest ligand representatives. Therefore precipitations with aqueous ammonia solutions were investigated. Finding a pH-value at which Mn<sup>+2</sup> is nearly fully precipitated as the hydroxide,

without dissolving  $Zn(OH)_2$  as an ammonia-complex, has not yet been accomplished. Further reactions with other amine bases, for example, tetramethylammoniumhydroxide (TMAH), are planned.

As bidentate complexing agents, ammonium oxalate, aminoacids or hydroxyacids are well suited. With ammonium oxalate an almost quantitative precipitation was observed.

The generation of porosity by thermal decomposition reveals an additional effect of these complexing agents which can be controlled by steric modifications.

#### ***4. Inert Liquids***

In the continuing research for a suitable inert liquid for slurry operations, synthesizing a decalin analogue with a higher boiling point was attempted in order to improve the separation characteristics in the continuous three phase system. Starting from 2-methylnaphthalene, the fully saturated product, 2-methyldecalin could be obtained quantitatively by hydrogenation reaction with  $Pd/Al_2O_3(5\%)$  at 560 K and 200 bars. The product was characterized by MS. In stability tests with syngas at 620 K and 200 bars, this compound showed the same behavior as decalin.

#### **TASK 4: PROGRAM SUPPORT**

Much of the planned work in this task will be carried out Bechtel. A subcontract with Bechtel is currently being arranged and is expected to be in place by the end of the next quarter. Although Bechtel's principal responsibilities will lie in the area of syngas generation and cleanup, Air Products is currently negotiating to add a further, high priority item to its slate. A combination of reduced manpower at Air Products coupled with Bechtel's abilities in the area of process innovation and techno-economic evaluation is leading to their assuming prime responsibility for the work under Task 4.1, Research Support Studies. A FY95 deliverable in this section is the preparation of isobutanol synthesis catalyst performance requirements for coal-based, resid-based and natural gas-based coproduction routes to MTBE. The target in the Alternative Fuels I contract (1990-94) was 50 gms/hr of isobutanol per kg catalyst, this in turn leading ultimately to a MTBE price of \$1.20/gal. With a revised target of MTBE @ \$.70/gal for 1995-2000, the new performance requirements need calculating as guidance for the university programs at Aachen, Delaware, and Lehigh.

#### **TASK 5: PROGRAM MANAGEMENT**

##### **5.1 Reports and Presentations**

A draft topical report entitled "Catalytic Dehydration of Isobutanol in a Slurry-Phase Reactor" was sent to DOE for review. This report described the LaPorte 8/93 results of dehydrating a feed of mixed alcohols, predominately isobutanol, to isobutylene, the necessary precursor to MTBE.

Monthly technical progress reports for October, November, and December were prepared and submitted to DOE.

The results of the second Fischer-Tropsch campaign at LaPorte were summarized and submitted in abstract form for presentation at the 14th North American Meeting of the Catalysis Society. The paper, entitled "Productivity Improvements for Fischer-Tropsch Synthesis," will be co-authored by DOE, Shell and Air Products personnel.

## 5.2 Management Activities

- Preaward work started in October at Air Products on the new cooperative program with DOE entitled "Alternative Fuels and Chemicals from Synthesis Gas." The Cooperative Agreement is not expected to be in place until December, however, DOE has formally notified us of their willingness to allow cost reimbursement back to October 3. The universities of Lehigh, Aachen, and Delaware will roll their work over from the Alternative Fuels I contract although their official subcontracts will not be in place until early spring. Eastman and Bechtel's subcontracts will also probably not start until then.

At the end of December, DOE approved the Cooperative Agreement. The program will be funded in full for FY95, \$8.8 million in total.

- A confidentiality agreement was signed between Air Products and Syncrude Technology (STI). Technical discussions were held through December between Air Products, STI, and DOE-PETC personnel for a proposed F-T run at LaPorte. The objective of the run would be to evaluate performance of catalyst-reactor system to confirm the design basis. A preliminary process flow diagram has been developed based on STI's desired operational envelope. Four line specifications were generated for new equipment required at LaPorte. Equipment and materials cost for the modifications was estimated at \$425,000. The total cost of the run is expected to be \$2,028,000.
- Bogdan Slomka from Iowa State University visited LaPorte in early November. He has been working on sonic-assisted cross-flow filtration. For removal of solids from coal liquefaction products, they have demonstrated a 2.7 fold increase in filtrate flux with sonic treatment. They plan to evaluate the F-T spent slurry from LaPorte (F-T I) next.
- A visit to Institut Francais du Petrole (IFP) revealed that they have stopped work on their (linear) higher alcohols process because of the unfavorable economics relative to MTBE production. They have switched their syngas work over to Fischer-Tropsch chemistry.
- An abstract was submitted for a presentation of the F-T II results at the 14th North American Meeting of the Catalysis Society. The paper entitled "Productivity Improvements for Fischer-Tropsch Synthesis" will be co-authored by Shell and DOE personnel.

# Quarterly Progress Report III: Preparation, Examination and Characterization of the Factorially Designed Catalyst Matrix

Center for Catalytic Science and Technology  
University of Delaware

Dr. Henry C. Foley  
Director and Associate Professor

April 12, 1995

For the Period October–December 1994

**Summary:** Factorially designed catalysts are prepared for the evaluation of the effects of variation in the primary oxide components on the activity and selectivity of higher alcohol synthesis catalysts. Namely, a two level, three factor full factorial design was performed on the ratios of MnO/CuO, ZrO<sub>2</sub>/CuO, and ZnO/CuO, which resulted in an eight sample catalyst matrix. All these catalysts were examined between 300–425°C and at 1000 psi of total reaction pressure. The XRD patterns of the catalysts before and after use were collected to characterize their solid state structures. Gas components and liquid products were analyzed by on- and off-line GCs to derive conversion and selectivity data. Experimental results showed that each of the factors indeed had significant influence on the higher alcohol synthesis performance of the catalysts, which in turn provided important information for optimizing the catalyst composition toward better isobutanol productivity. Basically, chemometric treatment of the reaction data indicated that increasing the ZrO<sub>2</sub>/CuO ratio and decreasing the MnO/CuO ratio significantly enhanced the isobutanol selectivity and suppressed the n-propanol production. The XRD patterns of the used catalysts show the presence of crystalline metallic copper, ZrO<sub>2</sub>, ZnO, and MnO with different relative intensities depending on their contents. In contrast the fresh samples before reduction and reaction display low crystallinity and more amorphous-like diffraction patterns.

## Introduction

In this quarter, our reaction testing and characterization mainly focused on the factorially designed catalysts for evaluation of the individual components of the previously examined catalysts. The basic idea is to systematically change the metal oxide compositions to explore the effects of them on the higher alcohol synthesis selectivity and activity with specific interest on isobutanol production from CO hydrogenation. With the help of the chemometric evaluation of the reaction data, we were able to determine the major effects of the oxide components on higher alcohol synthesis. X-ray diffraction was carried out to characterize the bulk structural changes of the catalysts. The performance of the catalysts in a stainless-steel reactor and copper-lined reactor also were compared.

## Experimental

The catalyst design and preparation are as follow: according to the literature and our previous results, CuO, MnO, ZnO and ZrO<sub>2</sub> are most essential components of the higher alcohol synthesis catalysts, especially for isobutanol synthesis, therefore, we chose the MnO/CuO, ZnO/CuO, and ZrO<sub>2</sub>/CuO ratios as our main factors and we changed their ratios from high to low levels. This results in a three factor, two level full factorial sample matrix. The catalyst preparation procedure was reverse precipitation, i.e., the catalysts were prepared by dropping corresponding amounts of metal nitrate solution into the K<sub>2</sub>CO<sub>3</sub> basic solution until a neutral pH was reached. The precipitates were then washed with deionized water, dried at 130°C (overnight), calcined at 400°C (2h in air), pelletized and sieved. Each sample also included a fixed amount of CoO. The calcined catalysts were doped with 4wt% of K<sub>2</sub>CO<sub>3</sub>. The coding and basic compositions of the catalysts are listed in the Tables 1 and 2.

After finishing the catalyst preparations of the factorially designed sample matrix, we carried out the reaction testing of the catalysts at T=300-425°C, P=1000psig, CO/H<sub>2</sub>=1, and at a GHSV=2800/h.



## Results and Discussions

### *Chemometric Evaluation of the Catalysts*

Generally, this set of catalysts shows significantly different performance than the last set of six catalysts reported in the previous two quarterly reports. This difference arises from the significant changes that we have made in component levels.

Examination of the reaction data collected from the factorially designed sample matrix has been carried out by the chemometric regression method. The compositions and alcohol productivities of the factorially designed catalysts are listed in the Tables 2 and 3. Clearly, n-propanol is the major higher alcohol product on the most of the catalysts, which is also shown in the detailed selectivity data listed in the Table 4. However, by changing the oxide compositions, n-propanol was successfully suppressed and the isobutanol selectivity was significantly enhanced on F5K and F6K, where we employed a high ZrO<sub>2</sub>/CuO ratio and a low MnO/CuO ratio. The effects of the MO<sub>x</sub> to CuO ratios on the alcohol productivities become even evident when we applied the multiple linear regression analysis to the experimental data to evaluate the effect of each factor on the isobutanol productivity quantitatively:

$$y = b_0 + b_1x_1 + b_2x_2 + b_3x_3 + b_4x_1x_2 + b_5x_1x_3 + b_6x_2x_3 + b_7x_1x_2x_3$$

Here  $y$  is the isobutanol productivity;  $x_1$ ,  $x_2$ ,  $x_3$  are the MnO/CuO, ZrO<sub>2</sub>/CuO, and ZnO/CuO factors and the  $b$ 's are regression coefficients. The coefficients obtained from regression analysis are listed in the Table 5.

Clearly, the first order terms represent the main contributions to isobutanol productivity. Not surprisingly, the MnO/CuO and ZrO<sub>2</sub>/CuO ratios turn out to be the most significant. Their signs indicate that a decrease in the MnO/CuO and an increase in the ZrO<sub>2</sub>/CuO ratios would improve the productivity of isobutanol. The second order terms reflect the interactions between the factors. Therefore, decreasing the interaction between MnO and ZrO<sub>2</sub> by decreasing the MnO/CuO ratio also would be helpful for isobutanol production. Similarly, we performed the regression analysis

on the isobutanol selectivity and n-propanol selectivity. The results of the evaluation are listed in the last two rows of the Table 5.

Therefore, an increase in the  $ZrO_2/CuO$  ratio, and a decrease in the  $MnO/CuO$  ratio, both first order terms, would be beneficial for enhancing isobutanol selectivity and suppressing n-propanol selectivity. This is crucial since as we have pointed out in our previous reports, these catalysts as originally composed did produce high levels of n-propanol indicating that the slow step between  $C_1$  and  $C_2$  alcohols was effectively catalyzed. Hence, it seemed logical to explore a means to shifting the selectivity more favorably towards isobutanol. These results constitute the first indications of how this may be achieved. The second order terms are showing similar effects on the isobutanol selectivity as discussed above. However, second order interactions are relatively more complex, especially for n-propanol selectivity. They may have a major effect on the product selectivity in the limiting cases of the first order terms. Therefore, we can optimize the product selectivity by adjusting the component ratios as defined by the factorial design, which helps us to minimize the catalyst screening process and to get to a more fundamental evaluation of the catalysts. But this small factorial design is by no means complete. For a complete evaluation of the catalysts, we would need to examine more factors on such a systematic basis.

#### *Performances of the Catalysts*

The performances of the catalysts discussed in this report are summarized in the Table 6. Generally, CO and  $H_2$  conversions are low (less than 10%) when temperature is lower than  $350^\circ C$ , but the conversions are drastically increased at  $425^\circ C$ . At a temperature higher than  $350^\circ C$ , the  $CO_2$  selectivity could be as high as 50%, which is apparently due to fast water gas reaction at high temperature. The  $CO_2$  formation could be beneficial in that the reaction would remove the water produced by the FT reaction and higher alcohol synthesis reaction. However, the contribution from FT reaction to the production of water and hydrocarbon is not very significant, which can be inferred from the hydrocarbon selectivity data listed in the Table 6. The hydrocarbon selectivity is generally less than 15% even at temperatures as high as  $425^\circ C$ .

Most of the catalysts discussed here are tested at three different temperature levels and over a period of 20 hours at each temperature, therefore, total reaction time on stream for the catalysts is over 60 hours. During this period, the catalysts showed fairly stable CO and H<sub>2</sub> conversions, CO<sub>2</sub> and hydrocarbon selectivities (see the plots of catalytic performance versus reaction-time-on-stream in Figures 1 to 9.)

#### *Stainless Steel Reactor versus Copper Lined Reactor*

In order to examine the possible influence of stainless steel reactor materials on the hydrocarbon productivity during the synthesis reaction, we have tested a copper-lined reactor. The experimental results do not show any significant difference between the two types of reactors with regard to total CO conversion, oxygenate selectivity, or hydrocarbon selectivity (see F6K and F6K/Cu in Tables 4 and 6, and Figures 6 and 7.) This result is reassuring since our previously reported data were taken in an unlined stainless steel reactor tube, and the similar performance of the two types of reactor now rules out the possible catalytic contribution of the reactor materials. Nonetheless, we will use the copper lined-reactor to run all reactions from this point forward to avoid the possible background reactions from the stainless steel reactor.

#### *X-ray Powder Diffraction Characterization of the Catalysts*

All of the catalysts, 8 fresh samples prior to the reduction and reaction, and the 8 corresponding samples after reduction and use in the actual catalytic reaction, have been subject to XRD measurement in the range of 2 Theta from 10 to 90 degree at 30mA and 40KV. The approximate compositions of the samples are listed in the Table 2. All of the fresh catalyst samples show low crystallinity and more amorphous-like XRD features. But after reduction and use in the higher alcohol synthesis reaction, the samples show sharp XRD lines. This provides an indication of the phase transformations that occur during reduction and the course of reaction.

Not copper oxide but metallic copper is observed on the XRD patterns of the used catalysts. The relative intensities of the XRD lines correspond well to the original content of the materials.

No other metal phase is detected by XRD on the used samples. The metal oxide phases that can be seen on the used catalysts include MnO, ZrO<sub>2</sub> and ZnO. Among these, MnO's XRD lines are always relatively weak—even at loadings of 43 wt%. ZnO's XRD lines are relatively strong and sharp; ZrO<sub>2</sub> shows strong XRD lines at high loading but they are always somewhat broadened. The XRD patterns of the catalysts before and after reactions are shown in the Figures 10 to 17.

For the catalysts with high ZrO<sub>2</sub>/CuO and low MnO/CuO ratios, F5K and F6K, which have shown enhanced isobutanol selectivity, the XRD patterns show very weak to unobservable MnO lines but relatively strong ZrO<sub>2</sub> diffraction lines (see Figures 14 and 15.) There are other minor XRD lines in the XRD patterns of the used catalysts that have not been identified, but which might be due to spinel formation during the catalytic reaction.

### **Future work**

From these experimental results using the chemometric design we have gotten important information with regard to the critical compositional factors that can lead to optimizing these catalysts for isobutanol production. Exploring the effects of the other components and factors of the catalysts and reactions, specifically, the alkali metal oxides (such as Li, K, Cs), the minor transition metal components (such as Co, Rh, Ir, Pd), different preparative procedures (such as precipitation pH, temperatures), and calcination conditions (such as air versus N<sub>2</sub> calcination) will be important aspects of the future work of this project.

Table 1. Sample matrix

$\bar{M}O_n/CuO$ ratio	F1K	F2K	F3K	F4K	F5K	F6K	F7K	F8K
MnO/CuO	+1	+1	+1	+1	-1	-1	-1	-1
ZrO <sub>2</sub> /CuO	+1	+1	-1	-1	+1	+1	-1	-1
ZnO/CuO	+1	-1	-1	+1	+1	-1	+1	-1

Note: All the catalysts are composed of MnO, ZrO<sub>2</sub>, ZnO, CuO in addition to the constant amounts of Co and K<sub>2</sub>CO<sub>3</sub>, "+1" and "-1" represent the  $\bar{M}O_n/CuO$  ratio of 2 and 0.5, respectively.

Table 2. Approximate compositions (wt%) of the factorially designed catalysts(calculation)

	F1K	F2K	F3K	F4K	F5K	F6K	F7K	F8K
MnO	22.5	27.9	43.8	31.8	6.8	8.8	10.4	16.3
ZrO <sub>2</sub>	39.1	48.4	19.0	13.8	47.0	61.3	18.1	28.3
ZnO	25.8	8.0	12.6	36.5	31.1	10.1	48.0	18.7
CuO	12.6	15.7	24.6	17.9	15.2	19.8	23.4	36.6

Table 3. Alcohol productivity of the catalysts (425°C, 1000psi, CO/H<sub>2</sub>=1) (mg/g/h)

Catalysts	MeOH	EtOH	iPrOH	nPrOH	2BuOH	iBuOH	nBuOH
F1K	9.96	4.55	9.23	32.0	5.04	8.49	2.71
F2K	9.14	6.20	6.41	19.0	3.47	6.09	1.68
F3K	4.34	7.68	6.77	20.8	3.64	4.75	3.23
F4K	10.7	8.49	9.54	20.0	6.56	4.92	1.49
F5K	15.7	3.87	5.42	13.8	5.81	13.7	2.32
F6K	9.68	2.44	5.17	13.2	3.85	16.2	1.32
F7K	1.38	2.94	8.83	11.6	11.0	6.44	2.76
F8K	2.55	1.85	10.8	16.4	15.1	7.13	3.96

Table 4. Analysis of Liquid Products

<i>Cut</i>	<i>MeOH</i>	<i>EtOH</i>	<i>iPrOH</i>	<i>nPrOH</i>	<i>2BuOH</i>	<i>iBuOH</i>	<i>nBuOH</i>	<i>Other</i>	<i>yield</i> (g/g/h)
F1K	8.3%	4.1%	8.3%	28.7%	4.6%	7.5%	2.4%	36.1%	1.23E-01
F2K	9.0%	6.5%	6.8%	20.0%	3.7%	6.3%	1.7%	46.0%	1.05E-01
F3K	4.5%	8.3%	7.4%	22.7%	4.0%	5.1%	3.4%	44.5%	1.01E-01
F4K	7.5%	6.3%	7.0%	14.8%	5.0%	3.6%	1.1%	54.8%	1.49E-01
F5K	12.5%	3.3%	4.7%	11.8%	5.1%	11.5%	1.9%	49.2%	1.29E-01
F6K	10.6%	2.9%	6.0%	15.4%	4.6%	18.7%	1.5%	40.2%	9.40E-02
F6K/cu	11.5%	4.1%	4.4%	16.0%	3.4%	15.1%	1.5%	44.0%	8.80E-02
F7K/cu	7.5%	8.3%	9.5%	30.6%	4.4%	8.8%	3.0%	28.0%	1.02E-01
F8K/cu	10.0%	8.5%	7.5%	28.9%	5.4%	12.2%	6.3%	21.2%	8.00E-02

Note: Reaction conditions: 425°C, 1000psi, CO/H<sub>2</sub>=1.

F6K/cu indicates F6K in copper lined reactor.

Table 5. Coefficients obtained from the multiple linear regression analysis

	<i>b</i> <sub>0</sub>	<i>b</i> <sub>1</sub>	<i>b</i> <sub>2</sub>	<i>b</i> <sub>3</sub>	<i>b</i> <sub>4</sub>	<i>b</i> <sub>5</sub>	<i>b</i> <sub>6</sub>	<i>b</i> <sub>7</sub>
i-BuOH product.	8.48	-2.42	2.67	-0.07	-1.44	0.71	0.06	0.49
iBuOH selec.	7.8	-2.8	2.2	-1.0	-1.0	0.93	-0.38	1.0
nPrOH selec.	16.8	2.8	0.45	-1.1	2.1	1.3	2.2	1.6

Table 6. Performance of the Factorially Designed Catalysts

Catalysts	T °C	CO Conv.	H <sub>2</sub> -Conv.	Yield (g/g.h)	Selectivity		C <sub>2</sub> OH+ in liquid
					CO <sub>2</sub>	HC	
F1K	300	3.1%	2.9%	0.004	5.7%	0.7%	2.1%
	350	4.7%	4.3%	0.030	35.0%	6.4%	12.9%
	425	32.8%	23.7%	0.120	40.2%	10.7%	55.6%
F2K	300	1.7%	1.1%	/	11.6%	1.7%	
	350	5.4%	3.2%	0.012	29.7%	7.5%	20.7%
	425	31.5%	22.4%	0.110	31.2%	10.0%	45.0%
F3K	300	2.5%	0.3%	/	9.0%	1.7%	
	350	7.2%	3.7%	0.008	20.2%	5.8%	22.3%
	425	39.7%	29.0%	0.096	38.4%	17.1%	51.1%
F4K	300	3.6%	3.7%	0.012	6.1%	1.0%	4.0%
	350	6.4%	6.0%	0.025	30.1%	7.7%	14.3%
	425	42.9%	32.1%	0.160	42.1%	16.5%	37.8%
F5K	300	3.8%	3.3%	0.002	6.2%	0.8%	
	350	5.9%	4.8%	0.022	27.3%	5.5%	
	425	37.9%	25.8%	0.129	39.1%	9.9%	38.2%
F6K	300	3.8%	2.4%	/	0.0%	1.5%	
	350	4.8%	3.8%	0.015	0.0%	7.7%	
	425	32.4%	22.8%	0.094	32.1%	11.9%	49.2%
F6K/cu	350	4.0%	3.6%		0.0%	8.0%	
	425	28.0%	17.0%	0.088	33.4%	12.3%	44.6%
F7K/cu	350	7.0%	2.4%	0.017	0.0%	6.9%	
	425	25.5%	16.7%	0.102	23.1%	14.8%	64.5%

Figure 1. Reaction on F1K (425°C, 1000psi, CO/H2=1)

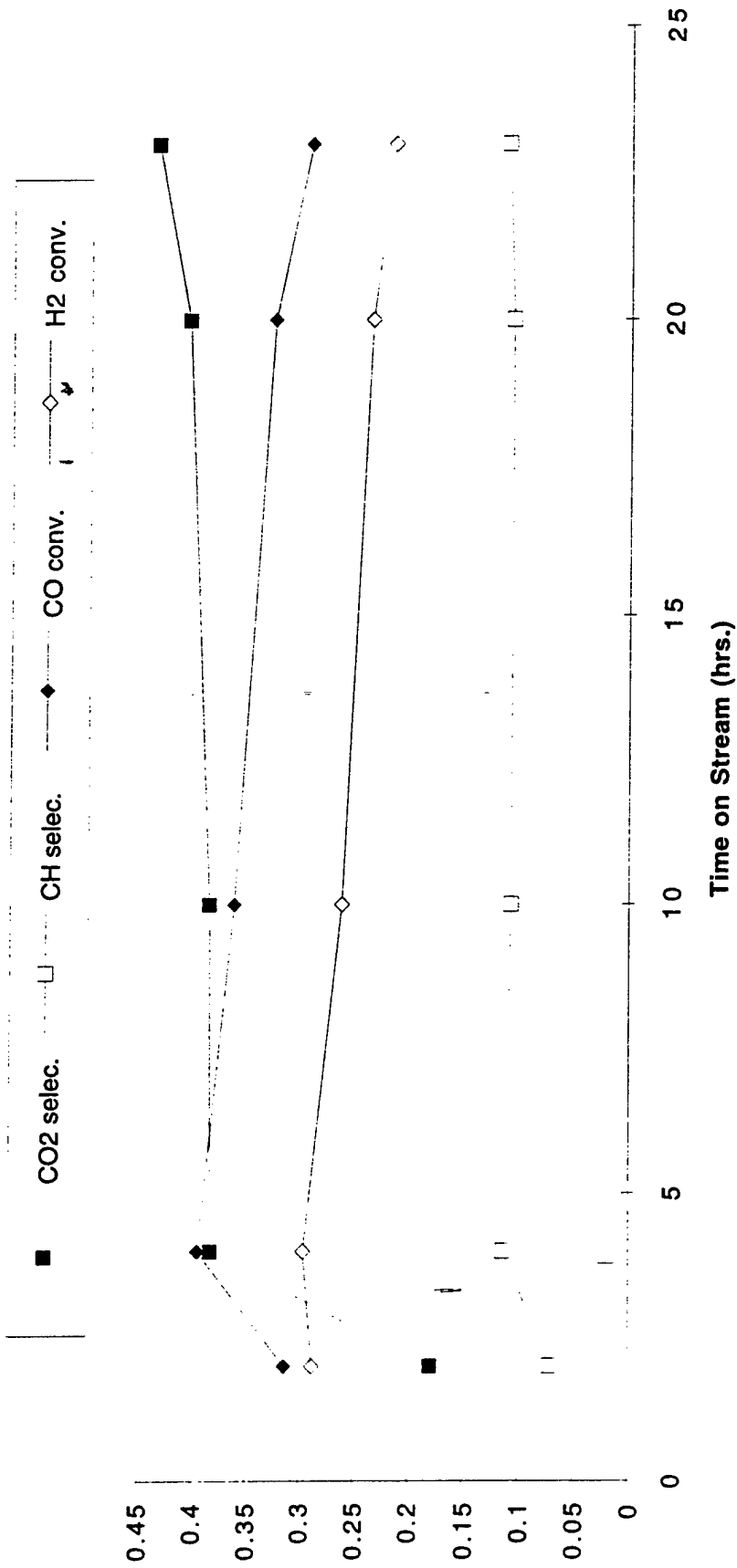




Figure 2. Reaction on F2K (425°C, 1000psi, CO/H<sub>2</sub>=1)

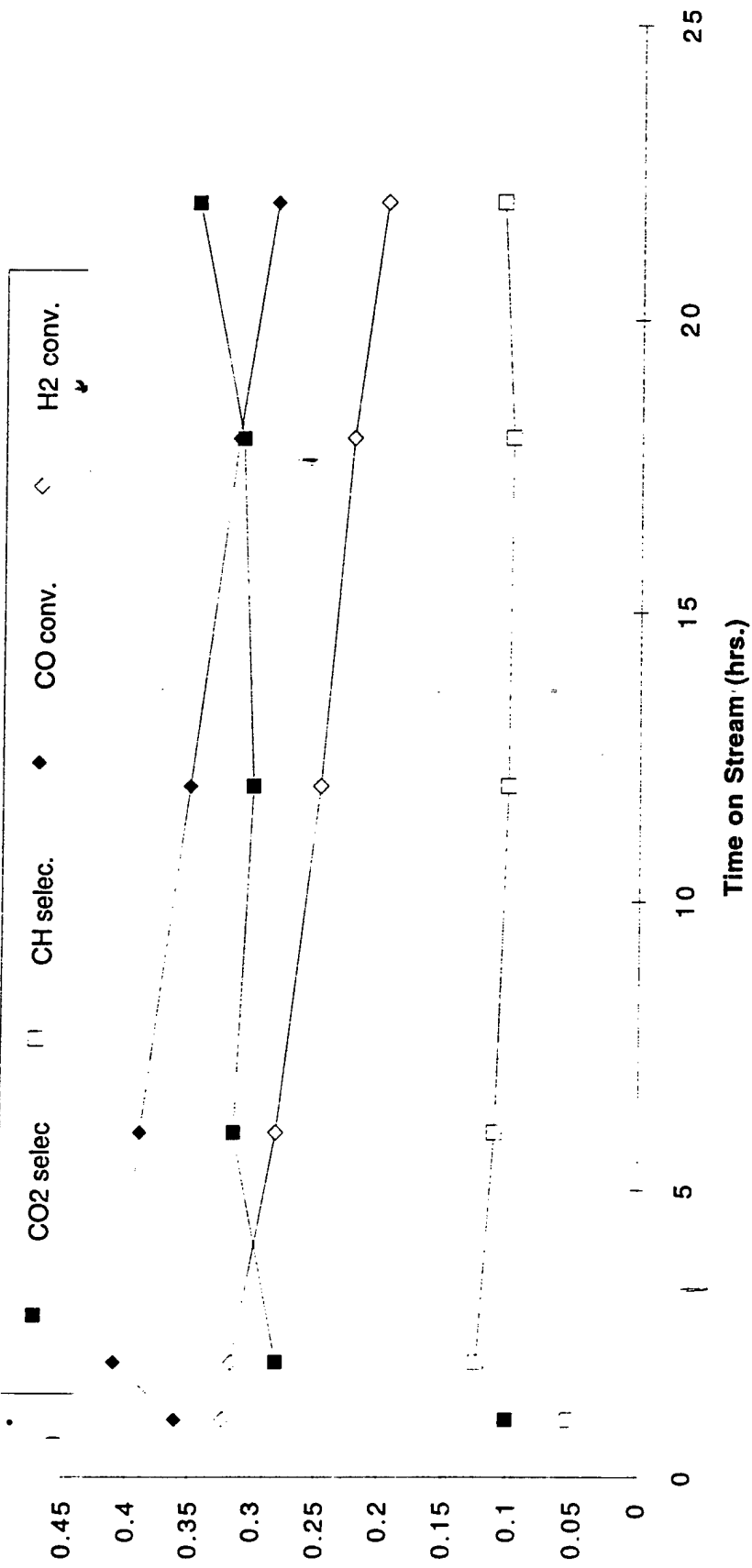


Figure 3. Reaction on F3K (425°C, 1000psi, CO/H<sub>2</sub>=1)

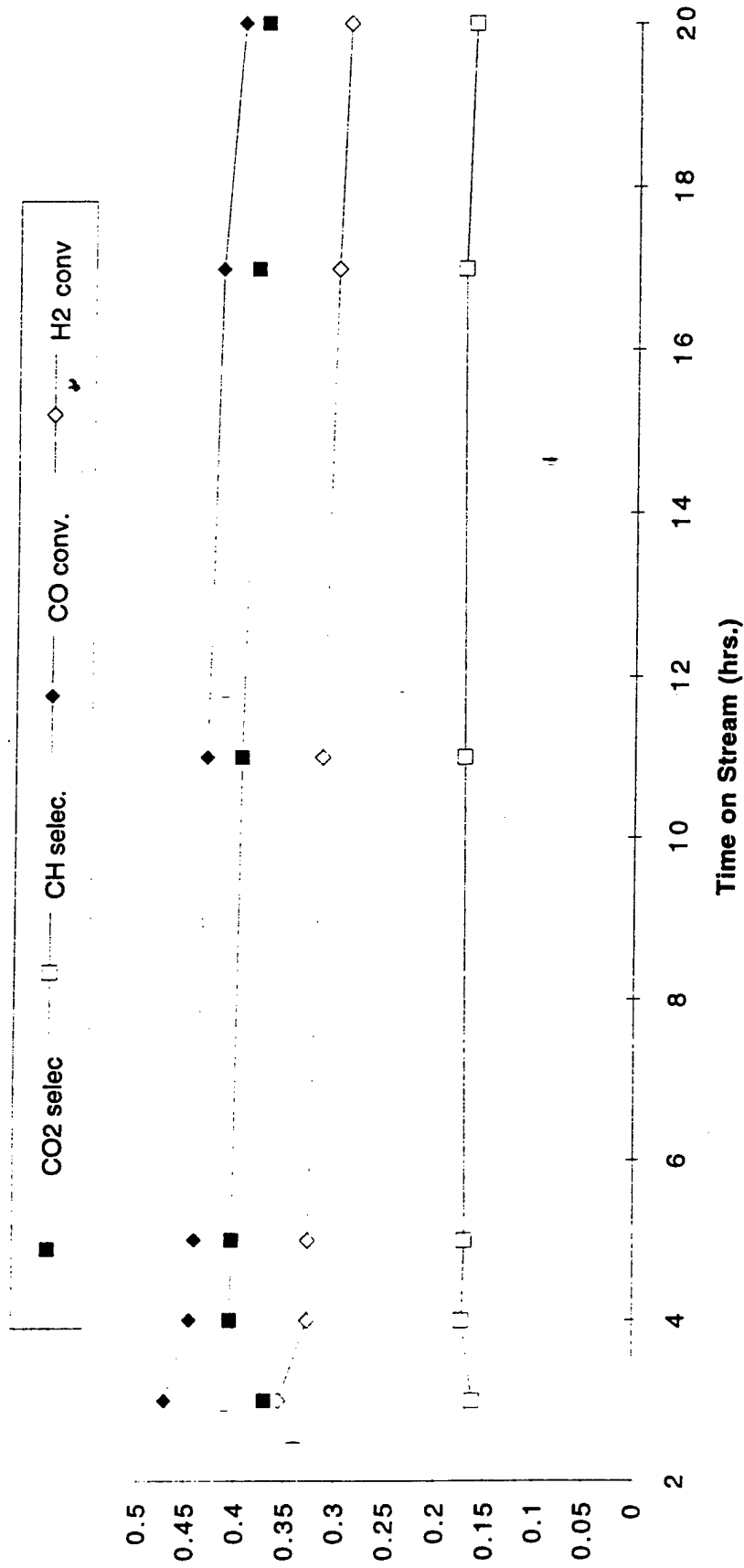


Figure 4. Reaction on F4K (425°C, 1000psi, CO/H<sub>2</sub>=1)

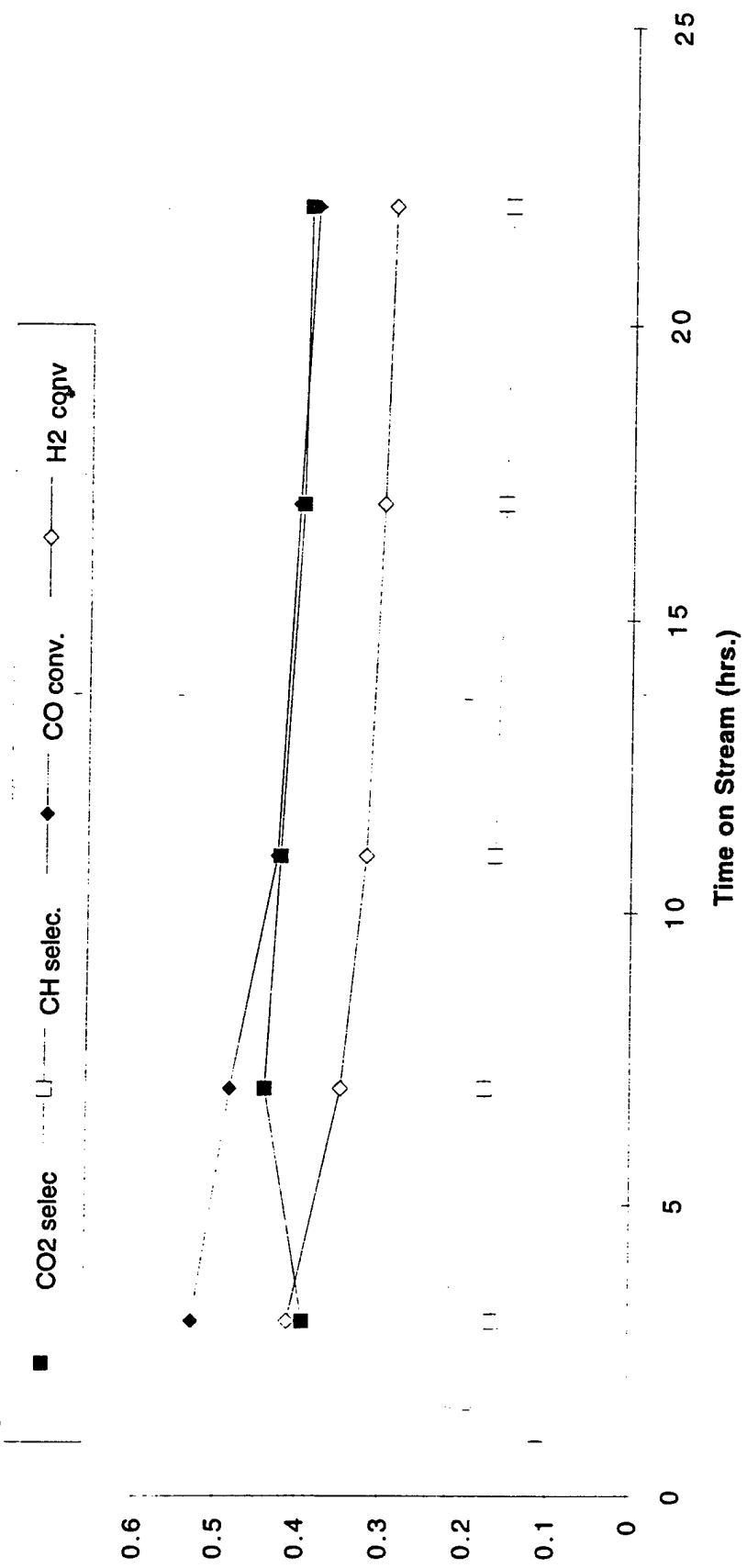


Figure 5. Reaction on F5K (425°C, 1000psi, CO/H2=1)

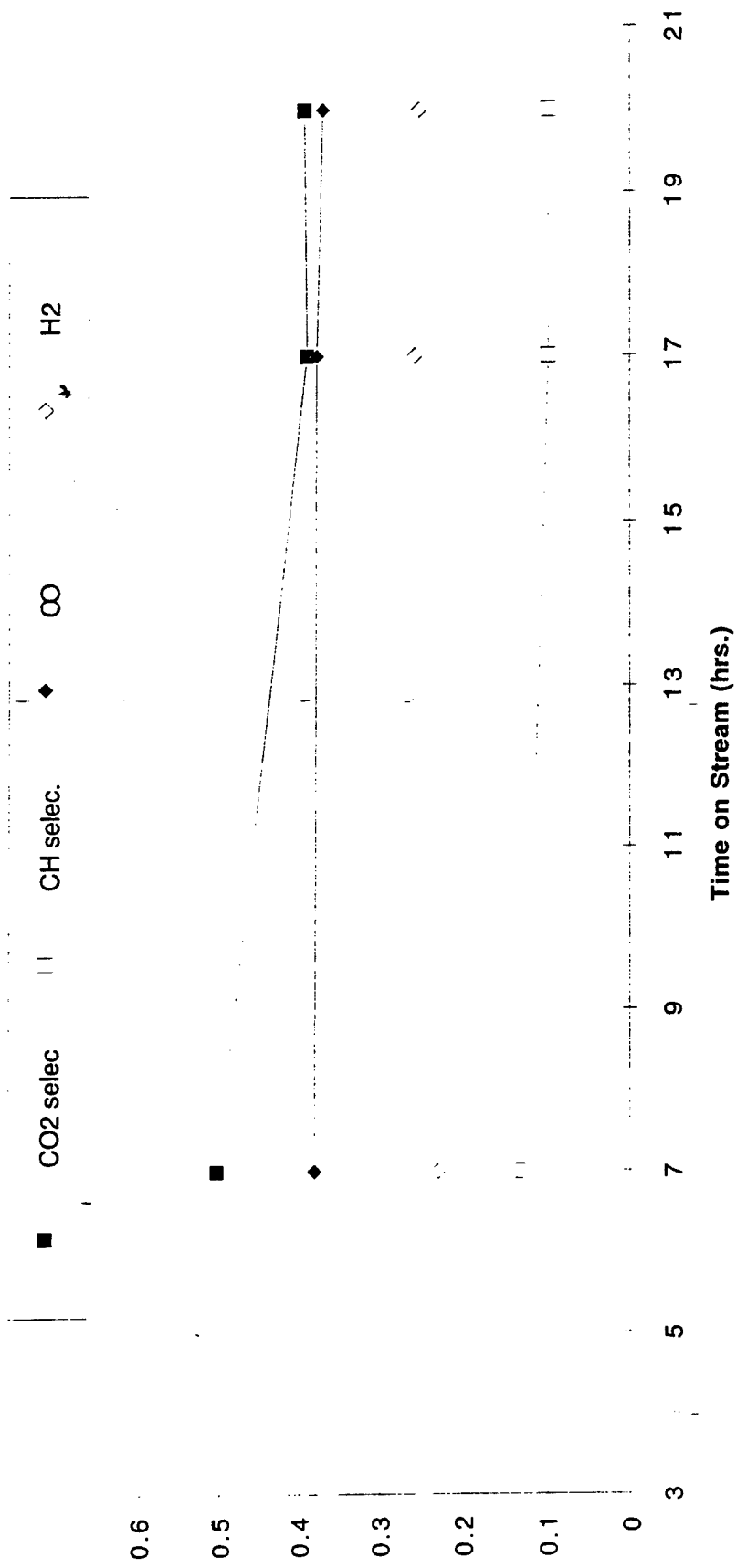


Figure 6. Reaction on F6K (425°C, 1000psi, CO/H2=1)

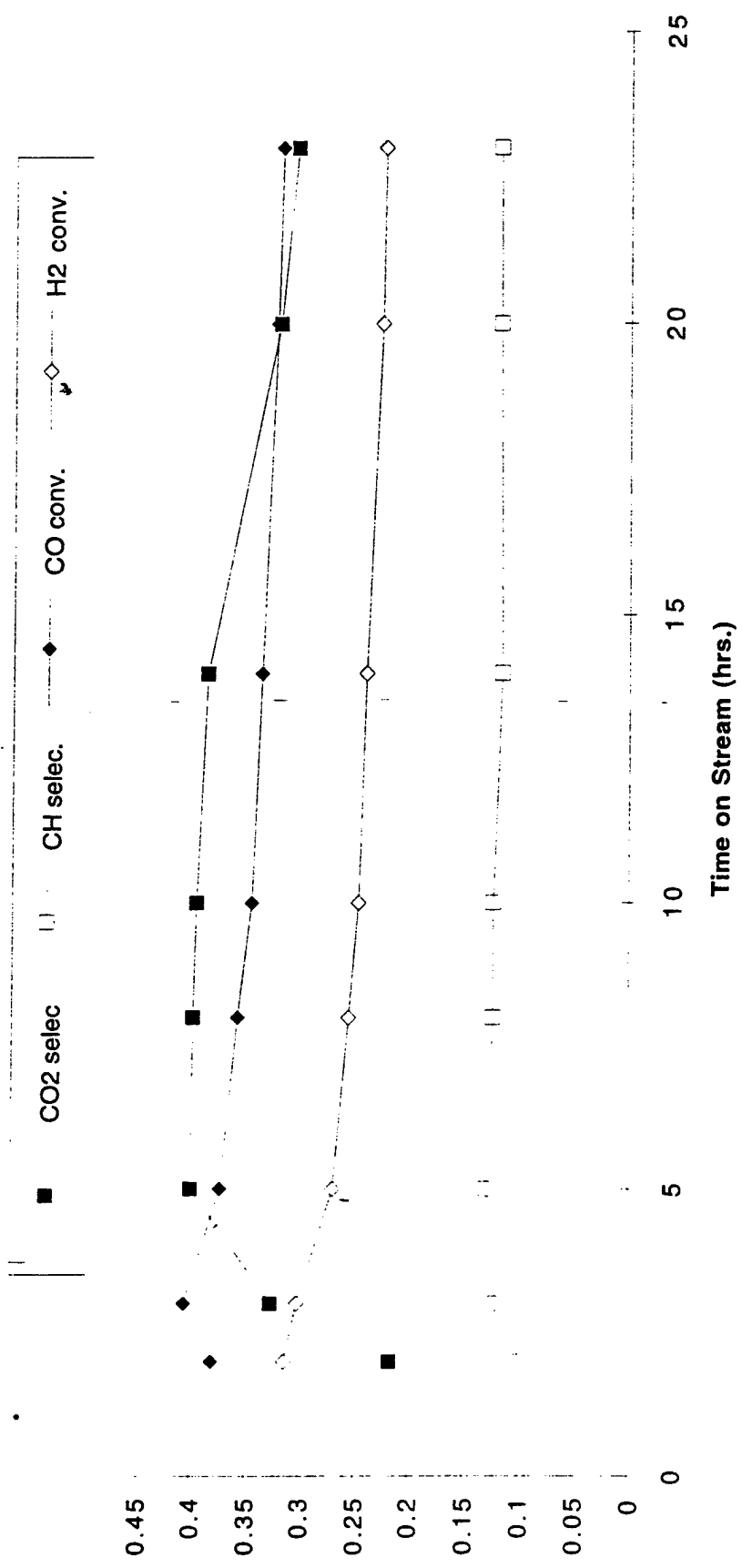


Figure 7. Reaction on F6K (cu)(425°C, 1000psi, CO/H<sub>2</sub>=1)

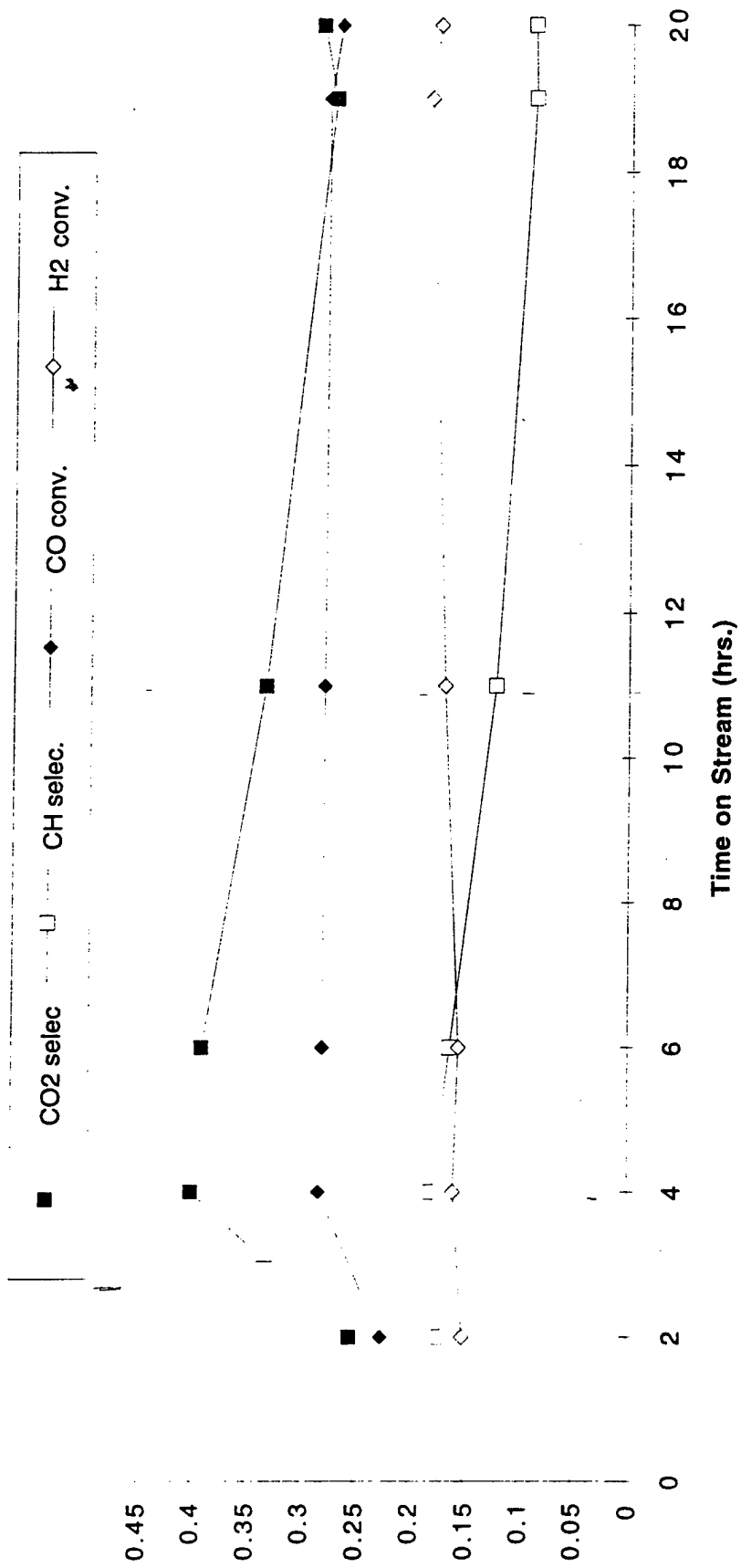


Figure 8. Reaction on F7K (425°C, 1000psi, CO/H<sub>2</sub>=1)

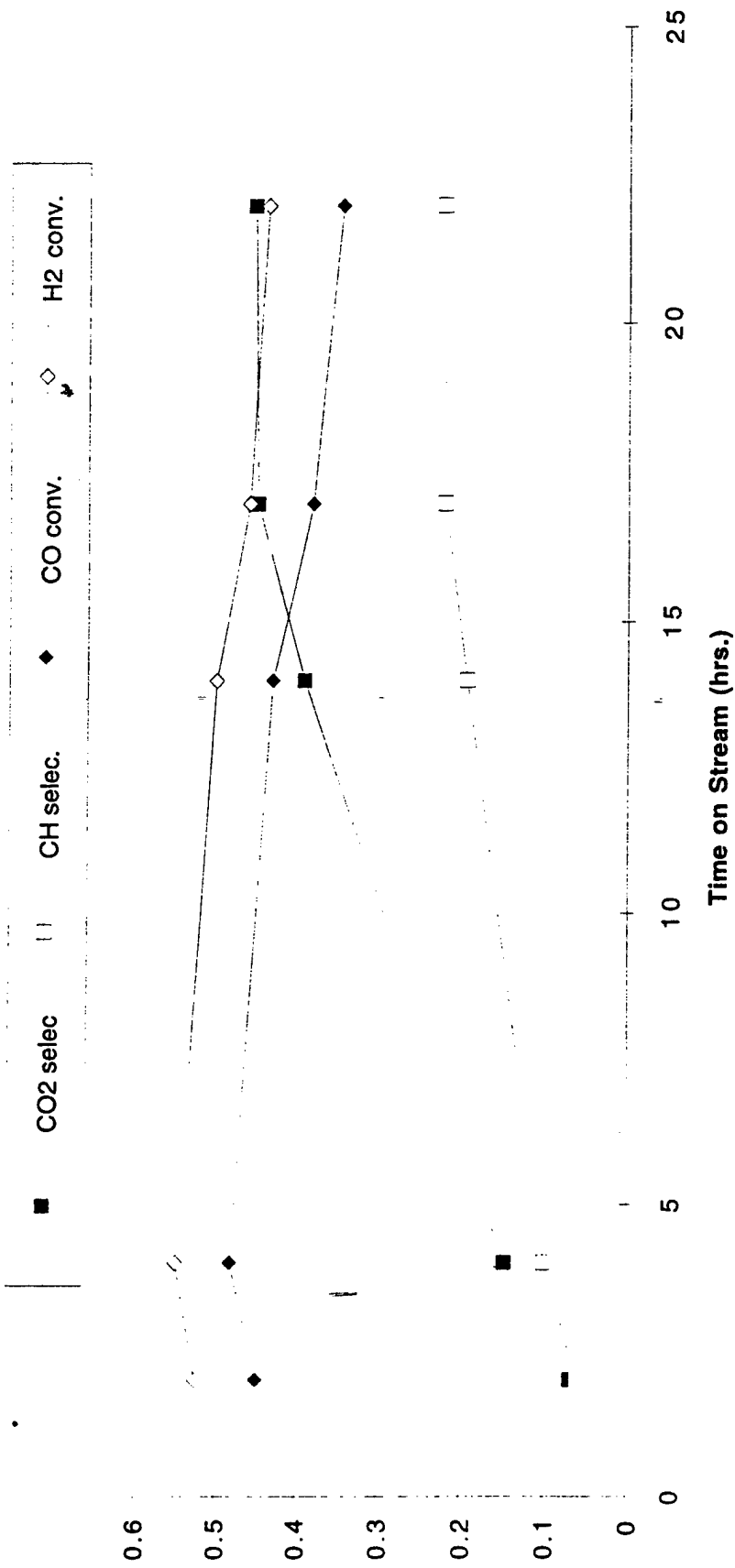


Figure 9. Reaction on F8K (425°C, 1000psi, CO/H<sub>2</sub>=1)

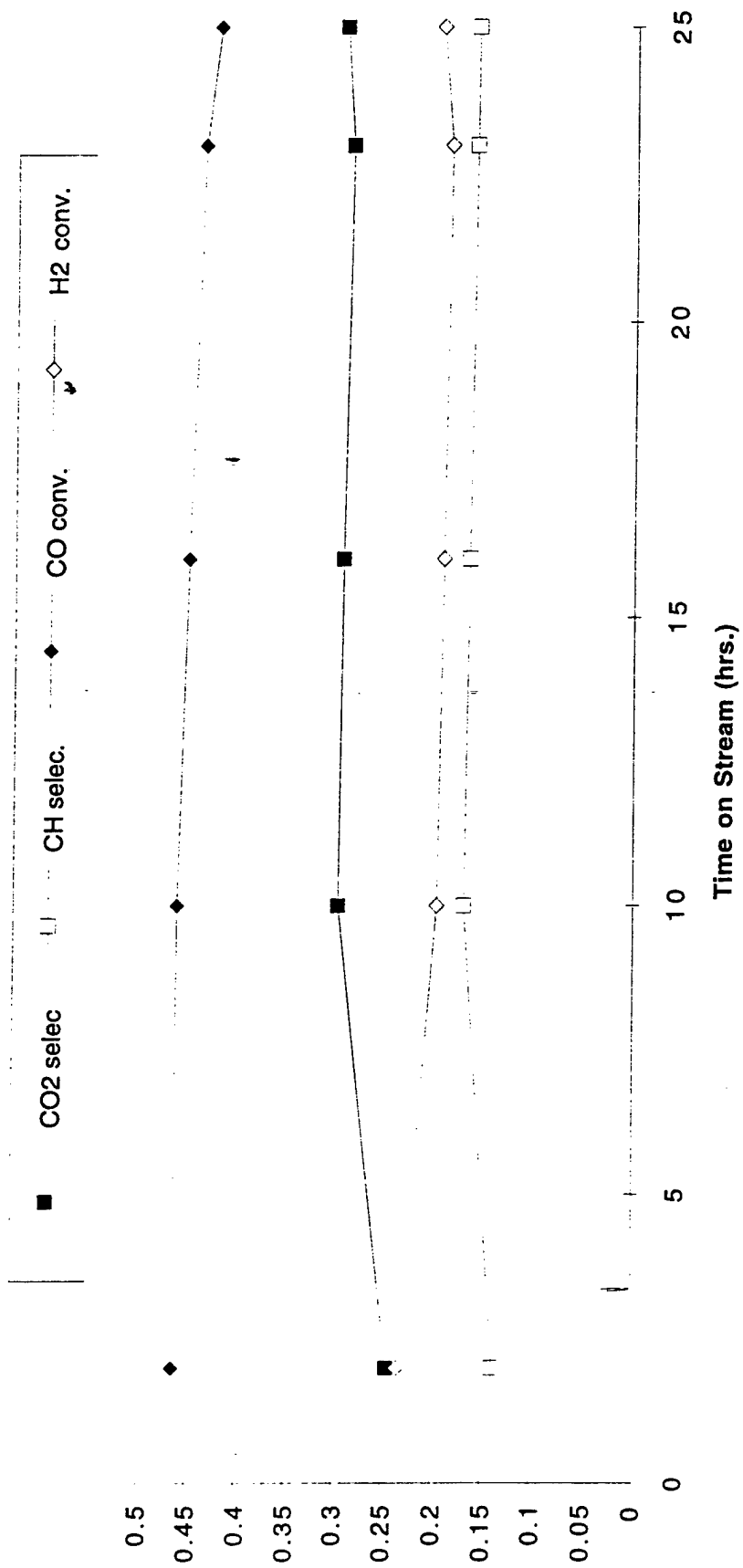




Fig.10 XRD for F1K&Used-F1K

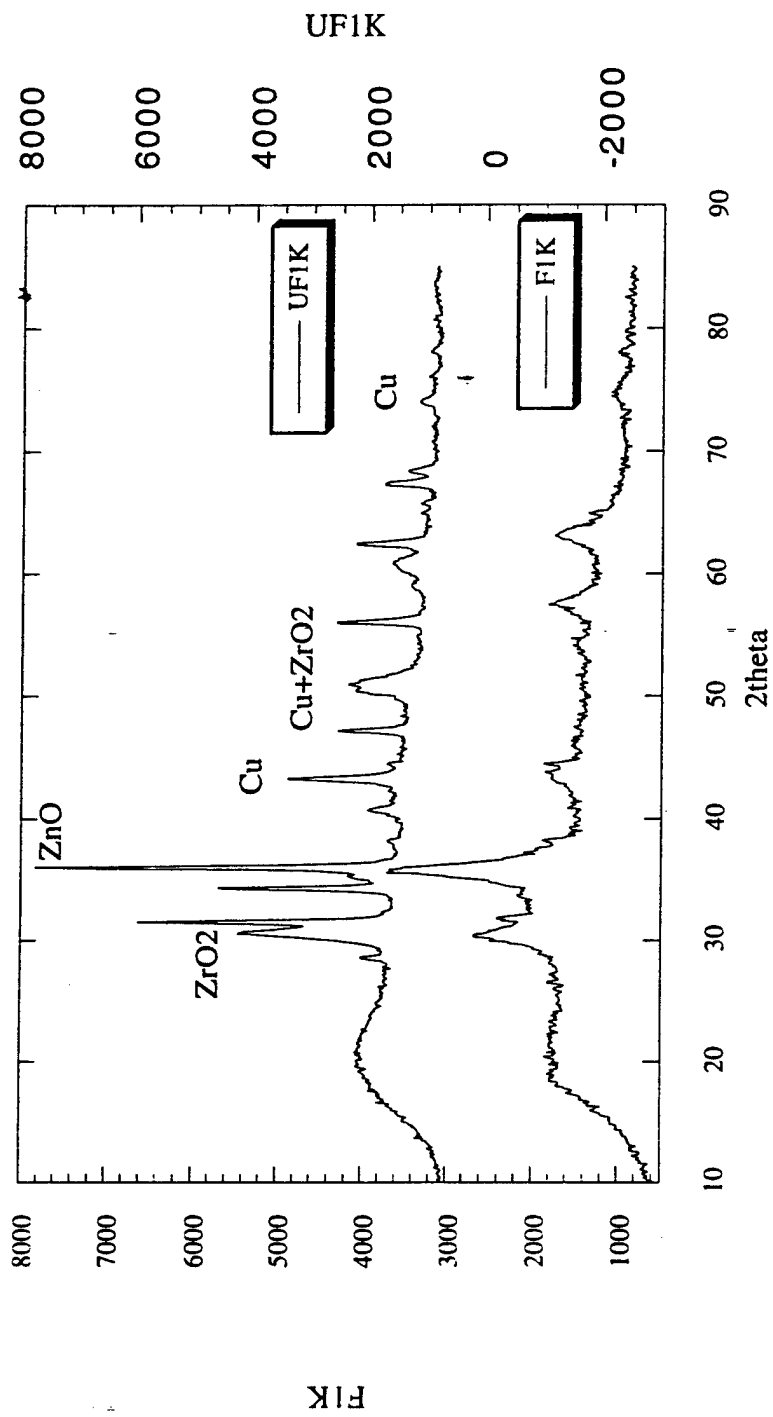


Fig.11 XRD for F2K&Used-F2K

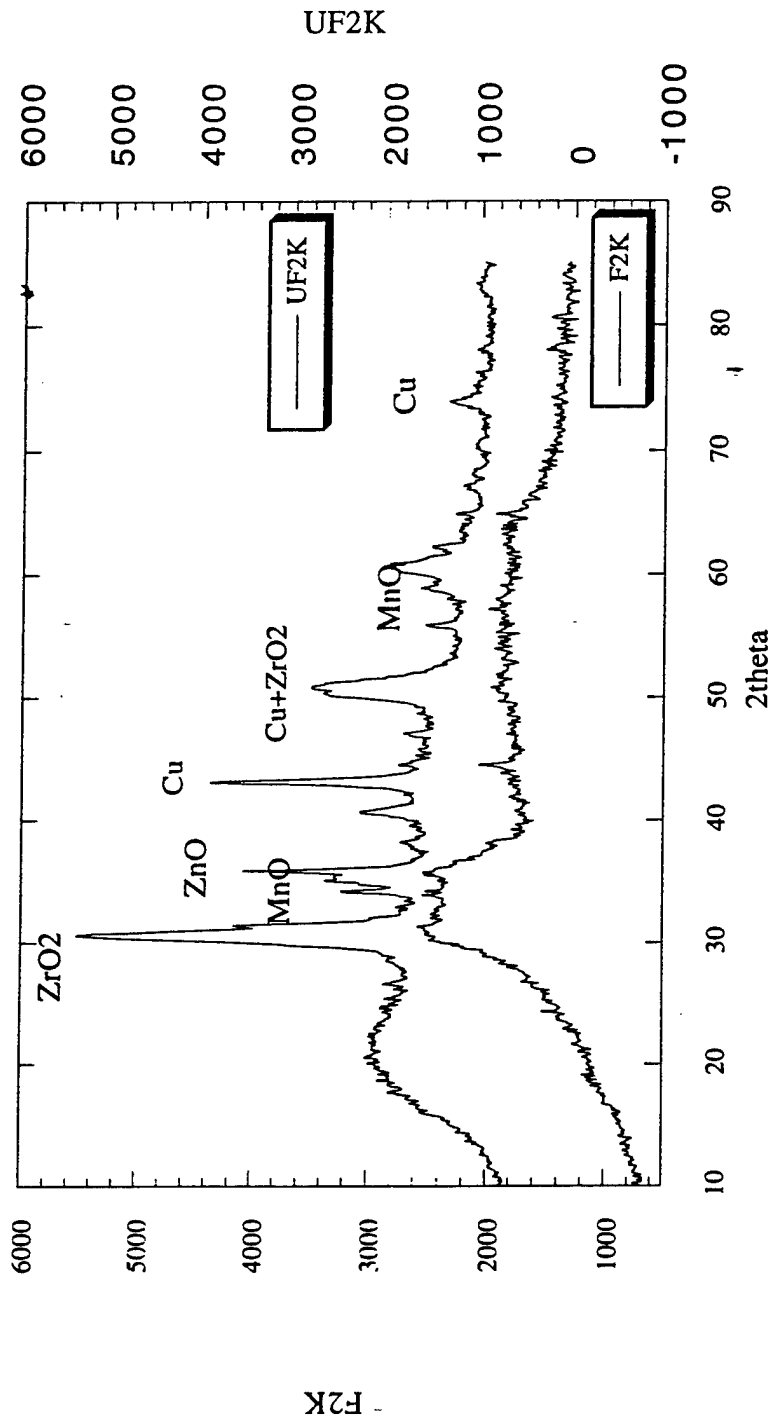


Fig.12 XRD for F3AK&Used-F3AK

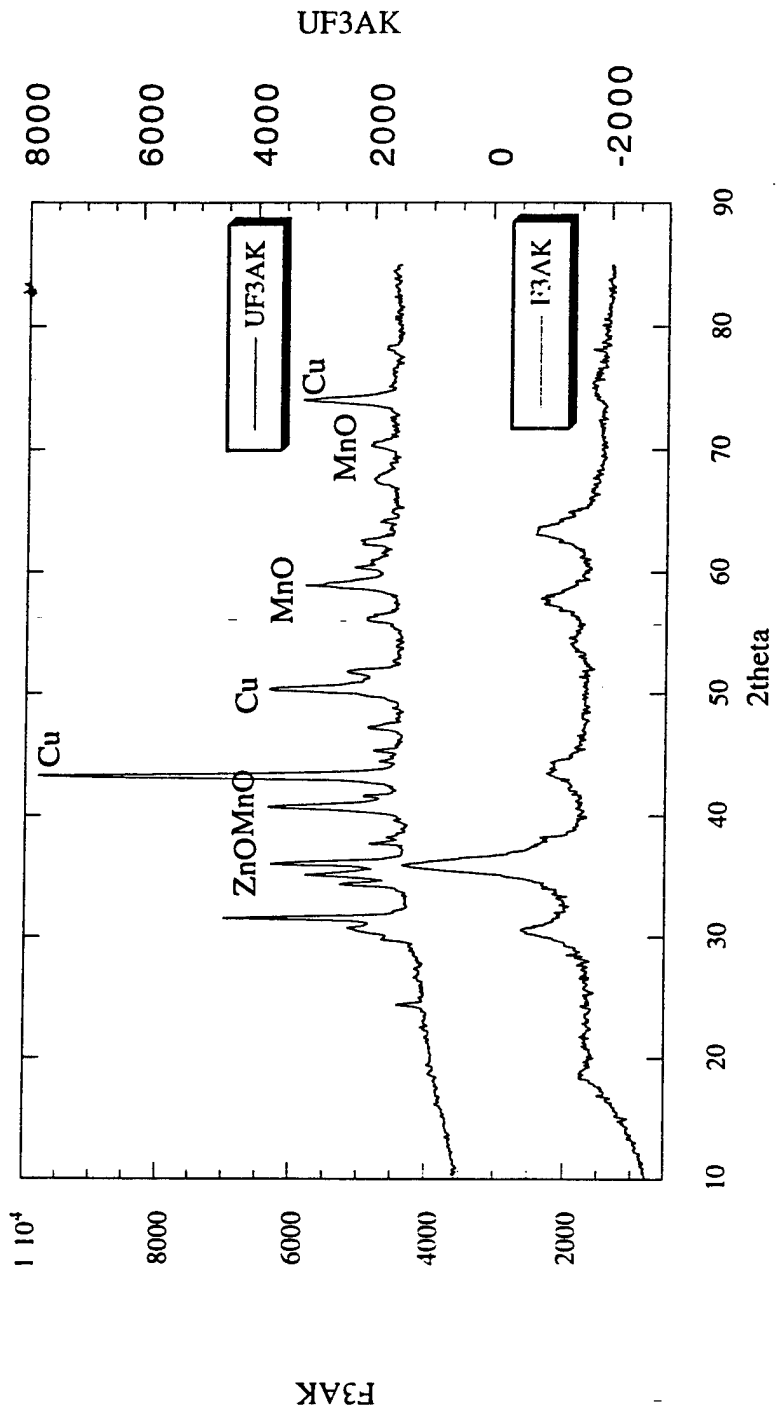


Fig.13 XRD of F4AK and Used-F4AK

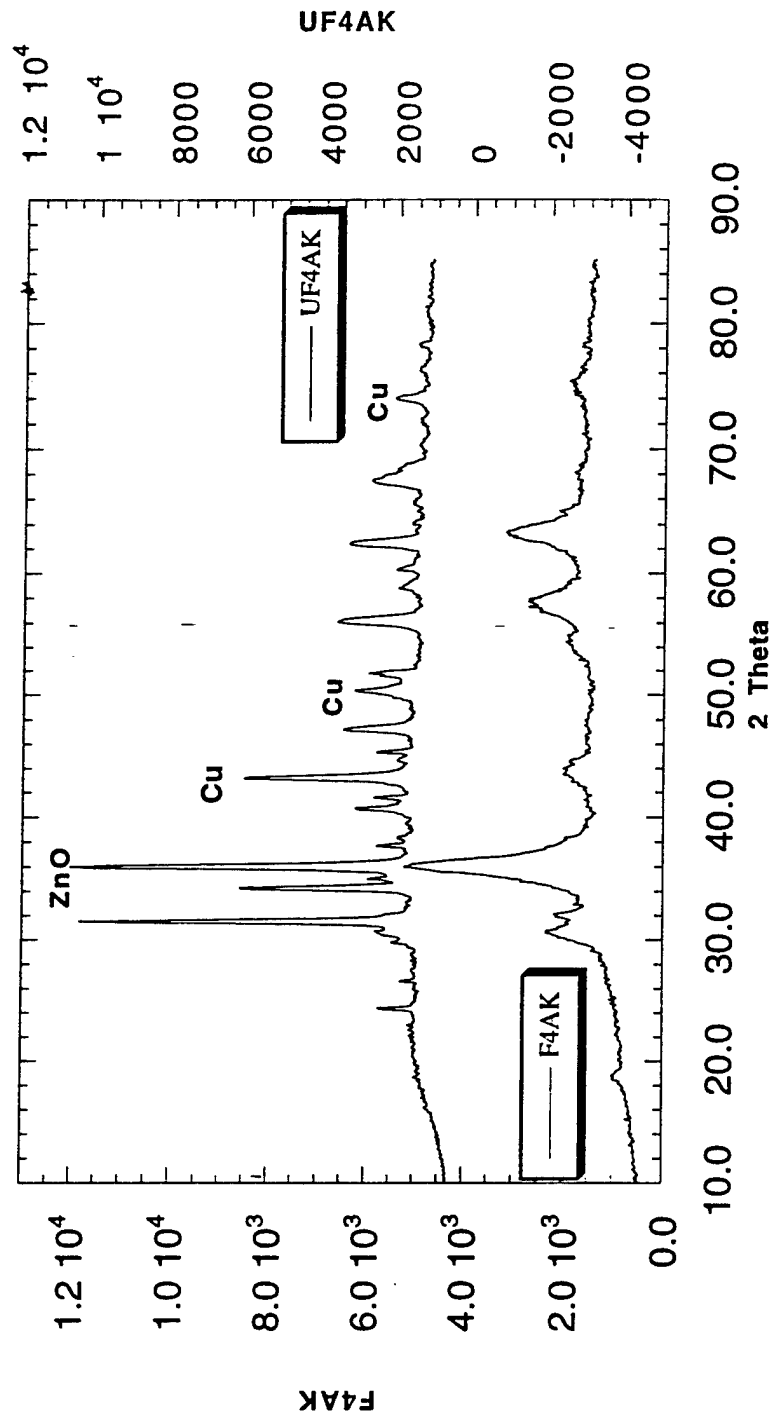


Fig.14 XRD for F5K & Used-F5K

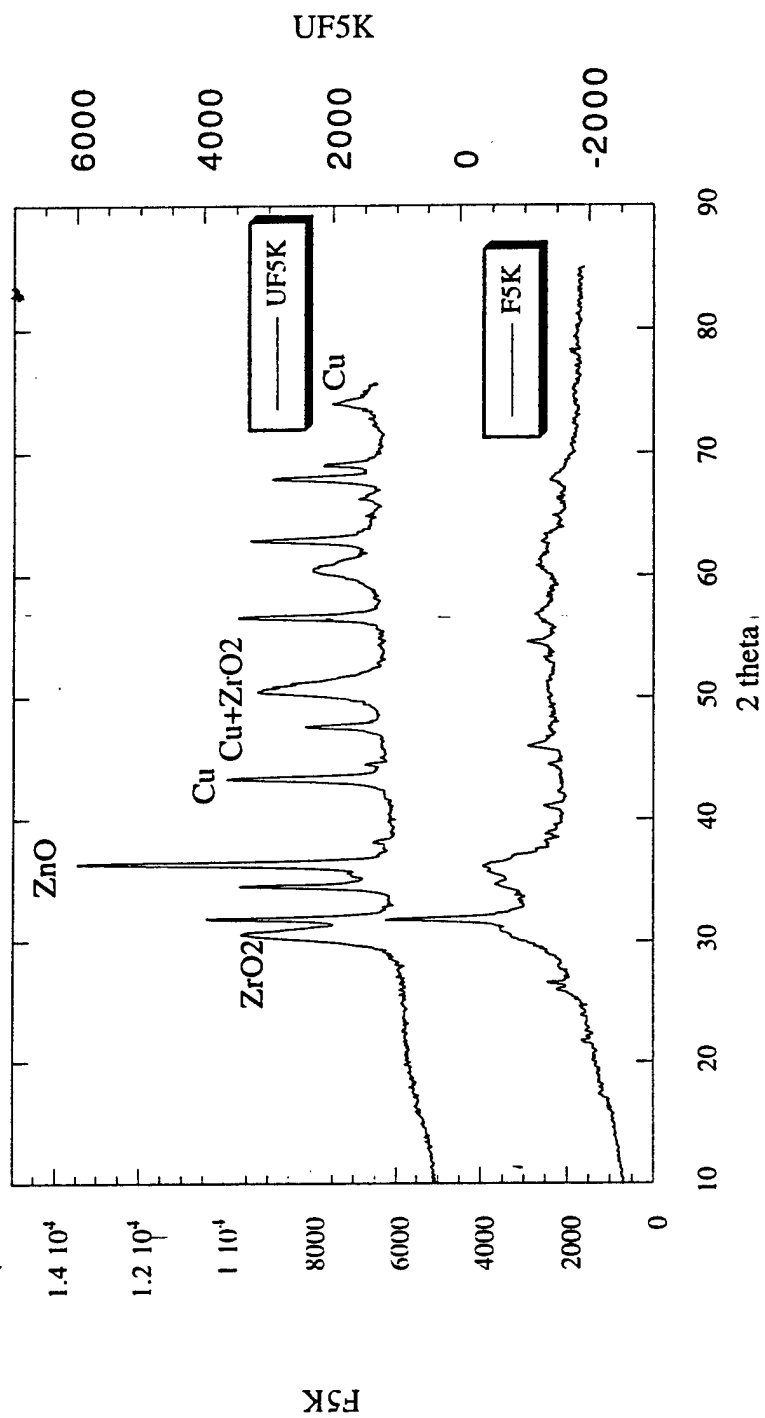


Fig.15 XRD of F6K and Used-F6K

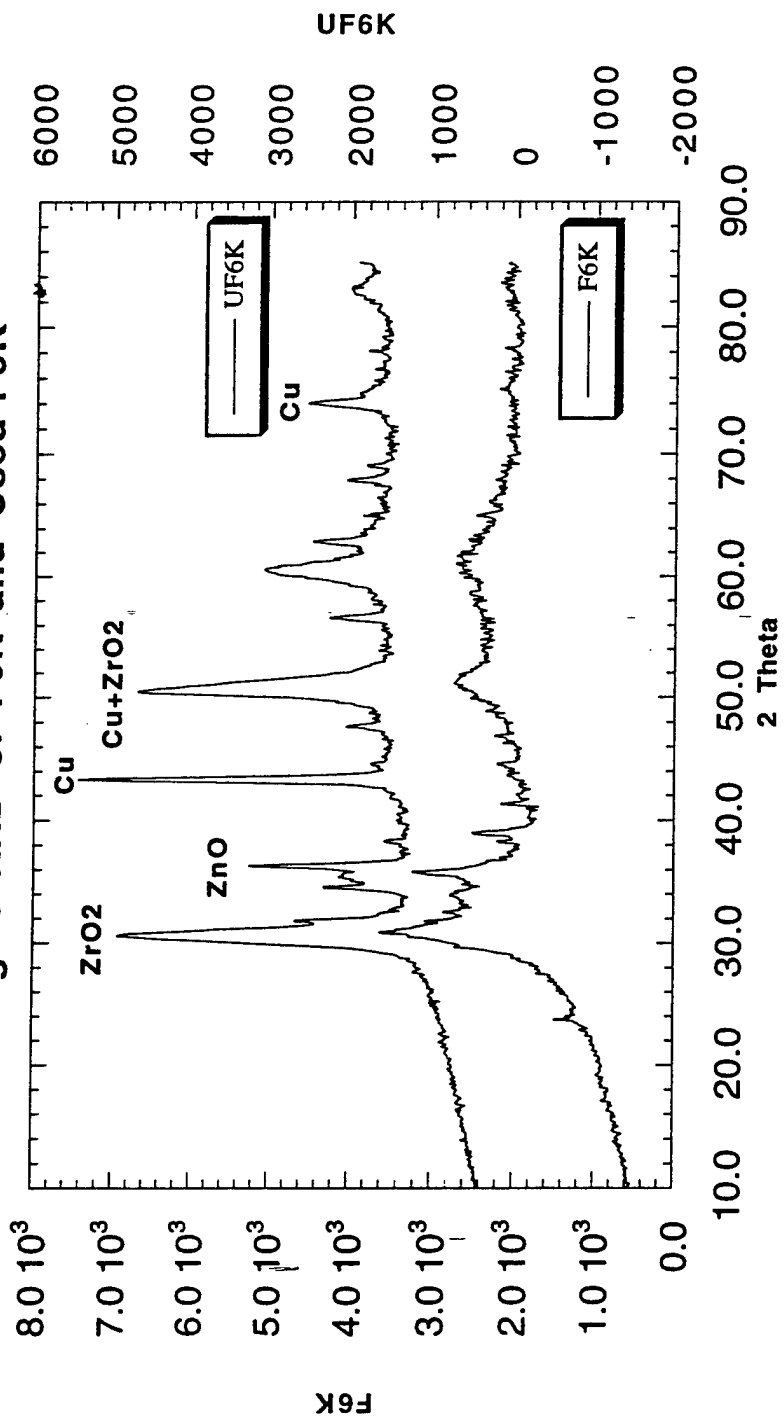


Fig.16 XRD for F7K and Used-F7K

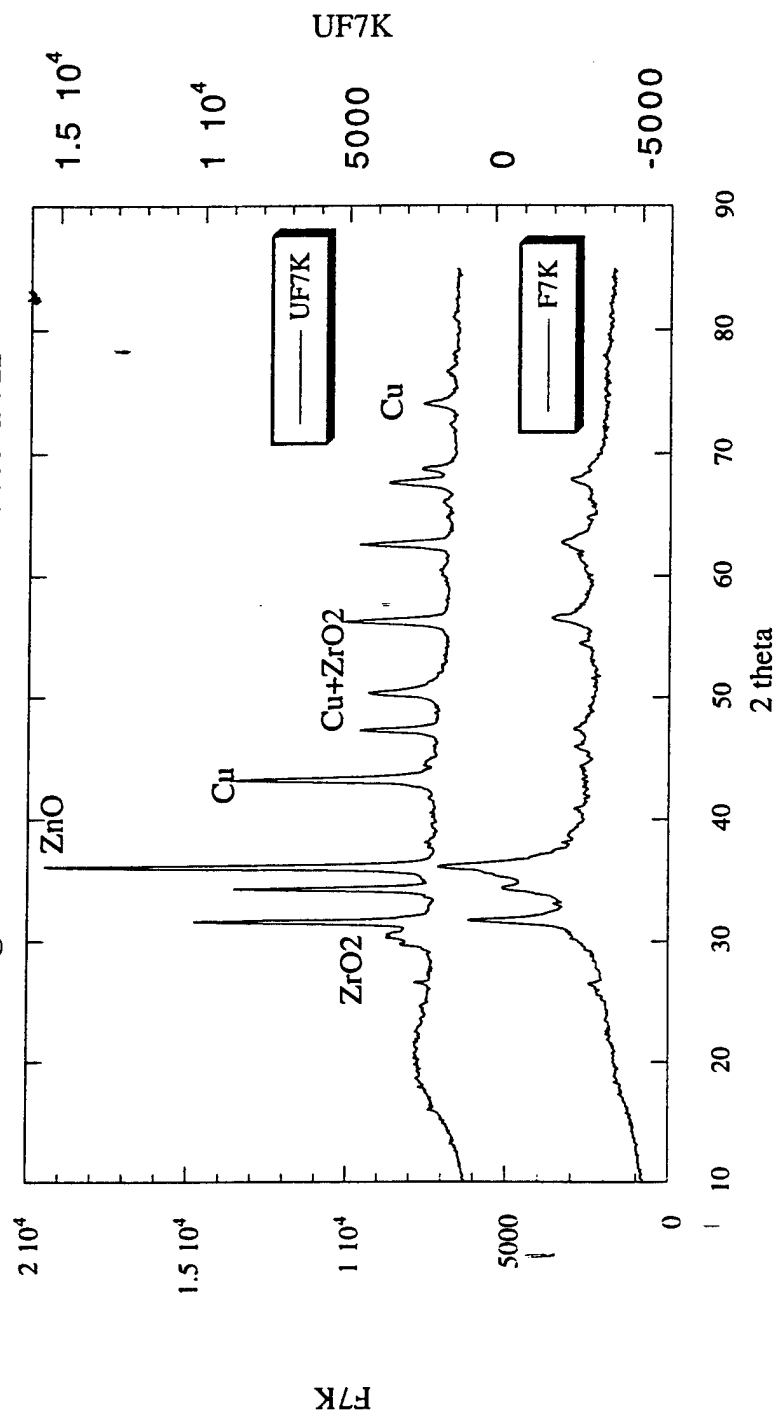
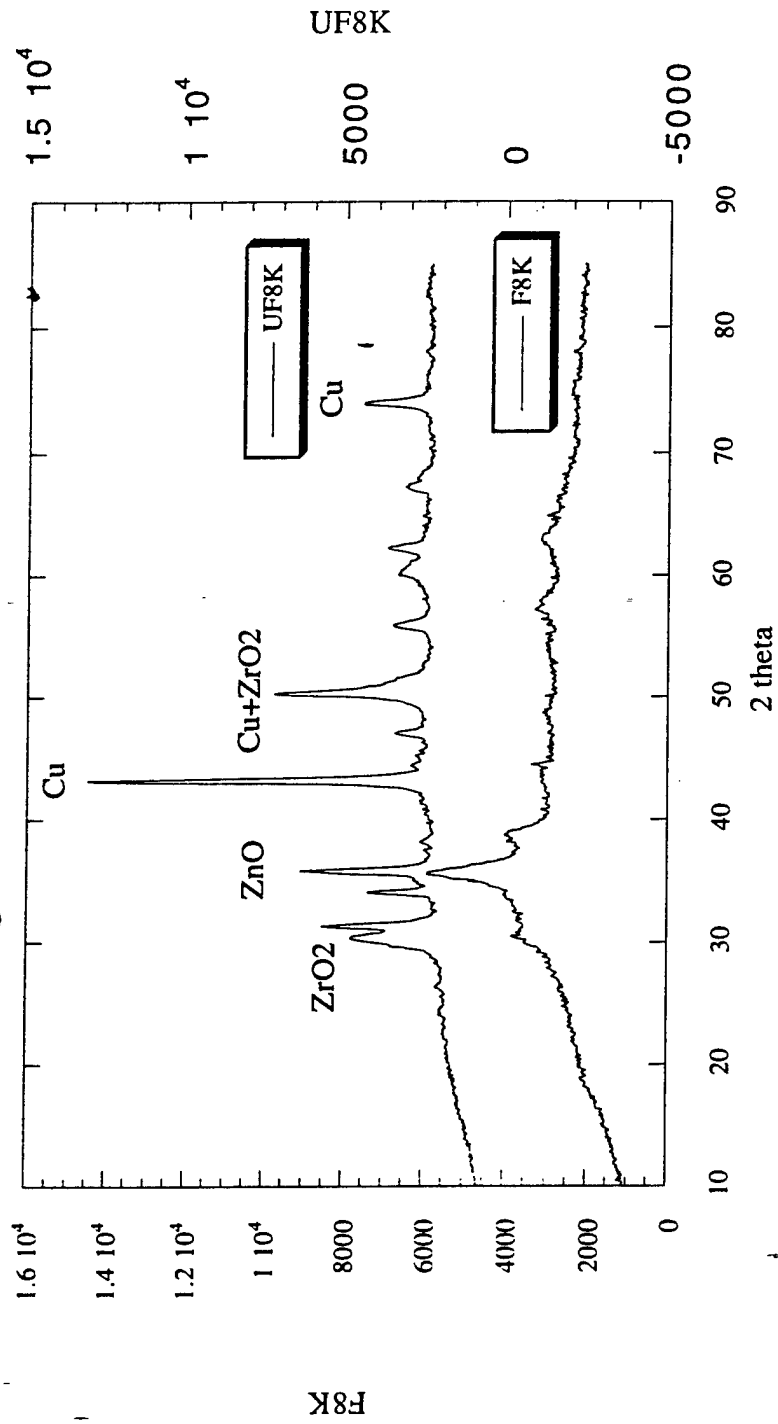


Fig.17 XRD for F8K&Used-F8K





M97054566



Report Number (14) DOE/PC/93052--T4

\_\_\_\_\_  
\_\_\_\_\_  
\_\_\_\_\_

Publ. Date (11) 1990 7 10

Sponsor Code (18) DOE/FE, XF

JC Category (19) UC-~~101~~ 101, DOE/ER

DOE